

12-14-2015

# Regulation of Stress Response and Innate Immunity by DSRNA-Binding Proteins PACT and TRBP

Lauren S. Vaughn

University of South Carolina - Columbia

Follow this and additional works at: <https://scholarcommons.sc.edu/etd>

 Part of the [Biology Commons](#)

---

## Recommended Citation

Vaughn, L. S. (2015). *Regulation of Stress Response and Innate Immunity by DSRNA-Binding Proteins PACT and TRBP*. (Doctoral dissertation). Retrieved from <https://scholarcommons.sc.edu/etd/3219>

This Open Access Dissertation is brought to you by Scholar Commons. It has been accepted for inclusion in Theses and Dissertations by an authorized administrator of Scholar Commons. For more information, please contact [dillarda@mailbox.sc.edu](mailto:dillarda@mailbox.sc.edu).

REGULATION OF STRESS RESPONSE AND INNATE IMMUNITY BY DSRNA-BINDING PROTEINS  
PACT AND TRBP

by

Lauren S. Vaughn

Bachelor of Science  
University of Texas at Dallas, 2010

---

Submitted in Partial Fulfillment of the Requirements

For the Degree of Doctor of Philosophy in

Biological Sciences

College of Arts and Sciences

University of South Carolina

2015

Accepted by:

Rekha C. Patel, Major Professor

Lewis H. Bowman, Committee Member

Deanna S. Smith, Committee Member

David Reisman, Committee Member

Caryn E. Outten, Committee Member

Lacy Ford, Senior Vice Provost and Dean of Graduate Studies

© Copyright by Lauren S. Vaughn, 2015  
All Rights Reserved.

## DEDICATION

I would like to dedicate this work to my family who provides constant support and encouragement- especially my amazing husband, Andrew, who has happily moved around the country with me to help me follow my dreams.

## ACKNOWLEDGEMENTS

First, I would like to thank my mentor, Dr. Rekha Patel, for being everything I was looking for in a mentor and beyond what I thought I needed. She has pushed me to be my best, giving critiques when needed, but all while providing support, mentoring, and knowledge to show me how to become a better researcher and member of the scientific community. She has helped me to grow tremendously in graduate school by being both a mentor and a friend. As I grew as a scientist, she has trusted my judgement and has let me make my own (small) mistakes to ultimately help me to learn to trust my own judgement and intuition. Every step of the way, Rekha has not only shown me how to improve, but also how and why those changes will help me be a better writer, researcher, and member of the community. I cannot even think of a way to thank her enough for all that she has done for me, and I'm sure will continue to do for me even when I have moved on. I would also like to thank my committee, all of whom have all gone out of their way to encourage, teach, and push me to get the most out of my graduate degree and leave as the best doctoral student I could be. Dr. Waldman, who should really be considered an honorary member of my committee, has also provided support and mentorship to help me (and many other students) improve and learn along the way.

I also have to thank my incredible family and friends. My family has provided endless support, never-ending belief in me, and the push to keep me moving forward. I was also lucky enough to start and end graduate school with Andy, who has been my partner in crime the entire way. We are able to laugh and joke together but also help each other by giving advice and support when we both need it. I am also enormously grateful for Evelyn's friendship as she is the only person who will answer my endless stream of questions and discuss anything and everything with me while we work. I have also been lucky enough to be surrounded by wonderful fellow graduate students, who have been essential to my achievements, both personally and scientifically. I would also like to thank Indhira and Shekhar who provided a supportive environment and made us all feel like we are surrounded by family and friends. Last, I would also like to thank Dr. Santosh D'Mello for giving me the wonderful opportunity to work in his lab as a post-bac student and gain invaluable experience for my future. In the D'Mello lab I made lifelong friends including my graduate mentor, Jason, as well as Valerie and Pragya who give continuous support and friendship.

Lastly, I would like to thank the funding and fellowships that I was lucky enough to have throughout my time in graduate school. The majority of my research was funded by the Dystonia Medical Research foundation and a University of SC Aspire grant. Additional support was provided by: University of SC's Presidential Fellowship and the University of SC's Dean's Dissertation award.

## ABSTRACT

An integral aspect of innate immune response to viral infections is the ability to detect non-self molecules to initiate antiviral signaling via pattern recognition receptors (PRRs). One subset of these receptors are cytoplasmic receptors that contain double stranded (dsRNA) binding domains, which allow them to identify non-self dsRNA produced during a viral infection and mount a protective cellular response. PKR is a dsRNA-activated eIF2 $\alpha$  kinase that is a key regulator of cellular antiviral and stress response pathways. Activation of PKR's catalytic activity requires binding to one of its activators, viral dsRNAs or the cellular protein PACT (PKR activator). Although PACT also binds to dsRNA, in uninfected cells PACT activates PKR by a direct interaction in the absence of dsRNA in response to oxidative stress, ER stress, and serum starvation. Prolonged PKR activation and downstream eIF2 $\alpha$  phosphorylation and inhibition leads to cell death by apoptosis. A third dsRNA-binding protein TRBP (TAR-RNA-binding protein), which is homologous to PACT, inhibits PKR by a direct interaction as well as by sequestration of dsRNA and PACT. Recently, an inherited, early-onset form of the neuromuscular disorder dystonia has been identified to be associated with multiple missense mutations in the coding region of PACT. We investigated alterations in PACT activity caused by DYT16 mutations by examining changes in interactions with known

protein partners and ability to activate PKR during cellular stress. Our results establish that each point mutation may alter PACT's functions differently. Patient lymphoblasts containing homozygous mutant P222L activate PKR with slower kinetics, albeit more robustly and for longer duration, as compared to wt lymphoblasts. In addition, the affinity of PACT-PACT and consequently PACT-PKR interaction is enhanced *in vivo* in these P222L dystonia lymphoblast lines, thereby leading to intensified PKR activation and consequently enhanced cellular death. Our results elucidate new mechanistic details of PKR regulation by PACT and shed new light on its impact on stress induced cellular apoptosis.

Another cytoplasmic dsRNA receptor similar to PKR is the RNA helicase RIG-I, which has the ability to detect and be activated by 5'triphosphate uncapped dsRNA as well as the viral mimic dsRNA polyI:C. Once activated, RIG-I's CARD domains oligomerize and initiate downstream mitochondrial anti-viral signaling (MAVS) to induce interferon (IFN) production. PACT stimulates RIG-I signaling in response to polyI:C treatment, in part, by stimulating RIG-I's helicase activity and resulting in an enhanced induction of IFN. Despite the domain homology and similar structure of PACT and TRBP, the role of TRBP is unknown in RIG-I like receptor (RLR) signaling. We investigated the role of TRBP in RIG-I signaling and IFN production. Our results establish an inhibitory role of TRBP on RIG-I signaling, opposing PACT's activating role. This inhibitory effect is also seen in the absence of PACT and PKR, indicating a direct role in RIG-I inhibition. The effect of DYT16 causing mutations in PACT on RIG-I signaling in response to viral stress mimics was also investigated and appears to be unaffected by the DYT16 mutations.



## TABLE OF CONTENTS

|   |     |
|---|-----|
| DEDICATION.....   | iii |
| ACKNOWLEDGEMENTS .....  | iv  |
| ABSTRACT.....   | vi  |
| LIST OF FIGURES.....  | x   |
| LIST OF ABBREVIATIONS.....  | xii |
| CHAPTER 1: INTRODUCTION .....   | 1   |
| 1.1 PKR ACTIVATOR PROTEIN PACT .....  | 2   |
| 1.2 PACT'S FUNCTIONAL ROLE DURING CELLULAR STRESS.....  | 5   |
| 1.3 PACT AND VIRAL INFECTIONS.....  | 10  |
| 1.4 PACT AND MOVEMENT DISORDER DYSTONIA .....   | 14  |
| 1.5 STRUCTURE OF DISSERTATION .....   | 17  |
| CHAPTER 2: INHIBITION OF PKR PROTECTS AGAINST TUNICAMYCIN-INDUCED APOPTOSIS IN<br>NEUROBLASTOMA CELLS ..... | 20  |
| 2.1 ABSTRACT .....  | 21  |
| 2.2 INTRODUCTION.....   | 22  |
| 2.3 MATERIALS AND METHODS .....   | 25  |
| 2.4 RESULTS.....  | 28  |
| 2.5 DISCUSSION .....  | 37  |

|  |     |
|--|-----|
| CHAPTER 3: ALTERED ACTIVATION OF PROTEIN KINASE PKR AND ENHANCED APOPTOSIS IN DYSTONIA CELLS CARRYING A MUTATION IN PKR ACTIVATOR PROTEIN PACT ..... | 44  |
| 3.1 ABSTRACT .....   | 45  |
| 3.2 INTRODUCTION.....  | 46  |
| 3.3 MATERIALS AND METHODS .....  | 49  |
| 3.4 RESULTS.....   | 56  |
| 3.5 DISCUSSION .....   | 78  |
| CHAPTER 4: OPPOSING ROLES OF TWO DSRNA BINDING PROTEINS PACT AND TRBP ON RIG-I INDUCED INTERFERON PRODUCTION.....                                    | 86  |
| 4.1 ABSTRACT .....   | 87  |
| 4.2 INTRODUCTION.....  | 88  |
| 4.3 MATERIALS AND METHODS .....  | 91  |
| 4.4 RESULTS.....   | 96  |
| 4.5 DISCUSSION .....   | 108 |
| CHAPTER 5: GENERAL DISCUSSION .....  | 115 |
| REFERENCES.....  | 119 |
| APPENDIX A- <i>GENE</i> REPRINT PERMISSION .....   | 142 |
| APPENDIX B- <i>THE JOURNAL OF BIOLOGICAL CHEMISTRY</i> REPRINT PERMISSION .....  | 143 |

## LIST OF FIGURES

|  |    |
|--|----|
| Figure 1.1 Domain Structure of PACT, PKR, TRBP, and RIG-I.....   | 3  |
| Figure 1.2 PKR Mediated Signaling .....  | 7  |
| Figure 1.3 DYT16 mutations.....  | 15 |
| Figure 2.1 Overexpression of K296R mutant inhibits PKR activity in SK-N-SH cells .....   | 29 |
| Figure 2.2 Inhibition of PKR activity reduces apoptosis in response to tunicamycin.....  | 31 |
| Figure 2.3 Overexpression of K296R inhibits PKR activation in response to tunicamycin .....  | 34 |
| Figure 2.4 Overexpression of K296R inhibits eIF2 $\alpha$ phosphorylation in response to tunicamycin.....  | 36 |
| Figure 2.5 Overexpression of K296R inhibits induction of ATF4 and CHOP (GADD153) in response to tunicamycin.....   | 38 |
| Figure 3.1 Effect of P222L mutation on dsRNA-binding .....   | 57 |
| Figure 3.2 Effect of P222L mutation on PACT-PKR interaction .....  | 58 |
| Figure 3.3 Effect of P222L mutation on PKR activation .....  | 62 |
| Figure 3.4 Tunicamycin-induced apoptosis is enhanced in dystonia patient lymphoblasts.....   | 64 |
| Figure 3.5 PACT-PKR interaction, PKR activation, and eIF2 $\alpha$ phosphorylation in response to tunicamycin in normal and dystonia patient lymphoblasts..... | 68 |
| Figure 3.6 P222L mutation affects TRBP-PACT and PACT-PACT interactions.....  | 72 |

|   |     |
|---|-----|
| Figure 3.7 Effect of P222L mutation on molecular interactions with PACT's binding partners in yeast two-hybrid assay..... | 77  |
| Figure 3.8 A schematic model of PKR activation in wt and dystonia cells .....   | 81  |
| Figure 4.1 Domain structure of PKR, PACT, TRBP, and RIG-I.....  | 89  |
| Figure 4.2 TRBP inhibits RIG-I mediated interferon production in response to polyI:C and 5'ppp dsRNA.....                 | 97  |
| Figure 4.3 TRBP-mediated inhibition of RIG-I requires neither PACT nor PKR.....   | 100 |
| Figure 4.4 Mapping the domains of PACT and TRBP required for influencing RIG-I mediated signaling.....                    | 101 |
| Figure 4.5 Phosphorylation of PACT and TRBP does not influence RIG-I mediated signaling .....                             | 105 |
| Figure 4.6 dsRNA binding ability of TRBP but not PACT influences RIG-I induced IFN production.....                        | 107 |
| Figure 4.7 Neither PACT nor TRBP affect RIG-I's ATPase activity in the presence of dsRNA.....                             | 109 |
| Figure 4.8 Regulation of RIG-I activation by dsRNA-binding proteins PACT and TRBP ..                                      | 113 |

## LIST OF ABBREVIATIONS

|                     |   |
|---------------------|---|
| 3AT .....           | 3-Amino-1,2,4-Triazole                          |
| ALS.....            | Amyotrophic Lateral Sclerosis                   |
| ATF-4 .....         | Activating Transcription factor 4               |
| ATP .....           | Adenosine Triphosphate                          |
| CHOP .....          | C/EBP Homologous Protein                        |
| CHOP .....          | C/EBP Homologous Protein                        |
| CTD .....           | Carboxy-Terminal Domain                         |
| DAPI.....           | 4',6-diamidino-2-phenylindole                   |
| dsRBM .....         | dsRNA-Binding Motif                             |
| dsRNA.....          | Double-Stranded Ribonucleic Acid                |
| EBV .....           | Epstein Barr Virus                              |
| eIF2 $\alpha$ ..... | Eukaryotic Initiation Factor 2 Subunit $\alpha$ |
| ER .....            | Endoplasmic Reticulum                           |
| GCN2 .....          | General Control Non-Derepressible-2             |
| GFP .....           | Green Fluorescent Protein                       |
| HEK293T .....       | Human Embryonic Kidney 293T cells               |
| HIV.....            | Human Immunodeficiency Virus                    |

|                |                                       |
|----------------|---------------------------------------|
| IFN .....      | Interferon                            |
| IRES.....      | Internal Ribosome Entry Site          |
| IRF3 .....     | Interferon Regulatory Factor 3        |
| K296R PKR..... | Dominant Negative Mutant PKR          |
| MAVS.....      | Mitochondrial Anti-Viral Signaling    |
| MEFs.....      | Mouse Embryonic Fibroblasts           |
| PACT .....     | PKR Activator                         |
| PBM.....       | PACT Binding Motif                    |
| PERK .....     | PKR-like Endoplasmic Reticulum Kinase |
| PKR .....      | Protein Kinase R                      |
| Prbp.....      | Protamine RNA Binding Protein         |
| PRR .....      | Pattern Recognition Receptor          |
| RAX .....      | PKR Activator X                       |
| RIG-I.....     | Retinoic Acid Inducible Gene 1        |
| RLR .....      | RIG-I like receptor                   |
| RNAi.....      | RNA Interference                      |
| SH-SY5Y .....  | Human Neuroblastoma Cell line         |
| SK-N-SH .....  | Human Neuroblastoma Cell Line         |
| TAR .....      | Trans-Activation Response Element     |
| TRBP .....     | TAR RNA binding protein               |
| UPR.....       | Unfolded Protein Response             |
| WT.....        | Wild Type                             |

## CHAPTER 1: INTRODUCTION<sup>1</sup>

---

<sup>1</sup>To be adapted into a comprehensive PACT Review. Vaughn LS and Patel RC. "PACT: multiple roles as a dsRNA-binding protein", *manuscript in preparation*.

## 1.1 PKR activator protein PACT

PACT is a double-stranded (ds) RNA-binding protein that was originally identified as a protein kinase R (PKR)-interacting protein in a yeast two-hybrid screen using the dominant negative mutant of PKR as bait (Patel and Sen 1998). PKR is an interferon (IFN)-induced protein kinase that plays a central role in antiviral innate immunity. PACT (also designated as PRKRA, DYT16) is a 313 amino acid long protein containing three dsRNA-binding and dimerization motifs homologous to those present in PKR and other dsRNA-binding proteins (Figure 1.1) (Patel and Sen 1998). Despite PACT's functional role in activation of PKR, it is not induced by IFN or dsRNA treatment (Patel and Sen 1998). PACT was named for its ability to work as an endogenous activator of PKR in the absence of dsRNA, PKR's only known activator at that time (Patel and Sen 1998). While human PACT was first identified by Dr. Rekha Patel while working for Dr. Ganes Sen at Cleveland Clinic, PACT's murine homolog was subsequently identified by Dr. Takahiko Ito in Stratford May's lab at the University of Texas Medical Branch by a similar yeast two-hybrid screen (Ito et al. 1999). The murine homolog of PACT was named RAX (PKR-associated protein X) (Ito et al. 1999). Both labs found PACT to be ubiquitously expressed in multiple cell lines and in all human and murine tissues tested (Patel and Sen 1998, Ito et al. 1999, Gupta and Patel 2002).

Although the dsRNA-binding motifs (dsRBMs) are evolutionarily conserved motifs present in proteins from bacteria to humans, some of the proteins belonging to



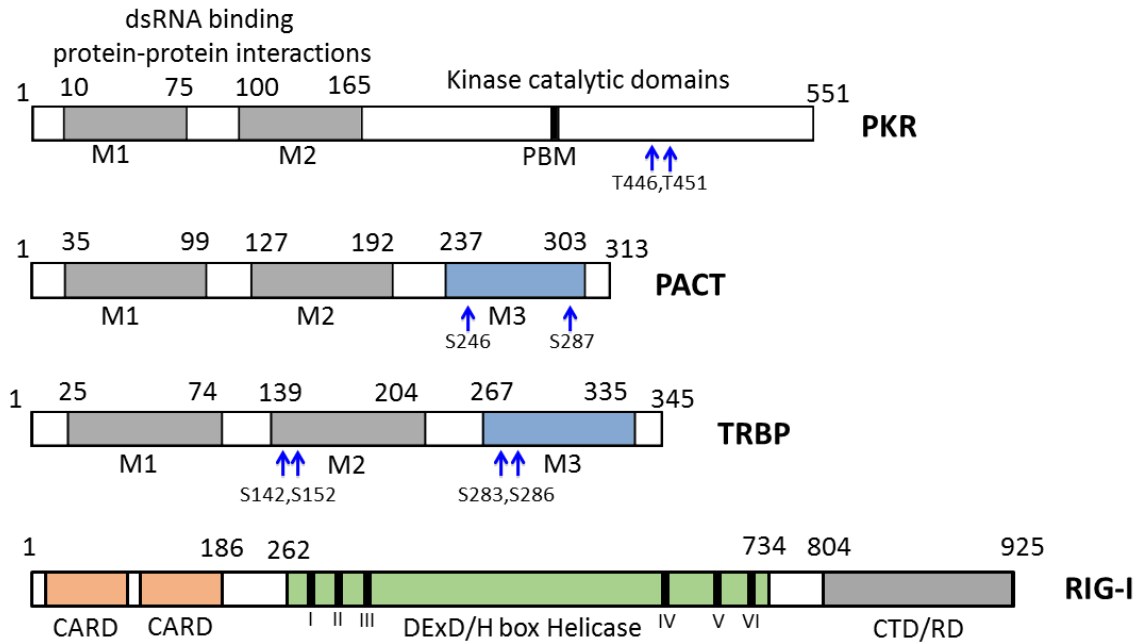


**Figure 1.1: Domain structure of PKR, PACT, TRBP, and RIG-I.** *M1 and M2* of PKR, PACT, and TRBP are conserved dsRNA binding motifs (dsRBMs) that also mediate protein-protein interactions. *PBM*, PACT Binding Motif. *M3* of PACT is essential for PKR activation. *M3* (aka medial domain) of TRBP mediates TRBP's interactions with Merlin, Dicer, and PACT. *Blue Arrows* indicate known sites of phosphorylation on each protein. *CARD*, Caspase activation and recruitment domain, site of oligomerization with other *CARD* domains. *DExD/H Helicase*, helicase domain with inherent ATPase activity. *CTD/RD*, C-terminal domain and regulatory domain, interaction site of PACT. *I-VI*, conserved helicase motifs.

this class share the most homology with PACT. These include Xenopus (Xlrpba), Drosophila (RAX/loqs/R3D1, R2D2), human (TRBP), and mouse (Prbp) proteins (Gatignol et al. 1991, Eckmann et al. 1997, Patel and Sen 1998, Ito et al. 1999). PACT contains three dsRBMs, of which the two amino-terminal motifs M1 and M2 are true dsRBMs that exhibit dsRNA-binding activity (Figure 1.1) (Patel and Sen 1998, Huang et al. 2002). In addition, the M1 and M2 dsRBMs of PACT bind to the amino-terminal dsRBMs of other PACT molecules as well as other dsRBM containing proteins such as TRBP and PKR (Figure 1.1) (Patel and Sen 1998, Peters et al. 2001, Gupta et al. 2003, Chang and Ramos 2005) to form homo- and heterodimers. The third, carboxy-terminal motif M3 has significant homology to the consensus dsRBM but is not a functional dsRBM and does not bind dsRNA (Figure 1.1) (Huang et al 2002, Li et al 2006).

Analysis of PACT expression has shown that PACT mRNA is expressed ubiquitously in various human organs, with the highest levels of expression seen in placenta, colon, and testis (Fasciano et al. 2007, Patel and Sen 1998, Ito et al. 1999, Gupta and Patel 2002). To better understand PACT's expression pattern and characterize the promoter region, PACT's transcription start site was mapped by primer extension (Fasciano et al. 2007). Surprisingly, PACT's promoter sequence contains no TATA box, and the only recognizable regulatory elements identified were GC boxes, the known binding sites for the general transcription factor Sp1 (Fasciano et al. 2007, Rowe and Sen 2001). Six Sp1 binding sites were identified within the first 300 bp upstream of PACT's transcription start site, and the minimal basal promoter was mapped to -101 bp upstream of transcription start site containing a single Sp1 binding site (Fasciano et al.

2007). A promoter including all six Sp1 binding sites, -309 bp upstream of transcription start, was able to increase reporter expression 2 fold (Fasciano et al. 2007). A five-fold increase was seen with a -414 bp promoter, which contains no additional GC box Sp1 binding sites, but does include a CCAAT box at position -404 to -400 (Fasciano et al. 2007, Rowe and Sen 2001). No significant increase was seen with inclusion of further upstream sequences to -2002 bp (Fasciano et al. 2007). Individual mutation of each of the six GC boxes showed no significant effect on promoter activity, indicating redundancy within the promoter (Fasciano et al. 2007). Further analysis showed that the first two GC box sites upstream of transcription start appear to have the most significant effect on expression, with either the first or second GC box site upstream being essential for full activity of the PACT promoter (Fasciano et al. 2007). Sp1 was shown to bind to both the first and second GC box site of the PACT promoter *in vitro* as well as in HeLa cells (Fasciano et al. 2007). It has been observed that in cell lines PACT's expression level remains unchanged during various cellular and viral stresses, though untransformed peripheral blood mononuclear cells (PBMCs) infected with HIV-1 show an increase in PACT expression at the peak of infection (Clerzius et al. 2013, unpublished data).

### **1.2 PACT's Functional Role during Cellular Stress**

Cells respond to various stress signals by inducing phosphorylation of the  $\alpha$ -subunit of eukaryotic initiation factor 2 (eIF2) (Donnelly et al. 2013). Phosphorylation of eIF2 $\alpha$  on serine 51 leads to a sharp decline in de novo protein synthesis and is considered as

an important strategy in cellular response against stressful insults including viral infection, the accumulation of misfolded proteins in the endoplasmic reticulum (ER), oxidative stress, and starvation (Donnelly et al. 2013). The phosphorylation of eIF2 $\alpha$  is carried out by a family of four kinases, PERK (PKR-like ER kinase), PKR (protein kinase double-stranded RNA-dependent), GCN2 (general control non-derepressible-2), and HRI (heme-regulated inhibitor) (Donnelly et al. 2013). Each kinase primarily responds to a distinct type of stress or stresses (Donnelly et al. 2013). Of these, PKR is an IFN-induced serine/threonine kinase that is expressed ubiquitously and plays a central role in mediating IFN's antiviral actions as well as in regulating cellular survival and apoptosis in response to several stress signals (Garcia et al. 2006). Although IFNs increase PKR's cellular abundance via transcriptional induction, PKR's kinase activity requires binding to one of its activators leading to autophosphorylation and enzymatic activation (Meurs et al. 1990). Double-stranded RNA, a replication intermediate for several viruses, was one of the first well-characterized activators of PKR (Figure 1.2) (Galabru and Hovanessian 1987, Meurs et al. 1990). PKR binds dsRNA via its two dsRNA-binding motifs M1 and M2 (Figure 1.1) (Lee et al. 1992, Patel and Sen 1992), which changes the conformation of PKR to expose the ATP-binding site (Nanduri et al. 2000) and leads to its autophosphorylation (Cole 2007). The two dsRBMs also mediate dsRNA-independent, protein-protein interactions with other proteins that carry similar domains (Patel et al. 1995, Chang and Ramos 2005). Among these are proteins inhibitory for PKR activity such as TRBP (human immunodeficiency virus (HIV)-1 transactivation-responsive (**T**AR) **R**NA-binding **p**rotein) (Benkirane et al. 1997) and proteins that activate PKR such as PACT

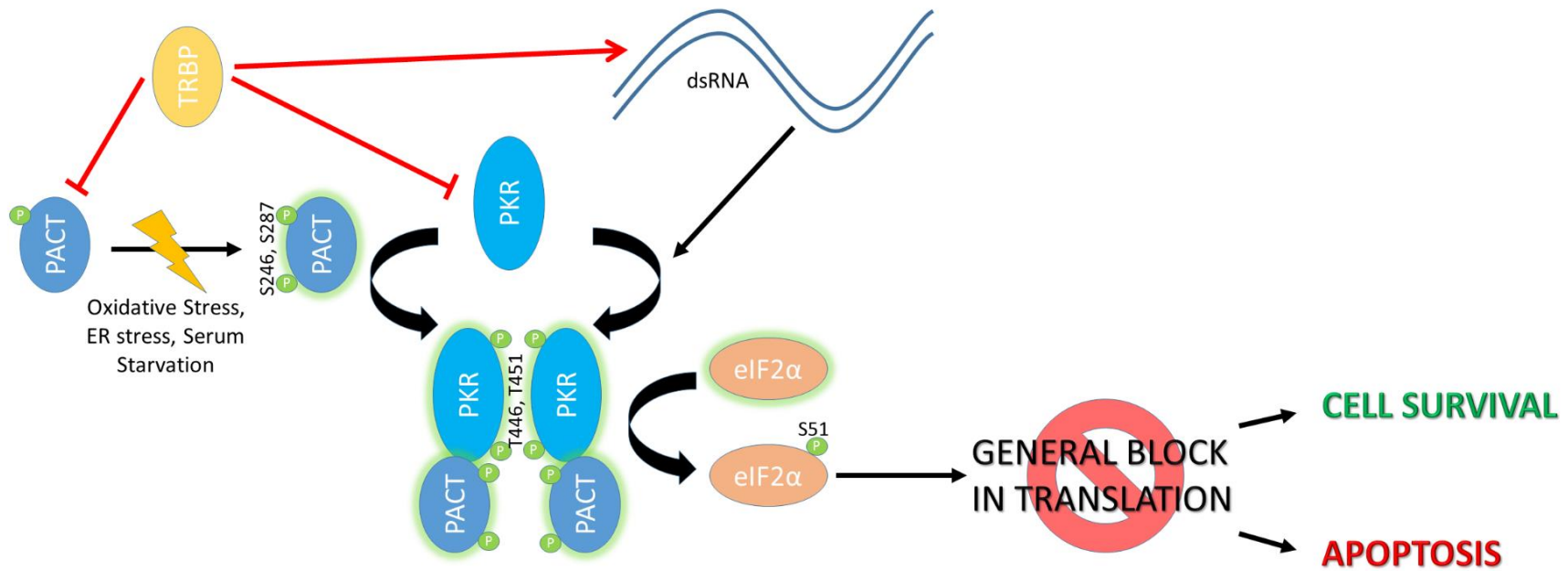


**Figure 1.2: PKR-Mediated Signaling.** In the absence of stress, TRBP binds to and sequesters PACT and PKR, keeping PKR signaling inactive. At this time, PACT is constitutively phosphorylated at serine 246. During viral stress, dsRNA produced by viruses binds directly to and activates PKR. TRBP works to counter PKR during viral stress by binding to dsRNA and sequestering it from PKR. During cellular stress (no dsRNA, e.g. endoplasmic reticulum stress), PACT is activated by phosphorylation at serine 287, which increases PACT's affinity for PKR while simultaneously decreasing PACT's affinity for TRBP. When either activator binds to PKR, it changes PKR's conformation to expose PKR's ATP binding pocket, which leads to autophosphorylation of PKR at threonine 446 and 451 and PKR activation. Once activated, PKR phosphorylates eIF2 $\alpha$  on Serine 51. This phosphorylation of eIF2 $\alpha$  inhibits protein synthesis by blocking recycling of GDP to GTP within the eIF2 complex, halting initiation of translation. This block in translation allows the cells to alleviate the stress (e.g. unfolded proteins, viral stress) or if unable to recover, undergo apoptosis.

(Figure 1.2) (Patel and Sen 1998). Of PACT's three dsRBMs, M1 and M2 are essential for binding to the corresponding M1 and M2 dsRBMs of PKR (Figure 1.1) (Peters et al. 2001, Huang et al. 2002). The third motif (M3) of PACT is essential for activation of PKR during cellular stress and binds to a specific region in the kinase domain of PKR with low affinity, this region is called the PACT binding motif (PBM) (Figure 1.1) (Peters et al. 2001, Li et al 2006, Huang et al. 2002). The PBM in PKR spans from amino acids 326-337, with five of the residues (D328, D333, D331, G329, Y332) being essential for the interaction with PACT (Li et al. 2006). Although purified, recombinant PACT can activate PKR by direct interaction *in vitro* (Patel and Sen 1998), PACT-dependent PKR activation in cells occurs in response to a cellular stress signal (Ito et al. 1999, Patel et al. 2000, Bennett et al. 2004, Singh et al. 2009). PACT-mediated activation of PKR occurs in response to cellular stressors such as arsenite, hydrogen peroxide, growth factor withdrawal, thapsigargin, tunicamycin, and actinomycin. PKR activation results in phosphorylation and inhibition of the translation initiation factor eIF2 $\alpha$  and subsequent apoptosis (Ito et al. 1999, Patel et al. 2000, Bennett et al. 2004). PACT (and its murine homolog RAX) is phosphorylated in response to the stress signals leading to its increased association with PKR and is essential for PKR activation in the absence of dsRNA (Ito et al. 1999, Patel et al. 2000, Bennett et al. 2004).

TRBP, while structurally alike to PACT, inhibits PKR's activity (Figure 1.2) (Gupta et al. 2003, Daher et al. 2001). Similar to PACT, TRBP has three copies of dsRBMs with only the two amino terminal copies M1 and M2 being capable of binding dsRNA (Gatignol et al. 1991, Gatignol et al. 1993, Erard et al. 1998, Daviet et al. 2000), but the third

carboxy-terminal copy (M3/medial domain) mediating protein-protein interactions with several proteins including Dicer (Daniels et al. 2009) , merlin (Xu et al. 2004), and PACT (Laraki et al. 2008) (Figure 1.1). In virally infected cells TRBP inhibits PKR by direct binding as well as by sequestering virally produced dsRNAs (Gupta et al. 2003, Daher et al. 2001). However, in uninfected cells TRBP inhibits PKR by direct binding (Cosentino et al. 1995) and by forming heterodimers with PACT and preventing it from activating PKR (Daher et al 2009, Singh et al 2011). TRBP-PACT and TRBP-PKR heterodimers are present in unstressed cells and after the onset of stress, PACT-TRBP and TRBP-PKR dimers dissociate (Daher et al. 2009, Gupta et al. 2003, Singh et al. 2011). Thus, TRBP regulates the activation of PKR in response to stress by controlling its accessibility to PACT (Singh et al. 2011, Gupta et al. 2003). Changes in the interactions between PACT, PKR, and TRBP have been shown to be mediated in part by phosphorylation of both PACT and TRBP (Peters et al. 2006, Singh et al. 2011, Paroo et al. 2009, Nakamura et al. 2015).

Phosphorylation of two serine residues S246 and S287 in PACT's PKR activation domain (M3) is required for PACT's ability to activate PKR in response to stress signals (Peters et al. 2006). Constitutive phosphorylation of serine 246 is a pre-requisite for stress-induced phosphorylation of serine 287 of PACT (Peters et al. 2006). Stress induced phosphorylation of serine 287 in PACT causes dissociation of PACT-TRBP complexes while at the same time increasing PACT's affinity for other PACT molecules as well as PKR, ultimately leading to PKR activation (Singh et al. 2009, Singh et al. 2011). Recently, phosphorylation sites of TRBP were identified and phosphorylation at all four sites (S142, S152, S283, S286) has been implicated in TRBP's ability to inhibit PKR, with

unphosphorylated TRBP unable to inhibit PKR activity (Paroo et al. 2009, Nakamura et al. 2015). Thus apoptosis induced by cellular stress is regulated by PACT-TRBP-PKR interactions, with each partner capable of forming heterodimer and homodimer interactions (Singh et al. 2011).

### **1.3 PACT and viral infections**

PACT's function during viral infections was investigated soon after PACT was characterized as a dsRNA-binding protein and it was reported that PACT could act as a positive regulator of type I interferon (IFN) genes during Newcastle Disease Virus infection (Iwamura et al. 2001). It was shown that PACT overexpression lead to enhanced gene expression mediated by IRF3, IRF7, and NFκB motifs in various promoters of innate immune response genes (Iwamura et al. 2001). Only one complete dsRNA binding motif (either M1 or M2) of PACT was necessary for enhanced gene expression (Iwamura et al. 2001). Subsequently, a viral protein Us11 (from Herpes Simplex Virus Type 1) was found to inhibit PACT's ability to activate PKR and decrease apoptosis (Peters et al. 2002). Interestingly, Us11 is unable to dissociate PACT from PKR but binds directly to PKR to inhibit PACT mediated PKR activation (Peters et al 2002).

The first mechanistic insight as to how PACT was altering gene expression during a viral infection did not come until 2011, when PACT was shown to directly enhance the signaling of a cytoplasmic pattern recognition receptor, RIG-I (Kok et al. 2011). Pattern recognition receptors (PRRs) function to detect non-self molecules by recognizing structures conserved among microbial species, called pathogen-associated molecular



patterns (PAMPs) (Takeuchi and Akira 2010). PACT is now known to regulate two of these PRRs, PKR and RIG-I (Patel and Sen 1998, Kok et al. 2011). RIG-I (Retinoic acid inducible gene-1) is a PRR that, like PKR, recognizes dsRNA produced during viral infections (Kok et al. 2011). PACT interacts directly with RIG-I through RIG-I's C-terminal domain (CTD) (Kok et al. 2011) to enhance RIG-I mediated induction of IFN. Thus, PACT is involved in RIG-I induced IRF3 activation as well as in stimulating RIG-I's ATPase/Helicase activity (Kok et al. 2011). PACT dependent increase in RIG-I's IFN inducing ability was seen both in the presence and absence of viral stress (polyI:C viral mimic and Sendai Virus infection) showing that PACT acts as an endogenous activator of RIG-I, similar to its actions on PKR (Kok et al. 2011). In addition, PACT's activation of RIG-I was shown to be independent of Dicer or PKR, further signifying a novel role for PACT during viral infection (Kok et al. 2011).

After it was established that PACT could increase IFN signaling through RIG-I in addition to activating PKR, PACT's association with viral protein Us11 was re-investigated. It was known that Us11 could inhibit IFN signaling through the RIG-I like receptors (RLRs) RIG-I and MDA5 (Xing et al. 2012). Since it was also known that Us11 could inhibit PACT signaling by direct binding to both PACT and PKR, the question arose if Us11 was also inhibiting IFN signaling by inhibiting PACT activation of RIG-I (Peters et al. 2002). Overexpression of Us11 could inhibit RIG-I activated IFN signaling, but only in the presence of PACT as basal RIG-I activity was unaffected by Us11 (Kew et al. 2013). PACT and Us11 were found to interact directly *in vitro* as well as co-fractionate from HSV-1 infected cells without involvement of an RNA molecule acting as a bridge (Kew et

al. 2013). Interaction of Us11 with PACT blocked its interaction with RIG-I, inhibiting downstream IFN production (Kew et al. 2013). Additional virally encoded proteins were also found to inhibit PACT's ability to activate RIG-I, including Ebola virus protein VP35 (Luthra et al. 2013), Middle East Respiratory Syndrome Coronavirus protein 4a (Siu et al. 2014), and Influenza A Virus proteins NS1 and NS2 (Tawaratsumida et al. 2014). Though most research has pointed to virally encoded proteins inhibiting PACT dependent signaling, Luthra et al. reported that PACT also inhibited Ebola Virus RNA Polymerase activity by disrupting interaction with VP35 and effectively blocking viral replication (Luthra et al. 2013). In addition, it has also been shown that PACT activates RIG-I like receptor MDA5's activity during viral infections (Siu et al. 2014).

An additional aspect of PACT signaling that has been addressed is PACT's ability to activate PKR during viral infections, in particular during HIV infection. PACT is known to activate PKR during multiple cellular stresses in the absence of dsRNA, but the role PACT plays in activating PKR during a viral infection was unknown (Figure 1.2) (Patel and Sen 1998). Initial research on the effect of TRBP (~40% homologous to PACT) on PKR activation in the context of HIV infection suggested that TRBP boosts HIV replication both by directly enhancing expression of TAR-containing viral mRNAs as well as by inhibiting PKR activation caused by TAR RNA that has a stem and loop structure (Daher et al. 2001, Dorin et al. 2003). Subsequently, TRBP was also reported to inhibit PKR both in the presence as well as the absence of a virus through sequestration of PKR's activators, PACT and dsRNA (e.g.TAR) (Figure 1.2) (Daher et al. 2009, Singh and Patel 2012). In the absence of viral infections, this inhibition of PKR activation by TRBP is

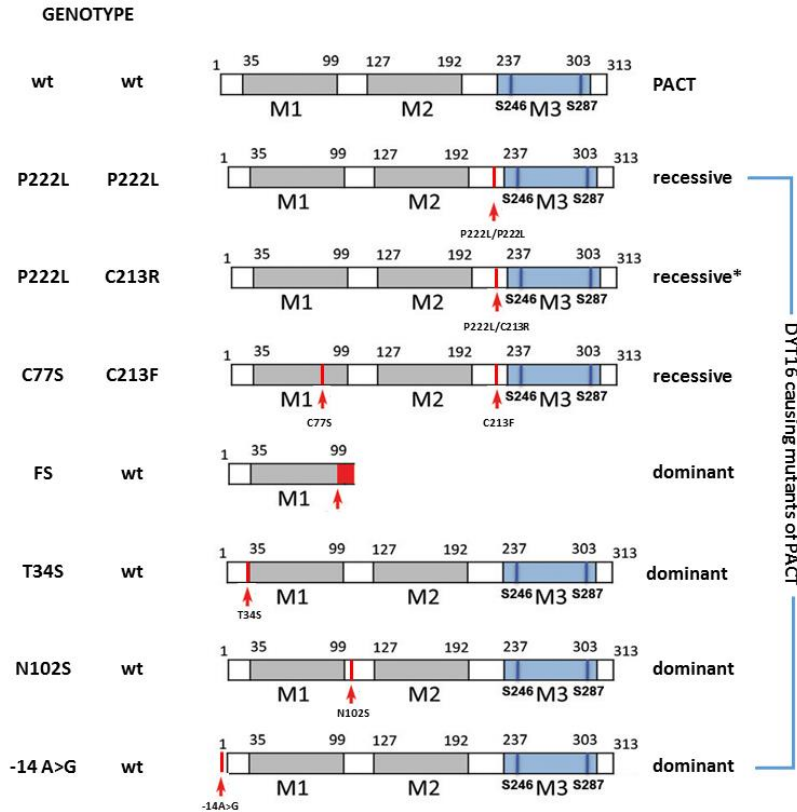
reversed by cellular stress when interactions shift from TRBP-PACT and TRBP-PKR to PACT-PACT and PACT-PKR due to changes in phosphorylation of PACT and TRBP (Daher et al. 2009, Singh et al. 2011, Singh and Patel 2012, Nakamura et al. 2015). Thus, as TRBP inhibits PKR during both viral infection and cellular stress and PACT activates PKR during cellular stress, it was predicted that PACT could also activate PKR during viral stress. However, initial research has shown that PACT is unable to activate PKR during HIV infection and in fact may inhibit PKR activation (Daher et al. 2009, Clerzius et al. 2013, ongoing research by Evelyn Chukwurah in Rekha Patel's lab).

In addition to this, PACT and TRBP also play a role in RNA interference (RNAi) via a direct interaction with Dicer and are believed to maintain fidelity of small RNA processing by properly recruiting miRNA precursors to RNAi machinery (Kok et al. 2007, Lee 2006, Lee et al. 2013, Takahashi et al. 2013, Wilson et al. 2015). While the functions of PACT and TRBP in RNAi often seem redundant, some differences have been identified. These include different binding preferences of the two proteins (siRNA binding versus homodimer formation) as well as size of resulting miRNAs produced by the dicer when associated with PACT versus TRBP (Kok et al. 2007, Lee 2006, Lee et al. 2013, Takahashi et al. 2013, Wilson et al. 2015, Heyam et al. 2015). The overlapping roles of TRBP and PACT in RNAi and antiviral innate immune response are not surprising, as in plants and insects RNAi functions as the main antiviral mechanism.

#### 1.4 PACT and movement disorder dystonia

In 2008, Camargos and colleagues described a recessively inherited form of early-onset dystonia due to a homozygous missense mutation in PACT (termed PRKRA in GenBank) and classified these mutations as DYT16 (Figure 1.3) (Camargos et al. 2008, Klein 2008). The dystonias (DYT1-DYT26) (Peall et al 2015; Mencacci et al. 2015; Bragg et al. 2011) are a heterogeneous group of movement disorders, in which affected individuals develop sustained, painful, involuntary muscle contractions, leading to twisted postures and permanent disabilities (Geyer and Bressman 2006). The mutation identified by Camargos is a point mutation resulting in substitution of a proline for a leucine at amino acid position 222 and is located between the two conserved M1 and M2 dsRNA binding motifs (Camargos et al. 2008, Klein 2008). Initially, seven individuals from two unrelated families in Brazil were diagnosed with dystonia and were identified as having this P222L homozygous mutation, whereas heterozygous family members were unaffected (Camargos et al. 2008). Additional dystonia patients, two brothers from Poland, have since been found to exhibit the same P222L homozygous phenotype as seen in the Brazilian patients (Zech et al. 2014). Soon after the initial mutation was identified, a group in Germany identified a German dystonia patient carrying a novel heterozygous mutation in PACT (Seiber 2008). In this patient, a deletion of two nucleotides (c.266\_267delAT) resulted in a frameshift and an early stop codon, resulting in a truncation of PACT protein after amino acid 88 followed by the 21 amino acids originating from the frameshift that are absent in the endogenous PACT protein (Figure 1.3) (Seibler et al. 2008).

A . PACT mutations identified in DYT16 dystonia patients



B. Sequence alignment of frameshift PACT mutation with M1 domain of PACT

```

ATG TCC CAG AGC AGG CAC CGC GCC GAG GCC CCG CCG CTG GAG CGC GAG GAC AGT 54
M S Q S R H R A E A P P L E R E D S>
GGG ACC TTC AGT TTG GGG AAG ATG ATA ACA GCT AAG CCA GGG AAA ACA CCG ATT 108
G T F S L G K M I T A K P G K T P I>

CAG GTA TTA CAC GAA TAC GGC ATG AAG ACC AAG AAC ATC CCA GTT TAT GAA TGT 162
Q V L H E Y G M K T K N I P V Y E C>
GAA AGA TCT GAT GTG CAA ATA CAC GTG CCC ACT TTC ACC TTC AGA GTA ACC GTT 216
E R S D V Q I H V P T F T F R V T V>
GGT GAC ATA ACC TGC ACA GGT GAA GGT ACA AGT AAG AAG CTG GCG AAA CAT AGA 270
G D I T C T G E G T S K K L A K H R>
CAG AGC
Q S

GCT GCA GAG GCT GCC ATA AAC ATT TTG AAA GCC AAT GCA AGT ATT TGC TTT GCA 324
A A E A A I N I L K A N A S I C F A>
TGC AGA GGC TGC CAT AAA CAT TTT GAA AGC CAA TGC AAG TAT TTG CTT TGC AGT
C R G C H K H F E S Q C K Y L L C S>

GTT CCT - wt sequence Continued till nucleotide 940 (PACT 313)|
V P
TCC TGA - frameshift mutation produces a truncated PACT protein (PACT88-21)
S *

```

**Figure 1.3: A. DYT16 Mutations.** Schematic representation of DYT16 dystonia mutations. \*unknown currently if C213R is recessive or dominant as this was a *de novo* mutation, not inherited. **B. Frameshift DYT16 nucleotide sequence aligned to wt PACT.** Alignment of frameshift DYT16 mutant with wtPACT showing two nucleotide (AT) deletion (bold and underlined). The resulting frameshift introduces 21 new amino acids (red) and an early stop codon producing a truncation.

Recently, an American dystonia patient was found to be heterozygous for the P222L mutation identified in the Brazilian and Polish patients in combination with a new mutation C213R (Lemmon et al. 2013). This patient inherited the P222L mutation from his unaffected mother, though the second mutation, C213R, appears to be a de novo event, as it was not found in either parent (Lemmon et al. 2013). The same group who identified the Polish patients with the P222L/P222L genotype, performed additional screening of dystonia patients' genotypes and were able to identify three new mutations, each identified currently only in a single patient, and surprisingly associated with a dominant inheritance (Zech et al. 2014). Two of the dominant mutations were within the coding region, N102S and T34S, and the third patient's mutation maps in the 5' UTR -14A>G (Zech et al. 2014). Last, an additional Brazilian patient was identified exhibiting two new mutations, C213F and C77S (de Carvalho Aguilar et al. 2015). This patient shows a pattern of recessive inheritance similar to the initial mutations, as heterozygous family members (for both mutations) are unaffected (de Carvalho Aguilar et al. 2015). While initially the link between PACT and dystonia seemed tentative, with the additional mutations (8 total) found only in dystonia patients as well as the global incidence (at least 4 countries, representing 3 continents), the causal link between PACT and dystonia DYT16 has now solidified. Further emphasizing this, is that none of these sequence variations were found in control samples obtained from the 1000 Genomes project, the National Heart, Lung, and Blood Institute Exome Sequencing Project (NHLBI-ESP), or dsSNP137 (a public-domain archive for a broad collection of simple genetic polymorphisms), as well as being absent in 2002 in house exomes at the Technische

Universität München and in the 376 controls used for that particular study (Zech et al. 2014).

Although additional roles for PACT in development and disease have been indicated, they have not been well defined. PKR has been identified to be overactive in many neurodegenerative diseases including Alzheimer's, where a possible involvement of PACT as the endogenous PKR activator has been suggested. (Onuki et al. 2004). Staining of Alzheimer's disease brains show increased co-localization of PACT and active p-PKR (Paquet et al. 2012). PACT has also shown to be important for migration of cerebellar granule neurons in the developing cerebellum. In addition, PACT is involved in post-natal pituitary development and differentiation, as well as skull and ear development based on study of PACT null mice and in mice with a missense point mutation (Yong et al. 2015, Rowe et al. 2006, Dickerman et al. 2006, Peters et al. 2009; Bennett et al. 2008) Depletion of PACT has also been shown to results in defective neuronal development in *Drosophila* (May 2008). These studies indicate the possibility of additional roles that PACT in neuronal development and disease, though currently the only direct link identified between PACT function and disease is within the context of dystonia.

### **1.5 Structure of Dissertation**

Chapter 2 of this dissertation focuses on examining PKR's ability to respond to cellular stress in a neuroblastoma cell line. This was addressed by establishing a human neuroblastoma cell line SK-N-SH that stably overexpresses the trans-dominant negative mutant of PKR. The level of apoptosis was then measured in this cell line compared to

the control SK-N-SH cells stably integrated with the empty vector at various time points after tunicamycin induced endoplasmic reticulum (ER) stress. The results showed a significant decrease in apoptosis in cells expressing trans-dominant negative PKR mutant, establishing that PKR signaling during ER stress regulates apoptosis in neuronal cells. This establishes the ubiquitous nature of the PKR stress response pathway and indicates a potential for altered stress response in neurons as a possible mechanism for DYT16 PACT mutations leading to neuronal abnormalities.

Chapter 3 investigates the changes in cellular stress response caused by the dystonia causing point mutation P222L in PACT. We investigated differences in the ability of cells carrying the P222L mutation to respond to stress as compared to wt cells. Lymphoblasts derived from patients bearing the P222L homozygous mutations exhibited enhanced apoptosis in response to ER stress as compared to wt lymphoblasts. This enhanced apoptotic response resulted from increased interactions of P222L protein with TRBP thereby leading to a slower kinetics of PKR activation following stress. In addition, P222L mutation also increased PACT-PACT homodimer interactions as well as PACT-PKR heterodimer interactions resulting in a delayed but more robust and sustained PKR activation also contributing to enhanced apoptosis. This work highlights the importance of regulating the speed and duration of PKR activation and eIF2 $\alpha$  phosphorylation in determining cellular fate as well as presenting a cellular consequence of one of the dystonia causing point mutations.

Chapter 4 investigates the role of TRBP in RIG-I mediated induction of interferon production during viral stress and examines any difference from the established role of



PACT in RIG-I signaling. To address the potential role of TRBP in RIG-I signaling, a transient overexpression system was used in the human embryonic kidney cell line HEK293T with an interferon  $\beta$  promoter driven luciferase reporter. The dsRNA viral mimics polyI:C and 5'pppdsRNA were used to induce viral stress in the transfected HEK293T cells where the resulting levels of IFN $\beta$  promoter driven luciferase activity could be measured. The results showed that TRBP is able to inhibit RIG-I induced IFN production, at least in part, by directly inhibiting RIG-I signaling during both polyI:C and 5'ppp dsRNA viral stress. This work establishes the functional interplay between the dsRNA-binding proteins PACT and TRBP in regulation of RIG-I like receptors and downstream interferon production with implications on viral susceptibility, disease progression, and antiviral immunity.

Chapter 5 provides overall conclusions of this dissertation.

CHAPTER 2: INHIBITION OF PKR PROTECTS AGAINST TUNICAMYCIN-INDUCED APOPTOSIS IN  
NEUROBLASTOMA CELLS<sup>1</sup>

---

<sup>1</sup>Vaughn LS, Snee BM, and Patel RC. 2014 *Gene*. 536(1):90-6  
Reprinted here with permission from publisher.

## 2.1 Abstract:

Endoplasmic reticulum (ER) dysfunction is thought to play a significant role in several neurological disorders, including Alzheimer's disease, Parkinson's disease, Huntington's disease, multiple sclerosis, amyotrophic lateral sclerosis, cerebral ischemia, and the prion diseases. ER dysfunction can be mimicked by cellular stress signals such as disruption of calcium homeostasis, inhibition of protein glycosylation, and reduction of disulfide bonds, which results in accumulation of misfolded proteins in the ER and leads to cell death by apoptosis. Tunicamycin, which is an inhibitor of protein glycosylation, induces ER stress and apoptosis. In this study, we examined the involvement of double stranded (ds) RNA-activated protein kinase PKR in tunicamycin-induced apoptosis. We used overexpression of the trans-dominant negative, catalytically inactive mutant K296R to inhibit PKR activity in neuroblastoma cells. We demonstrate that inhibition of PKR activation in response to tunicamycin protects neuronal cells from undergoing apoptosis. Furthermore, K296R overexpressing cells show defective PKR activation, delayed eIF2 $\alpha$  phosphorylation, dramatically delayed ATF4 expression. In addition, both caspase-3 activation and C/EBP homologous protein (CHOP, also known as GADD153) induction, which are markers of apoptotic cells, are absent from K296R overexpression cells in response to tunicamycin. These results establish that PKR activation plays a major regulatory role in induction of apoptosis in

response to ER stress and indicates the potential of PKR as possible target for neuroprotective therapeutics.

## **2.2 Introduction:**

Several chronic neurodegenerative diseases such as Alzheimer's, Parkinson's, Huntington's and Amyotrophic lateral sclerosis (ALS) exhibit abnormally folded proteins that aggregate and accumulate in neurons (Soto 2003; Ross and Poirier 2004). Presence of these aggregated proteins is closely related to initiation and progression of such neurodegenerative diseases. In recent years it has become clear that endoplasmic reticulum (ER) stress is also associated with neuronal death and contributes to the disease pathology (Doyle et al. 2011; Hoozemans and Scheper 2012). Depletion of calcium stores from ER lumen, inhibition of protein glycosylation, reduction of disulfide bonds, expression of mutated proteins, ischemic insults cause accumulation of misfolded or unfolded proteins in the ER and trigger activation of the ER stress pathway (Hetz 2012). ER stress response is a compensatory pathway that involves unfolded protein response (UPR), which is mediated by generalized suppression of protein synthesis via phosphorylation of initiation factor eIF2 $\alpha$ , increased expression of molecular chaperones to assist protein folding, and ER associated degradation of misfolded proteins (Walter and Ron 2011). These protective responses function to control the accumulation of misfolded proteins in the ER transiently, but sustained ER stress leads to apoptosis with characteristic nuclear chromatin condensation, DNA fragmentation, and shrinkage of cell bodies (Gorman et al. 2012; Stefani et al. 2012).

Although phosphorylation of eIF2 $\alpha$  causes a general block in translation, it paradoxically activates translation of the ATF4 mRNA (Donnelly et al. 2013), which encodes a transcription factor that binds to and activates the C/EBP homologous protein (CHOP) promoter (Tabas and Ron 2011). Thus, the expression of the transcription factor CHOP, also known as GADD153 is induced in response to eIF2 $\alpha$  phosphorylation (Oyadomari and Mori 2004; Wek et al. 2006). Cells lacking CHOP are significantly protected from ER stress induced apoptosis and thus CHOP is thought to be one of the major inducers of apoptosis in response to ER stress (Zinszner et al. 1998; Oyadomari et al. 2002).

PKR (protein kinase, RNA activated) is an interferon (IFN)-induced, double-stranded RNA activated serine-threonine protein kinase that plays a pro-apoptotic role during prolonged ER stress (Shimazawa and Hara 2006; Singh et al. 2009; Nakamura et al. 2010). Most of the early work on PKR elucidated its function in the IFN regulated antiviral pathways (Katze 1995). However, PKR also plays a central role in inducing apoptosis in response to cellular stress (Williams 1999). Activation of PKR's catalytic activity requires the binding of one of its activators also leading to PKR autophosphorylation (Sadler and Williams 2007). There are two possible activators of PKR; double-stranded (ds) RNA, produced during viral infections (Garcia et al. 2007), and the protein activator PACT, which is the only known cellular protein that activates PKR (Patel and Sen 1998). Although recombinant PACT protein can activate PKR by a direct interaction *in vitro*, PACT-dependent PKR activation in cells occurs only in response to a stress signal (Ito et al. 1999; Patel et al. 2000; Bennett et al. 2006; Singh et al. 2009). PACT is phosphorylated in response to stress signals leading to its increased association

with and consequent catalytic activation of PKR (Patel et al. 2000; Singh et al. 2009). Activated PKR phosphorylates the translation initiation factor eIF2 $\alpha$ , which results in an inhibition of protein synthesis and subsequent apoptosis (Patel et al. 2000). Our work has previously established that PACT-induced PKR activation in response to ER stress is essential for induction of apoptosis in neuronal cells (Singh et al. 2009). We demonstrated that PACT is phosphorylated in response to ER stressor tunicamycin (inhibitor of protein glycosylation) in neuroblastoma cells and is responsible for PKR activation by direct interaction. Furthermore, PACT as well as PKR null fibroblasts are markedly resistant to tunicamycin. Reconstitution of PKR and PACT expression in the null cells renders them sensitive to tunicamycin, thus demonstrating that PACT-induced PKR activation plays an essential function in induction of apoptosis.

Substantial evidence correlating presence of activated PKR with neurodegenerative disease pathology exists from studies performed on human brain tissue (Chang et al. 2002; Hugon et al. 2009). In the present study we investigated if inhibition of PKR activation would protect the neuronal cells from apoptosis in response to ER stress. We established neuroblastoma cell lines that overexpress PKR's catalytically inactive mutant K296R. The K296R mutation, which substitutes an arginine for lysine at position 296 within the catalytic subdomain II of PKR destroys its kinase activity (Ortega et al. 1996). It is well established that K296R prevents PKR activation in cells by direct interaction and heterodimer formation as well as by competition for activating molecules (Thomis and Samuel 1995). Our results indicate that K296R overexpressing cells are resistant to apoptosis in response to ER stressor tunicamycin.

Furthermore, this resistance can be attributed to a lack of PKR activation, delayed eIF2 $\alpha$  phosphorylation, and a lack of ATF4 and CHOP induction. These results support the idea that inhibition of PKR activity could be explored as a therapeutic option for neurodegenerative conditions.

## 2.3 Materials and Methods

### *Reagents, Cells, and Antibodies*

SK-N-SH cells were cultured in Dulbecco's modified Eagle's medium (DMEM) containing 10% fetal bovine serum and penicillin/streptomycin. The reagents used were as follows: tunicamycin (Santa Cruz), phosphatase Inhibitor cocktail (Sigma), pIRESpuro2 plasmid (Clontech), DAPI nuclear stain (Sigma). The following antibodies were used: Anti-Flag monoclonal M2 (Sigma A8592), Anti-PKR (human) monoclonal (71/10, R & D systems), Anti-phospho-PKR (Thr451) (Cell Signaling, 3075), Anti-eIF2 $\alpha$  (Invitrogen, AH01182), Anti-phospho-eIF2 $\alpha$  (ser51) (Epitomics, 1090-1; Cell Signaling, 9721), Anti-ATF4 (Santa Cruz, sc-200), and caspase-3 (Santa Cruz H-277).

### *DNA fragmentation analysis*

DNA fragmentation analysis was performed as described before (Singh et al. 2009).

Equal numbers of EV and K11 SK-N-SH cells were treated with either 2  $\mu\text{g}/\text{ml}$  or 5  $\mu\text{g}/\text{ml}$  tunicamycin for 72 hours. Adherent and non-adherent (apoptotic) cells in culture medium were harvested and washed twice with ice cold 1X PBS solution. Cells were then lysed in 100  $\mu\text{l}$  lysis buffer (10mM Tris-HCl pH 7.5, 10mM EDTA, 0.5% Triton X-100)

on ice for 5 minutes. Lysate was centrifuged at 13,000 xg for 5 minutes; supernatant was treated with proteinase K at 37°C for 1 h (1mg/ml). Nucleic acids were precipitated with 300 µM NaCl and 50% isopropanol at -20°C for at least an hour. Precipitates were collected at 13,000 xg for 5 minutes and the resulting pellet was left to air dry. Pellet was then re-suspended in modified TE buffer (10mM Tris-HCl pH 7.5, 10mM EDTA), treated with RNase A (20µg/ml) at 37°C for 30 min. The resulting DNA preparation was run and analyzed on a 1.5% agarose gel.

#### *DAPI staining*

After treatment with 5 µg/ml tunicamycin for indicated period of time, cells were washed twice with 1X PBS, then fixed in a 1:1 solution of methanol:acetone for 1 min. The fixative was washed with ice cold 1X PBS. DAPI stain (4,6-diamidino-2-phenylindole) at 0.5 µg/ml in PBS was placed onto the cells for 5 minutes at room temperature in the dark. After incubation, the cells were rinsed once with 1X PBS, and viewed under the fluorescence microscope and counted as live or apoptotic. % apoptotic cells were calculated using the formula, % apoptosis = (fluorescent dead cells/total fluorescent cells) X 100.

#### *Western Blot analysis*

Cells were treated with tunicamycin and harvested at indicated time points. Cells were collected, washed with two washes with ice cold 1X PBS. Harvested cells were lysed in western lysis buffer (2% Triton X-100, 20mM Tris-HCl pH 7.5, 100mM KCl, 200mM NaCl,



4mM MgCl<sub>2</sub>, Glycerol 40%, phosphatase inhibitor cocktail (Sigma) 1:100) for 5 minutes on ice. Lysate was centrifuged at 13,000 xg for 2 minutes. Protein concentration in the supernatant was quantified Bradford reagent. For the analysis of eIF2 $\alpha$  phosphorylation 25  $\mu$ g of the total protein was analyzed and for PKR phosphorylation, ATF4, and CHOP 50  $\mu$ g of the total protein was analyzed by western blot analysis.

#### *PKR kinase activity assay*

PKR activity assays were performed using an anti-PKR monoclonal antibody (R & D system; 71/10). EV and K11 cells were harvested when they were at 70% confluency. Cells were washed in ice-cold PBS and collected by centrifugation at 600 xg for 5 min. Cell extracts were prepared in lysis buffer (20 mM Tris-HCl pH 7.5, 5 mM MgCl<sub>2</sub>, 50 mM KCl, 400 mM NaCl, 2 mM DTT, 1% Triton X-100, 100 U/ml aprotinin, 0.2 mM PMSF, 20% glycerol). A 100  $\mu$ g aliquot of total protein was immunoprecipitated using anti-PKR monoclonal antibody (71/10) in high salt buffer (20 mM Tris-HCl pH 7.5, 50 mM KCl, 400 mM NaCl, 1 mM EDTA, 1 mM DTT, 1% Triton X-100, 100 U/ml aprotinin, 0.2 mM PMSF, 20% glycerol) at 4°C for 30 min on a rotating wheel. Then 20  $\mu$ l of Protein A-agarose beads were added and incubation was carried out for a further 1 h. The Protein A-agarose beads were washed four times in 500  $\mu$ l of high-salt buffer and twice in activity buffer (20 mM Tris-HCl pH 7.5, 50 mM KCl, 2 mM MgCl<sub>2</sub>, 2 mM MnCl<sub>2</sub>, 0.1 mM PMSF, 5% glycerol). The PKR assay was performed with PKR still attached to the beads in activity buffer containing 0.1 mM ATP and 1  $\mu$ Ci of [ $\gamma$  <sup>32</sup>P] ATP at 30°C for 10 min. The standard activators of the enzyme were 1  $\mu$ g/ml of polyI:polyC (dsRNA) or 0.116 pmol of pure

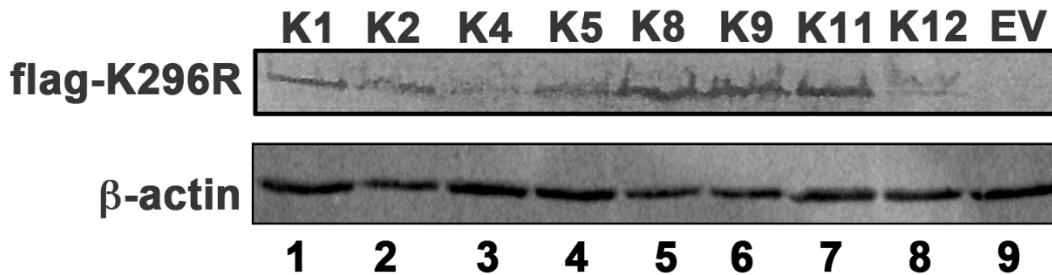
recombinant PACT protein. Labeled proteins were analyzed by SDS-PAGE on a 12% gel followed by autoradiography.

## 2.4 Results

### *Generation of K296R overexpressing SK-N-SH cell lines:*

In order to develop a system to test the effects of inhibition of PKR's kinase activity, we generated SK-N-SH lines that carried PKR's dominant negative mutant K296R stably integrated into the genome. SK-N-SH cells constitutively express a low level of endogenous wild type PKR. The flag epitope tagged mutant K296R reading frame was cloned into a bicistronic vector, pIRESpuro2. This allowed for high efficiency selection for a stable integration of the gene of interest. In this expression vector, K296R is cloned as a first reading frame and puromycin resistance marker for selection is expressed from a second, downstream reading frame. The presence of an internal ribosome entry site (IRES) element between the two reading frames allows for expression of K296R and puromycin resistance marker from the same mRNA molecule, thereby increasing the efficiency of isolating of clones that express the gene of interest among the puromycin resistant clones. Total 8 clones were expanded and analyzed for Flag-K296R PKR expression. As seen in Fig. 2.1 A, the western blot analysis showed expression of flag-K296R protein to different levels in various clones (lanes 1-8). The cells stably transfected with the empty vector (EV) pIRESpuro2 did not express any FLAG K296R (lane 9). Clone K11, which showed expression of flag-K296R at a high level was selected for further analysis of ER stress induced apoptosis. To ensure that

### A. western blot



### B. kinase assay

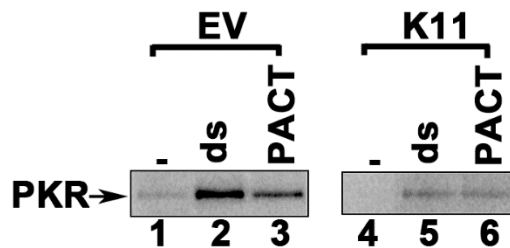


Fig. 1

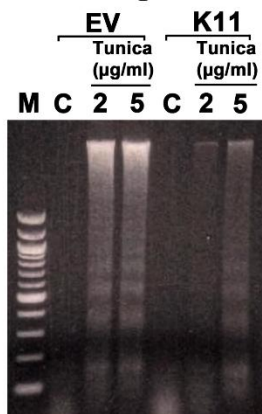
**Figure 2.1: Overexpression of K296R mutant inhibits PKR activity in SK-N-SH cells. A. Establishment of stable SK-N-SH lines overexpressing dominant negative K296R mutant PKR.** pIRESpuro2 empty vector (EV) and FLAG-K296R/pIRESpuro2 transfected (K1- K12) puromycin resistant clones were isolated and expanded. Expression of FLAG-K296R was verified by western blot analysis of 50  $\mu$ g total protein with anti-flag antibody. Monoclonal anti- $\beta$ -actin antibody was used on the same blot ensure all lanes were loaded equally. **B. Kinase activity assay.** PKR immunoprecipitated from EV or K11 cell extracts was activated by the addition of dsRNA or purified recombinant PACT. PKR activators were added as follows- Lane 1 and 4: no activator; Lane 2 and 5: 1  $\mu$ g/ml polyI.polyC; lane 3 and 6: 4 ng of pure PACT protein. Position of autophosphorylated PKR is indicated by an arrow.

overexpression of K296R does inhibit PKR activation in K11 cells, we performed a PKR kinase activity assay with extracts prepared from EV and K11 cells. As seen in Fig. 2.1 B, extract from EV cells showed a low level of PKR kinase activity in the absence of any activator (lane 1) and showed a robust activation in the presence of dsRNA and PACT (lanes 2 and 3). In contrast to this, extract from K11 cells showed undetectable levels of PKR kinase activity in the absence of activator (lane 4) and showed significantly reduced kinase activity in the presence of dsRNA as well as PACT (lanes 5 and 6). These results establish that an overexpression of K296R inhibits PKR activity in K11 cells very efficiently.

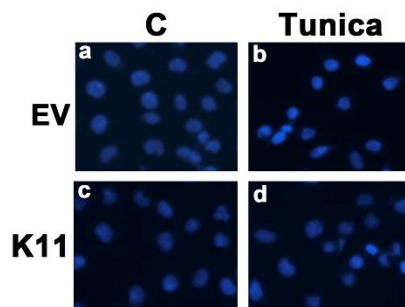
#### *Overexpression of K296R protects cells from tunicamycin-induced apoptosis*

In order to test the effect of K296R overexpression, we compared apoptosis of EV and K11 cells in response to tunicamycin treatment, which induces ER stress by blocking protein glycosylation in the ER. The progression of apoptosis was monitored by DNA fragmentation analysis 72 hours after tunicamycin treatment. Late apoptosis is associated with fragmentation of chromosomal DNA into multiples of the nucleosomal units, known as DNA laddering (Yeung 2002). As seen in Fig. 2.2 A, the EV cells show distinct fragmentation of DNA after 72 treatment at both 2  $\mu\text{g/ml}$  and 5  $\mu\text{g/ml}$  tunicamycin. In contrast, there is little or no DNA fragmentation seen with 2  $\mu\text{g/ml}$  tunicamycin treatment and only very slight fragmentation seen with 5  $\mu\text{g/ml}$  tunicamycin in the K11 cells. These results indicate that the K11 SK-N-SH cells are markedly resistant to apoptosis in response to tunicamycin treatment.

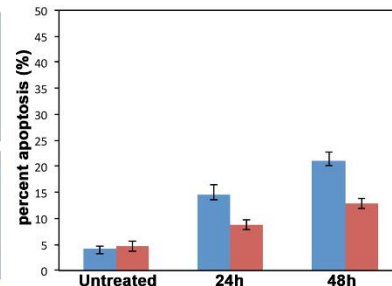
### A. DNA fragmentation



### B. DAPI staining



### C. percent apoptosis



### D. Caspase-3 activation

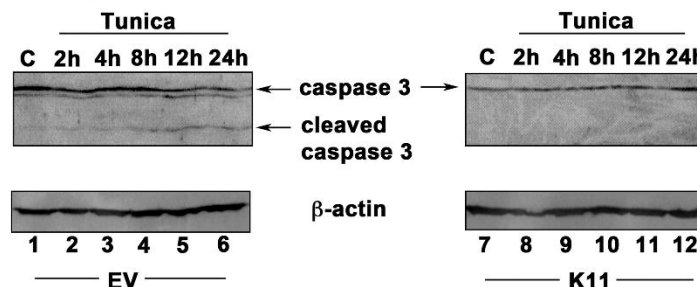


**Fig. 2**

**Figure 2.2: Inhibition of PKR activity reduces apoptosis in response to tunicamycin. A. DNA Fragmentation analysis.** EV and K11 were treated with either 2 µg/ml or 5 µg/ml tunicamycin as indicated for 72 h. The DNA fragmentation was analyzed 72 hours after treatment. Cell type and treatment concentration is indicated on top. C indicates untreated control cells and M indicates 100 bp ladder DNA size markers. **B. Chromatin condensation analysis.** EV and K11 were treated with 5 µg/ml tunicamycin for 24 h or 48 h, the data shown is from 24 h treatment samples. At the end of treatment period the cells were fixed and stained with DAPI nuclear stain. The fluorescent nuclei were analyzed under a microscope. **C. Quantification of chromatin condensation analysis.** Approximately 600 nuclei were counted either as normal or apoptotic based on DAPI intensity and nuclear morphology. Percentage of apoptotic nuclei was calculated and is represented as a bar graph. The error bars represent standard error. **D. Caspase-3 activation analysis.** EV and K11 cells were treated with 2 µg/ml tunicamycin and cell extracts were prepared at indicated times after treatment. Induction of caspase-3 cleavage was examined by western blot analysis with anti-caspase-3 antibody. The same blot was stripped and re-probed with anti-β-actin antibody. The treatment times are indicated on top of lanes and C represents untreated cells.

To further quantify the level of apoptosis in EV versus K11 cells, DAPI staining was performed on fixed cells at 24 and 48 h after tunicamycin treatment to assay for chromatin condensation. Cells were analyzed by looking at morphology of the nucleus. Viable, non-apoptotic cells show a diffuse blue fluorescence of the nucleus and apoptotic cells show nuclei that have intense blue fluorescence, often times these apoptotic nuclei exhibited densely fluorescent lobular appearance. Fig. 2.2 B shows representative images of both EV and K11 cells treated with 5  $\mu\text{g}/\text{ml}$  tunicamycin (Tunica) for 24 h compared to untreated cells (C). In the EV cells, there is a distinct increase in condensed nuclear morphology in response to tunicamycin treatment. In the K11 cells, there are fewer condensed, intensely fluorescent nuclei in the tunicamycin treated sample in comparison with the EV cells. Fig. 2.2 C shows the quantification of the data represented in fig. 2.2 B. More than 600 nuclei for each sample were counted as apoptotic (intense fluorescence) or non-apoptotic (dull, diffused fluorescence). The percentage of apoptotic nuclei was calculated and is represented in the bar graph. As seen in Fig. 2.2 C, tunicamycin treatment showed about 15% apoptosis at 24 h time point in EV cells, which increased further to about 22% at 48 h (blue bars). In contrast to this, K11 cells showed about 8% apoptosis at 24 h and about 13% apoptosis at 48 h (red bars). These results confirm that overexpression of K296R protein protects SK-N-SH cells from apoptosis in response to tunicamycin.

In order to further assay for apoptosis in response to tunicamycin, we studied activation of a well-established apoptosis marker, caspase-3. We assayed for caspase-3 activation using western blot analysis using an antibody that detects both the

procaspase-3 and the active cleaved caspase-3 forms. As seen in Fig. 2.2 D, caspase-3 cleavage product corresponding to active caspase-3 was observed at 12 and 24 h after tunicamycin treatment in EV cells (lanes 5 and 6). In contrast to this, no active caspase-3 cleavage products were detected in K11 cells in response to tunicamycin. These results further confirm that K11 cells are resistant to tunicamycin induced apoptosis.

#### *PKR activation in response to tunicamycin is inhibited in K11 cells*

Our previous work established that PACT is phosphorylated in response to tunicamycin induced ER stress and associates with PKR to activate its kinase activity (Singh et al. 2009). PKR activation in response to tunicamycin leads to phosphorylation of eIF2 $\alpha$ , which signals inhibition of protein synthesis as part of the ER stress response pathway. Thus, we next analyzed PKR activation in response to tunicamycin in K11 and EV cells. A western blot analysis was performed using a threonine 451 phosphospecific PKR antibody that specifically detects the catalytically active PKR. As seen in Fig. 2.3, the EV cells show serine 451 phosphorylation (and therefore activation of PKR) as early as 2 hours after tunicamycin treatment (lane 2) and PKR remains activated at 8 hours after treatment (lane 4). In K11 cells, PKR shows no phosphorylation at any time points and remains inactive even after 8 hours of treatment (lanes 5-8). The same blot was probed with anti-PKR monoclonal antibody to detect total PKR levels in cells, which showed equal amount of total PKR in all lanes of EV and K11. An increased amount of total PKR can be seen in the K11 cells (lanes 5-8), which can be accounted for by the Flag-K296R PKR being overexpressed in these cells in addition to the endogenous PKR. Flag

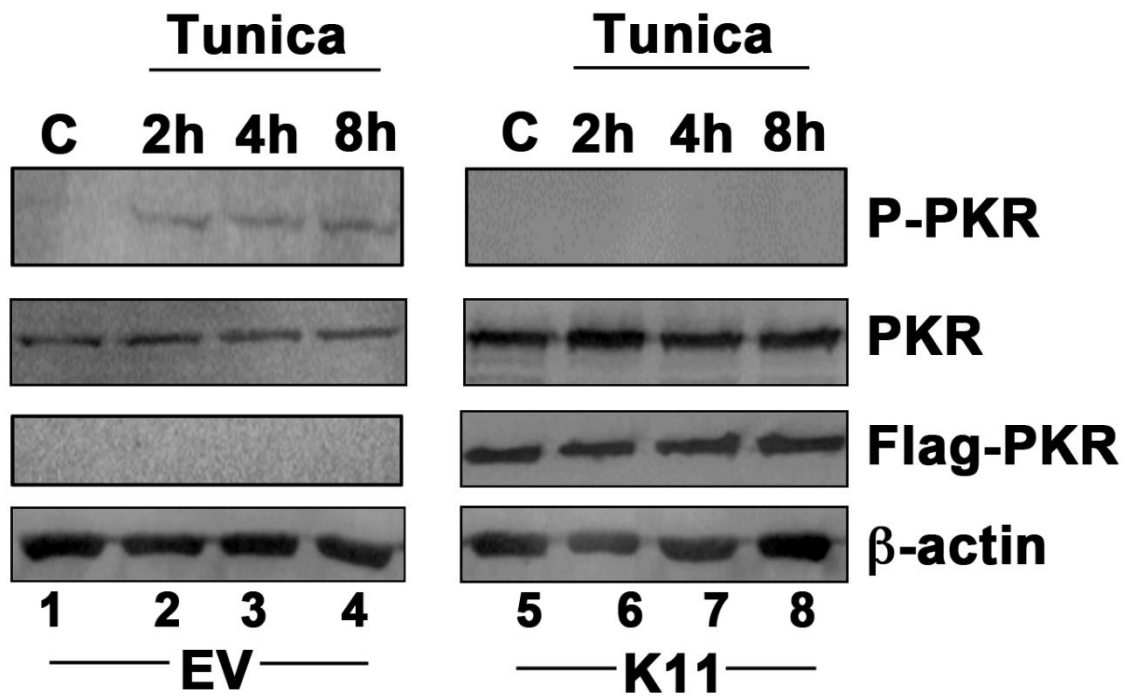


**Fig. 3**

**Figure 2.3: Overexpression of K296R inhibits PKR activation in response to tunicamycin.** EV and K11 cells were treated with 2  $\mu\text{g}/\text{ml}$  tunicamycin and cell extracts were prepared at indicated times after treatment. Phosphorylation of PKR was examined by western blot analysis with a phosphothreonine-451 specific antibody. The same blot was stripped and re-probed with an anti-PKR monoclonal, anti-flag monoclonal, and anti- $\beta$ -actin monoclonal antibodies. The treatment times are indicated on top of lanes and C represents untreated cells.



antibody showed presence of Flag-K296R protein in K11 cells and not in EV cells and  $\beta$ -actin antibody showed equal loading in all lanes.

*eIF2 $\alpha$  phosphorylation in response to tunicamycin is delayed in K11 cells*

To further investigate the effect of PKR inhibition on markers of ER stress response pathway, we investigated the phosphorylation status of eIF2 $\alpha$ . Western blot analysis was performed using a serine 51 phosphospecific anti-eIF2 $\alpha$  antibody. As shown in Fig. 2.4, EV cells have an initial increase in eIF2 $\alpha$  phosphorylation 2 h after tunicamycin treatment (lane 2). Phosphorylation of eIF2 $\alpha$  is maintained until 8 h (lane 4) after treatment and at 12 h it shows a decrease (lane 5) returning to basal levels by 24 h (lane 6). In contrast, the increase in eIF2 $\alpha$  phosphorylation is not seen until 12 hours after treatment (lane 11) in K11 cells. The same blot was probed with anti-eIF2 $\alpha$  antibody to ensure total eIF2 $\alpha$  protein levels remained unchanged and with anti- $\beta$ -actin antibody to ensure equal loading in all lanes.

*Induction of transcription factor ATF-4 in response to tunicamycin is delayed in K11 cells*

One of the consequences of eIF2 $\alpha$  phosphorylation is the induction of ATF-4, which is a transcription factor that plays a central role in promoting apoptosis. We analyzed the expression of ATF-4 in response to tunicamycin in K11 cells. As shown in Fig. 2.5 A, the induction of ATF4 was seen in EV cells at 4 h after treatment (lane 3), with a consistent increase until 24 h after treatment (lanes 4-6). However, K11 cells exhibited a very slight induction of ATF4 at 4 h after treatment (lane 9) with the larger induction

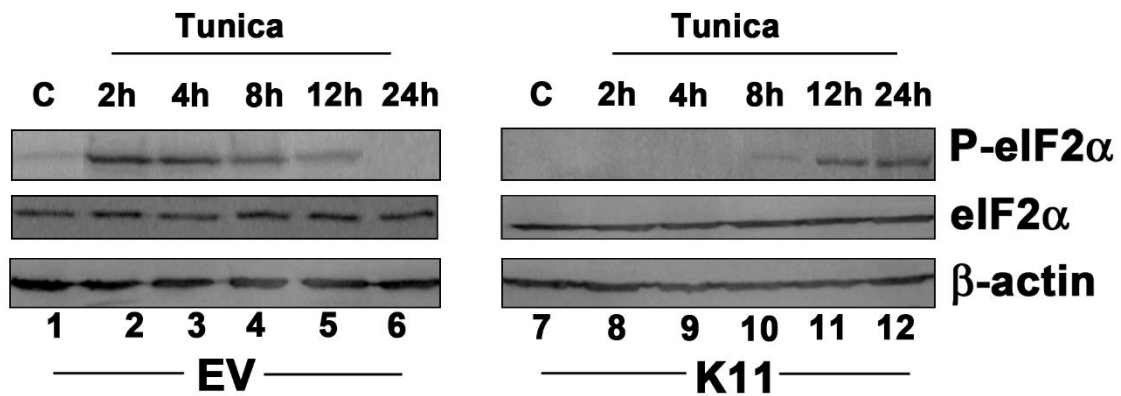


**Fig. 4**

**Figure 2.4: Overexpression of K296R inhibits eIF2 $\alpha$  phosphorylation in response to tunicamycin.** EV and K11 cells were treated with 2  $\mu$ g/ml tunicamycin and cell extracts were prepared at indicated times after treatment. Phosphorylation of eIF2 $\alpha$  was examined by western blot analysis with a phosphoserine-51 specific antibody. The same blot was stripped and re-probed with an anti-eIF2 $\alpha$ , and anti- $\beta$ -actin antibodies. The treatment times are indicated on top of lanes and C represents untreated cells.

being delayed until 24 h after treatment (lane 12). These results indicate that ATF-4 induction is compromised in K11 cells in response to tunicamycin.

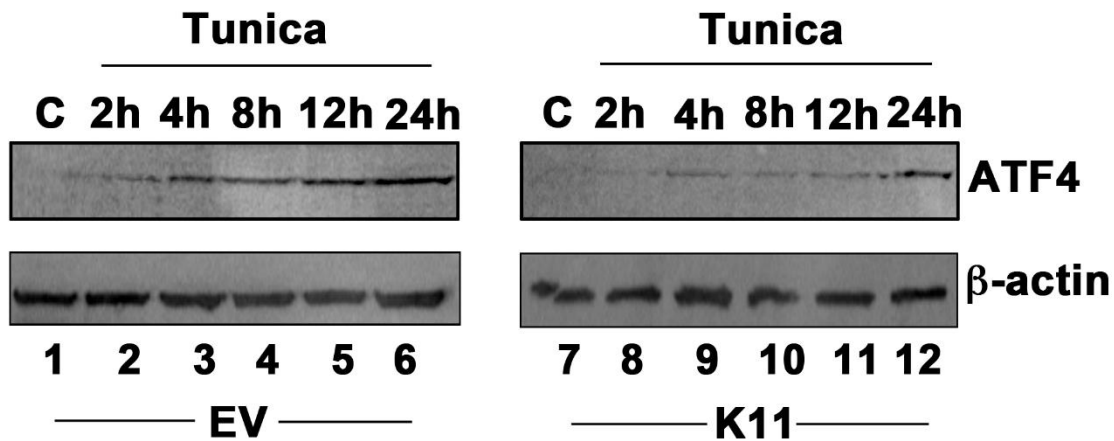
#### *Absence of CHOP induction in response to tunicamycin in K11 cells*

The essential role of transcription factor CHOP in the apoptotic pathway induced by ER stress is unequivocally established. Thus, we compared CHOP induction in response to tunicamycin in EV and K11 cells by western blot analysis. As shown in Fig. 2.5 B, CHOP induction was seen at 8 h and 12 h after tunicamycin treatment in EV cells (lanes 3 and 4) and declined at 24 h after tunicamycin treatment (lane 5). In contrast to this, there was no induction of CHOP expression in response to tunicamycin in K11 cells (lanes 6-10). These results demonstrate that the induction of pro-apoptotic protein CHOP is compromised in K11 cells.

## **2.5 Discussion**

Abnormally folded proteins have been shown to aggregate in neurons in several chronic neurodegenerative diseases and are closely correlated with either the initiation or development of disease symptoms (Aguzzi and O'Connor 2010). The neurodegeneration observed in such diseases is thought to result from ER stress caused by accumulation of misfolded protein aggregates (Rao and Bredesen 2004). One aim of cellular ER stress response is to inhibit protein synthesis globally to cope with folding of accumulated misfolded proteins and that is mainly achieved by phosphorylation of the initiation factor eIF2 $\alpha$  on serine 51 (Wek and Cavener 2007). There are two protein

A.



B.

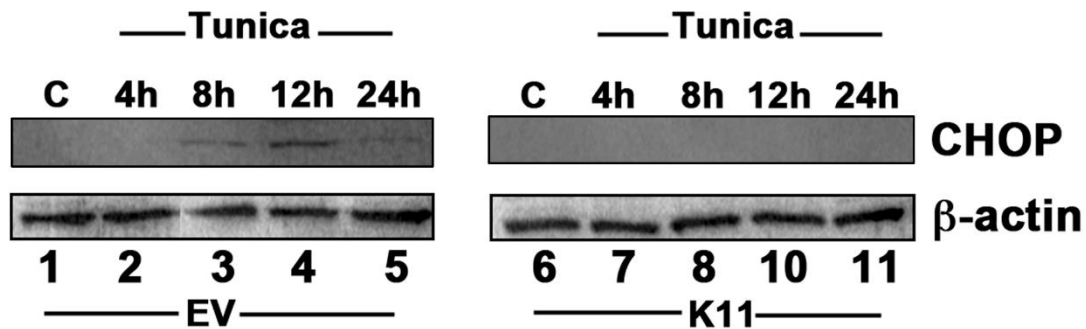


**Fig. 5**

**Figure 2.5: A. Overexpression of K296R inhibits induction of ATF4 in response to tunicamycin.** EV and K11 cells were treated with 2  $\mu$ g/ml tunicamycin and cell extracts were prepared at indicated times after treatment. Induction of ATF4 expression was examined by western blot analysis with anti-ATF4 antibody. The same blot was stripped and re-probed with anti- $\beta$ -actin antibody. The treatment times are indicated on top of lanes and C represents untreated cells. **B. Overexpression of K296R inhibits induction of CHOP (GADD153) in response to tunicamycin.** EV and K11 cells were treated with 2  $\mu$ g/ml tunicamycin and cell extracts were prepared at indicated times after treatment. Induction of CHOP expression was examined by western blot analysis with anti-CHOP antibody. The same blot was stripped and re-probed with anti- $\beta$ -actin antibody. The treatment times are indicated on top of lanes and C represents untreated cells.

kinases that respond to ER stress to phosphorylate eIF2 $\alpha$ ; PKR and PKR-like ER resident kinase (PERK). Phosphorylation of eIF2 $\alpha$  by PERK in response to ER stress is considered a protective response since it attenuates the new protein synthesis and the cells gain time to manage correct folding (Rao and Bredesen 2004) or degrade the accumulated misfolded proteins (Ron and Walter 2007). In accordance with this, homozygous mutations in PERK cause pancreatic beta-cell death and diabetes (Shi et al. 2003; Zhang et al. 2006). Thus, lack of PERK kinase activity and lack of eIF2 $\alpha$  phosphorylation makes the cells more vulnerable to apoptosis in response to ER stress (Harding et al. 2000). In contrast to this, PKR activation by ER stressors such as thapsigargin (which causes Ca<sup>+</sup> release from the ER) or tunicamycin leads to activation of apoptotic pathways (Srivastava et al. 1995; Scheuner et al. 2006). Although the primary result of PKR activation by ER stress is also phosphorylation of eIF2 $\alpha$  on serine-51, the outcome of this event is opposite of PERK activation and leads to cell death by apoptosis. In accordance with this, inhibition of PKR activation in response to ER stress leads to a reduction in apoptosis (Tang et al. 1999; Onuki et al. 2004) and PKR null cells are resistant to ER stress induced apoptosis (Singh et al. 2009). These apparently opposite effects of these two eIF2 $\alpha$  kinases probably arise from phosphorylation of proteins other than eIF2 $\alpha$ .

Previously our work on ER stress has established that PACT mediated PKR activation is essential for tunicamycin-induced apoptosis (Singh et al. 2009). Both PKR and PACT null fibroblasts are markedly resistant to ER stress induced apoptosis. We wanted to explore the requirement of PKR activity in neuronal cell apoptosis in response to ER stress because of its central importance in neurodegenerative diseases. Thus, in

the current study we used a specific inhibitor of PKR to block PKR activation in neuroblastoma cells after inducing ER stress and investigated its effect on neuronal apoptosis. Consistent with our previous observations, our results presented here indicate that inhibition of PKR inhibits apoptosis in neuroblastoma cells. Inhibition of apoptosis by PKR inhibition could be attributed to a lack of ATF4 and consequently CHOP induction. While phosphorylation of eIF2 $\alpha$  reduces the synthesis of a majority of cellular proteins, the translation of mRNAs containing small upstream open reading frames (uORFs) within their 5'UTR is selectively increased (Harding et al. 2000). The mRNA encoding ATF4 transcription factor contains uORFs and thus ATF4 synthesis is upregulated in response to eIF2 $\alpha$  phosphorylation. ATF4 promotes the expression of the proapoptotic transcription factor, CHOP (Fawcett et al. 1999; Harding et al. 2000). CHOP-deficient cells are modestly resistant to ER stress-inducing agents compared to their wild-type counterparts (Zinszner et al. 1998), while enforced CHOP expression sensitizes cells to ER stress (McCullough et al. 2001). Thus, the lack of CHOP induction in K11 cells is consistent with their insensitivity to tunicamycin. Furthermore, a lack of procaspase-3 cleavage to generate the active caspase-3 in K11 cells further establishes that K11 cells are protected from induction of apoptosis in response to tunicamycin.

The link between presence of activated PKR and neurodegeneration has been explored and confirmed for over a decade since the first report showed enhanced levels of activated PKR in brains of patients suffering from Huntington's disease (Peel et al. 2001). This was soon followed by a report establishing increased PKR activation and eIF2 $\alpha$  phosphorylation in Alzheimer's patients' brains, especially in degenerating

hippocampal neurons (Chang et al. 2002). Amyloid- $\beta$  peptide has been shown to induce PKR and eIF2 $\alpha$  phosphorylation in primary neurons and neuroblastoma cells, inhibition of which also blocks neuronal apoptosis (Chang et al. 2002; Suen et al. 2003). Neurons from PKR null mice were resistant to amyloid- $\beta$  toxicity compared to their wt counterparts (Suen et al. 2003). Inhibition of PKR using a randomized ribozyme library could protect SK-N-SH cells from ER stress induced apoptosis, however the mechanism of this protection was not investigated (Onuki et al. 2004). Phosphorylated PKR and eIF2 $\alpha$  co-localize with phosphorylated tau protein in affected degenerating neurons and senile plaques in AD patients as well as in transgenic mouse models (Peel and Bredesen 2003; Page et al. 2006). Elevated levels of active PKR and phosphorylated eIF2 $\alpha$  that correlated with cognitive decline were reported in blood lymphocytes of Alzheimer's patients (Paccalin et al. 2006). Enhanced neuronal immunoreactivity for phosphorylated PKR was seen in extrastriatal brain regions in brains from Parkinson's and Huntington's disease patients (Bando et al. 2005). In case of HIV-infected patients, the neurodegeneration caused by gp120 glycoprotein has been associated with dementia and correlates with PKR induction and activation (Alirezaei et al. 2007). In case of Creutzfeld-Jacob disease the presence of activated PKR in affected brains was reported using an antibody specific for activated PKR (Paquet et al. 2009). Thus, presence of activated PKR correlates well with neurodegeneration and apoptosis seen in various diseases.

In order to further investigate and establish involvement of PKR in neuronal apoptosis seen in various neurodegenerative diseases, it would be of value to test

disease progression in established mouse models of such diseases in either a PKR null background or in the presence of agents that modulate PKR activity. Studies can also be extended in primary cultured neurons established from PKR null mice to test if the lack of PKR protects the neurons from amyloid- $\beta$  toxicity and apoptosis.

Inhibition of PKR activation in response to ER stress thus may be beneficial in preventing apoptosis and neurodegeneration in patients. Inhibition of PKR activity by a small molecule inhibitor oxandol-imidazol compound C16 has been shown to offer protection against apoptosis in neuronal cell cultures (Shimazawa and Hara 2006). Using a different neuroblastoma cell line SH-SY5Y, and employing a pharmacological approach to inhibit PKR activity, these authors demonstrated that PKR activity plays an essential function in induction of apoptosis in response to ER stress. Thus, protection against neuronal apoptosis via use of PKR inhibition has now been tested in two different neuroblastoma cell lines by using different experimental approaches. Our results presented in this paper are obtained by using a specific trans-dominant negative mutant to inhibit PKR activation and thus rules out any non-specific off target effects that chemical inhibitors may exhibit. Indeed, such lack of specificity was recently reported for one of the small molecule inhibitors previously thought to be specific for PKR (Chen et al. 2008). A peptide inhibitor (PRI) of PKR has been described that has not been explored yet for inhibition of ER stress induced apoptosis (Nekhai et al. 2000). Such peptide inhibitors are likely to be more specific in targeting PKR activation as compared to chemical inhibitors. It also remains to be tested if PKR inhibition may relieve neurodegeneration in mouse models of Alzheimer's disease. Our results presented here



demonstrate that PKR inhibition using overexpression of a highly specific trans dominant negative mutant offers protection against neuronal apoptosis and support the idea that PKR may be a good target for drug development for treatment of neurodegenerative diseases.

CHAPTER 3: ALTERED ACTIVATION OF PROTEIN KINASE PKR AND ENHANCED APOPTOSIS IN  
DYSTONIA CELLS CARRYING A MUTATION IN PKR ACTIVATOR PROTEIN PACT<sup>1</sup>

---

<sup>1</sup>This research was originally published in the Journal of Biological Chemistry. Vaughn LS, Bragg DC, Sharma N, Camargos S, Cardoso F, and Patel RC. "Altered Activation of Protein Kinase PKR and Enhanced Apoptosis in Dystonia Cells Carrying a Mutation in PKR Activator Protein PACT." *J Biol Chem.* 2015; 290(37):22543-57. © the American Society for Biochemistry and Molecular Biology. Reprinted here with permission from the publisher.

### 3.1 Abstract

PACT is a stress-modulated activator of the interferon (IFN)-induced double-stranded (ds) RNA-activated protein kinase (PKR). Stress-induced phosphorylation of PACT is essential for PACT's association with PKR leading to PKR activation. PKR activation leads to phosphorylation of translation initiation factor eIF2 $\alpha$  inhibition of protein synthesis, and apoptosis. A recessively inherited form of early-onset dystonia DYT16 has been recently identified to arise due to a homozygous missense mutation P222L in PACT. In order to examine if the mutant P222L protein alters the stress-response pathway we examined the ability of mutant P222L to interact with and activate PKR. Our results indicate that the substitution mutant P222L activates PKR more robustly and for longer duration albeit with slower kinetics in response to the endoplasmic reticulum (ER) stress. In addition, the affinity of PACT-PACT and PACT-PKR interactions is enhanced in dystonia patient lymphoblasts, thereby leading to intensified PKR activation and enhanced cellular death. P222L mutation also changes the affinity of PACT-TRBP interaction after cellular stress, thereby offering a mechanism for the delayed PKR activation in response to stress. Our results demonstrate the impact of a dystonia-causing substitution mutation on stress induced cellular apoptosis.

### 3.2 Introduction

PKR is an interferon (IFN)-induced serine/threonine kinase expressed ubiquitously that mediates IFN's antiviral actions and regulates cellular survival and apoptosis in response to stress (Garcia et al. 2006). PKR's kinase activity requires binding to one of its activators leading to its autophosphorylation and enzymatic activation (Meurs et al. 1990). Double-stranded (ds) RNA, a replication intermediate for several viruses, binds to PKR's two dsRNA-binding motifs (dsRBMs) (Green and Mathews 1992; McCormack et al. 1992; Patel and Sen 1992), and activates PKR by unmasking the ATP-binding site (Nanduri et al. 2000) leading to its autophosphorylation (Cole 2007). The two dsRBMs also mediate dsRNA-independent protein-protein interactions with other proteins that carry similar domains (Patel et al. 1995; Chang and Ramos 2005). Among these are proteins TRBP (human immunodeficiency virus (HIV)-1 transactivation-responsive (TAR) RNA-binding protein) that inhibits PKR activity (Benkirane et al. 1997), and PKR activator protein PACT (Patel and Sen 1998).

PACT's association with PKR activates PKR in the absence of dsRNA (Patel and Sen 1998; Patel et al. 2000). PACT contains three copies of dsRBM (Fig. 3.1 A), of which the two amino-terminal motifs (M1 and M2) bind to the dsRBMs of PKR. The third, carboxy-terminal motif 3 (M3) is dispensable for interaction with PKR but is essential for PKR activation and interacts with a specific region in its kinase domain (Peters et al. 2001; Huang et al. 2002). Although purified, recombinant PACT can activate PKR by direct interaction *in vitro* (Patel and Sen 1998), PACT-dependent PKR activation in cells occurs in response to stress signals (Ito et al. 1999; Patel et al. 2000; Bennett et al. 2006; Singh

et al. 2009) such as arsenite, peroxide, growth factor withdrawal, thapsigargin, and tunicamycin, and leads to phosphorylation of the translation initiation factor eIF2 $\alpha$  and cellular apoptosis (Ito et al. 1999; Patel et al. 2000; Bennett et al. 2006). PACT (and its murine homolog RAX) is phosphorylated in response to stress leading to its increased association with PKR (Ito et al. 1999; Patel et al. 2000; Bennett et al. 2006).

Similar to PACT, TRBP is a dsRNA binding protein but unlike PACT it inhibits PKR. In uninfected cells and in the absence of cellular stress TRBP inhibits PKR by direct binding (Cosentino et al. 1995) and by forming heterodimers with PACT (Daher et al. 2009). Recently we have shown that cellular stress signals cause PACT to dissociate from TRBP leading to PACT-mediated PKR activation. TRBP-PACT heterodimers present in unstressed cells dissociate as PACT is phosphorylated on S287 in M3 in response to oxidative stress, serum starvation and ER stress (Peters et al. 2006; Singh et al. 2011) by a protein kinase yet to be identified. Stress-induced phosphorylation at serine 287 has a dual role in PACT mediated PKR activation as it causes dissociation of PACT-TRBP complex and at the same time increases PACT's affinity for PKR (Singh et al. 2011). Two PACT molecules can also interact via the conserved dsRBMs and phosphorylation of serine 287 enhances PACT-PACT interactions (Singh and Patel 2012). The PACT-PACT homodimers interact strongly with PKR leading to catalytically active PKR. Thus stress-induced phosphorylation of serine 287 of PACT serves to enhance PACT-PACT and PACT-PKR interactions in addition to reducing PACT-TRBP interactions. Consequently, apoptosis in response to stress signals is regulated by various PACT-TRBP-PKR

interactions, with each partner capable of forming homomeric interactions as well as interacting with the other two proteins.

Camargos and colleagues described a recessively inherited form of early-onset generalized dystonia due to a homozygous missense mutation in PACT (PRKRA) (Camargos et al. 2008). The dystonias are a heterogeneous group of movement disorders in which affected individuals develop sustained, often painful involuntary muscle contractions and twisted postures that can have devastating consequences (Geyer and Bressman 2006). For DYT16, the affected members from the two unrelated families have the same P222L mutation in PACT gene (Camargos et al. 2012). This point mutation lies between the conserved motifs M2 and M3 within PACT (Klein 2008). The other mutation reported in PACT that causes dystonia is a frameshift mutation which results in truncation of the protein after 88 amino acids (Seibler et al. 2008). Recently, three more recessive mutations (C77S, C213F, and C213R) were found in DYT16 patients (Brashear 2013; Lemmon et al. 2013; de Carvalho Aguiar et al. 2015). The three most recent mutations reported in Polish and German families (T34S, N102S, and c.-14A>G) indicate a worldwide involvement of PACT (PRKRA) gene in dystonia (Zech et al. 2014).

In spite of the identification of many genetic mutations that lead to dystonia, the molecular mechanisms involved in disease onset or progression have remained largely unknown (Bragg et al. 2011). In this report we have analyzed the effect of P222L mutation on PACT's biochemical properties such as dsRNA binding, PKR interaction, and PKR activation. P222L mutation does not affect PACT's ability to bind dsRNA, or its ability to interact with PKR *in vitro*. However, in mammalian cells the P222L mutant

protein interacts with higher affinity with TRBP, forms homodimers more efficiently, and in response to stress causes a delayed but much prolonged activation of PKR. In accordance to the altered biochemical properties of P222L protein, dystonia patient cells exhibit enhanced apoptosis in response to endoplasmic reticulum (ER) stressor tunicamycin. These results indicate that dystonia-causing PACT mutation alters the kinetics and duration of eIF2 $\alpha$  phosphorylation in response to ER stress and has deleterious implications on cell survival.

### 3.3 Materials and Methods

#### *Reagent, Cell Lines, and Antibodies:*

Patient B-lymphoblast cell lines were cultured in RPMI 1640 medium and HeLa M cells were cultured in Dulbecco's modified Eagle's medium (DMEM), both containing 10% fetal bovine serum and penicillin/streptomycin. The wt and DYT16 dystonia patient lymphoblast cell lines were Epstein Barr Virus (EBV)-transformed to create stable cell lines, as previously described (Anderson and Gusella 1984). The other reagents were as follows: tunicamycin (Santa Cruz), Phosphatase Inhibitor Cocktail (Sigma), The antibodies used are as follows: Anti-flag monoclonal M2 (Sigma A8592), Anti-PKR (human) monoclonal (71/10, R&D Systems), anti-phospho-PKR polyclonal (Thr451) (Cell Signaling, 3075), anti-eIF2 $\alpha$  polyclonal (Invitrogen, AH01182), anti-phospho-eIF2 $\alpha$  (ser51) polyclonal (Epitomics, 1090-1; Cell Signaling 9721), anti-PACT rabbit monoclonal (abcam 75749), and anti-myc monoclonal (Santa Cruz 9E10).

*Generation of P222L substitution mutation:*

Point mutation P222L was generated using a mutagenic primer for PCR amplification to change codon for Proline 222 from CCT to CTT. The primer sequences were as follows:

Upstream mutagenic primer:

5'CCTTGAGGAATTCTCTTGGTGAAAAGATCAAC-3'

Downstream primer:

5'GGGGATCCTTACTTTCTTTCTGCTATTATC-3'

The PCR product was sub-cloned into pGEMT-easy vector (Promega). Once the sequence of the point mutant (P222L) was verified, we generated full-length P222L ORF in pcDNA3.1<sup>-</sup> by a three-piece ligation of XbaI -EcoRI restriction piece from flag-PACT/BSIIKS<sup>+</sup>, EcoRI-BamHI piece from P222L point mutant/pGEMT-easy, and XbaI-BamHI cut pcDNA3.1<sup>-</sup>. The full-length P222L mutant in pcDNA3.1<sup>-</sup> has an amino-terminal flag or myc tag. Full length P222L mutant was sub-cloned into mammalian two-hybrid system vectors and pET15b (Novagen). TRBP constructs were as described before (Singh et al. 2011).

*dsRNA-binding assay:*

The *in vitro* translated, <sup>35</sup>S-labeled PACT proteins were synthesized using the TNT-T7 coupled reticulocyte lysate system from Promega and the dsRNA-binding activity was measured by using the previously established polyI-polyC-agarose binding assay (Patel and Sen 1992; Patel and Sen 1998). 4 µl of *in vitro* translation products were diluted



with 25  $\mu$ l of binding buffer (20 mM Tris, pH 7.5, 0.3 M NaCl, 5 mM MgCl<sub>2</sub>, 1 mM DTT, 0.1 mM PMSF, 0.5% Nonidet P-40, 10% glycerol) and incubated with 25  $\mu$ l of poly(I)-poly(C)-agarose beads at 30 °C for 30 min. The beads were washed 4 times with 500  $\mu$ l of binding buffer and the bound proteins were analyzed by SDS-PAGE and fluorography. For competition assay with soluble ssRNA or dsRNA, 1  $\mu$ g of poly(C) or poly(I)-poly(C) was incubated with the proteins for 15 min at 30 °C before the addition of poly(I)-poly(C)-agarose beads. To ascertain specific interaction between PACT proteins and poly(I)-poly(C)-agarose beads, *in vitro* translated, <sup>35</sup>S-labeled firefly luciferase protein was assayed for binding to the poly(I)-poly(C)-agarose beads using same conditions. The T lanes represent total radioactive proteins in the reticulocyte lysate and B lanes represent the proteins that remain bound to poly(I)-poly(C)-agarose beads after washing. The poly(I)-poly(C)-agarose binding was quantified on Typhoon FLA7000 by analyzing the band intensities in T and B lanes. The percentage of PACT proteins bound to poly(I)-poly(C)-agarose was calculated from these values (% binding = 100 X band intensity in B lane/band intensity in T lane), and was plotted as bar graphs.

*Co-immunoprecipitation with in vitro translated proteins:*

*In vitro* translated, <sup>35</sup>S-labeled PKR and flag epitope-tagged PACT proteins were synthesized using the TNT-T7 coupled reticulocyte system from Promega and the co-immunoprecipitation assay was performed as described before (Patel and Sen 1998).

#### *Co-immunoprecipitation Assay in HeLa cells:*

For PACT/P222L and PKR co-immunoprecipitations, HeLa cells were co-transfected in 6-well culture dishes with 500 ng of flag-PACT/pcDNA3.1<sup>-</sup> or flag-P222L/pcDNA3.1<sup>-</sup> using the Effectene (Qiagen). For PACT/P222L-TRBP, PACT-PACT, and P222L-P222L co-immunoprecipitations, HeLa cells were co-transfected in 6-well culture dishes with 250 ng each of (i) myc-TRBP/pcDNA3.1<sup>-</sup> and flag-wtPACT/pcDNA3.1<sup>-</sup>, (ii) myc-TRBP/pcDNA3.1<sup>-</sup> and flag-P222L pcDNA3.1<sup>-</sup>, (iii) flag-PACT/pcDNA3.1<sup>-</sup> and myc-PACT /pcDNA3.1<sup>-</sup>, and (iv) flag-P222L/pcDNA3.1<sup>-</sup> and myc-P222L /pcDNA3.1<sup>-</sup>. At 24 h post-transfection, co-immunoprecipitations were performed as described before.

#### *PKR kinase activity assays:*

PKR kinase activity assays were performed using HeLa M cell extracts as described before (Patel and Sen 1998; Singh et al. 2011). One  $\mu\text{g/ml}$  of poly(I)·poly(C) was used as the standard activator. Purified PACT or P222L proteins in amounts varying from 50 pg to 100 ng were tested their effect on PKR activity.

#### *DNA Fragmentation analysis:*

DNA fragmentation analysis was performed as described before (Singh et al. 2009).  $5 \times 10^6$  lymphoblast cells established from wt individuals and dystonia patients were treated with 0.5  $\mu\text{g/ml}$  tunicamycin for 48 hours followed by DNA fragmentation analysis. In order to quantify the DNA fragmentation, the fluorescence image was inverted and the total band intensities in the entire lanes were computed with

Imagequant software on Typhoon FLA 7000 phosphorimager (GE Healthcare and Life Sciences) and compared with untreated samples as well as between wt and patient cells. The band intensities in wt untreated samples were considered as 1.0 and fold increases in band intensities with respect to wt untreated samples were calculated and subjected to statistical analysis. A statistical analysis from four different experiments was performed to calculate p values to determine significant differences between wt and patient untreated and treated samples.

*Flow cytometry analysis:*

$5 \times 10^5$  lymphoblast cells established from wt individuals and dystonia patients were treated with 0.5  $\mu\text{g/ml}$  tunicamycin for 48h. After treatment, cells were washed once in 1X PBS, re-suspended in 70% ethanol and kept at  $-20^\circ\text{C}$  overnight. Cells were rinsed with 1X PBS, re-suspended in 0.5 ml 1X PBS, and 1 ml of PC Buffer (50mM  $\text{Na}_2\text{HPO}_4$ , 85mM sodium citrate, 0.1% Triton-X pH7.8) was added drop wise followed by incubation at RT for 35 min. Cells were rinsed with 1X PBS, labeled with propidium iodide (PI) (25  $\mu\text{g/ml}$  PI in PBS, 10  $\mu\text{g/ml}$  RNase A, 0.1% Triton-X) for 30 min. Cell cycle analysis was performed by the Flow Cytometry core at USC School of Pharmacy.

*Caspase 3/7 assay:*

Patient and wt B-lymphoblast cells were plated at  $2 \times 10^5$  and either left untreated or treated with 0.5  $\mu\text{g/ml}$  tunicamycin. Aliquots of untreated and treated cells were collected at indicated time points. After collection, aliquots were mixed with equal parts

of Promega Caspase-Glo 3/7 reagent and incubated for 45 minutes. Luciferase activity was measured with a negative control of cell culture medium alone used to normalize all readings.

*Western Blot analysis:*

Western blot analysis was performed using primary antibodies as described under reagents. Western blots were quantified using Imagequant LAS 4000.

*Expression and purification of recombinant wt PACT and P222L:*

The protein coding regions (wt or P222L mutant) were subcloned into pET15b (Novagen) to generate PACT/pET15b and P222L/pET15b resulting in the in-frame fusion of PACT ORF to the histidine tag. The recombinant proteins were expressed and purified as described (Patel and Sen 1998; Singh et al. 2011)

*Mammalian two-hybrid interaction assay:*

The wt PACT and P222L ORFs were sub-cloned into pSG424 (Addgene) such that it produces an in-frame fusion to GAL4 DBD and in VP16 AD vector pVP16AASV19N (Takacs et al. 1993; Patel et al. 1995) such that it produces an in-frame fusion to VP16 AD. Fusion proteins were tested for interaction in various combinations. COS-1 cells were transfected with 250 ng of each of the three (two test plasmids encoding proteins to be tested for interaction, and reporter plasmid pG5Luc) and 1 ng of pRLNull (Promega) to normalize the transfection efficiencies using Effectene (Qiagen). Cells were

harvested 24 h after transfection and assayed for luciferase activity. Western blot analysis was done using the anti-GAL4 DBD and -VP16 AD antibodies.

#### *Yeast two-hybrid interaction assay:*

PACT and its point mutants were expressed as GAL4 DNA-binding domain fusion proteins from pGBKT7 vector, while PACT and its point mutants, TRBP, and PKR was expressed as GAL4 activation domain fusion proteins from pGADT7 vector. Each pGBKT7 and pGADT7 construct was co-transformed into *S. cerevisiae* strain AH109 (clontech) and selected on double dropout SD minimal medium lacking tryptophan and leucine. Transformation of each of the PACT constructs in pGBKT7 and empty vector pGADT7 served as negative controls. In order to check for the transformants' ability to grow on quadruple dropout histidine, leucine, tryptophan, and adenine-lacking medium, 10  $\mu$ l of serial dilutions (of OD<sub>600</sub> = 10, 1.0, 0.1, 0.01) of an overnight liquid culture were spotted for each of the transformants on quadruple dropout SD medium plates lacking adenine, tryptophan, leucine and histidine containing 25 mM 3-amino-1,2,4-triazole. Plates were incubated for three days at 30°C.

#### *Quantifications and Statistics*

All western blot images and radioactive gel scans (Typhoon FLA7000) were quantified using GE Life Sciences ImageQuant TL software. To determine statistical significance of results of the western blots as well as DNA fragmentation, flow cytometry profiles, and caspase assay a two-tailed Student's T-test was performed,

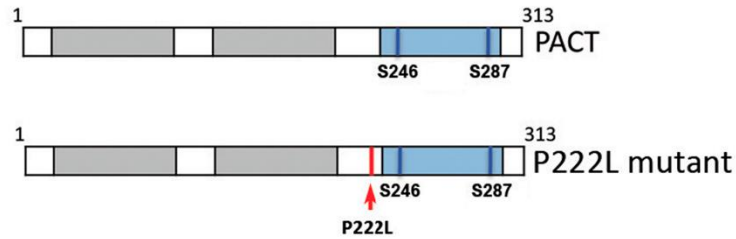
assuming equal variance. Each figure legend indicates p values as denoted by brackets and special characters. Note that our alpha level was  $p=0.05$ .

### 3.4 Results

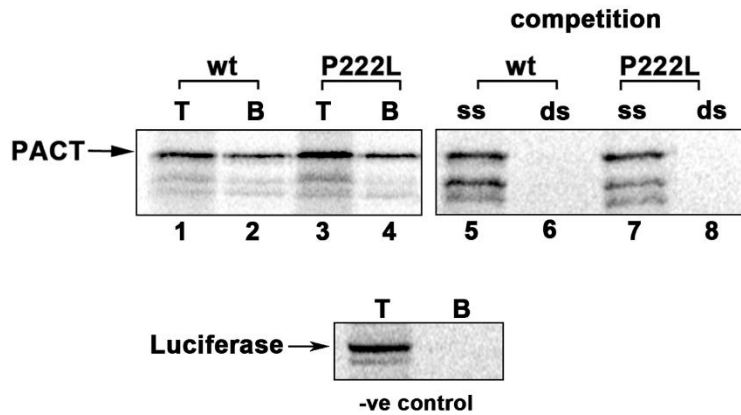
*P222L mutation does not affect PACT's dsRNA binding, but increases interaction with PKR:*

The P222L point mutation is between the conserved M2 and M3 motifs (Fig. 3.1 A). Currently there is no structural information on PACT to predict possible changes due to P222L mutation. In order to determine if the mutation affects PACT's dsRNA binding activity, an *in vitro* dsRNA-binding assay previously well established for PKR and PACT (Patel and Sen 1998) was performed (Fig. 3.1 B and C). As seen in Figure 3.1 B, both the wt PACT (lane 2) and P222L mutant (lane 4) bind to dsRNA. The binding to dsRNA immobilized on the beads could be competed out by exogenously added dsRNA (lanes 6 and 8) but not ssRNA (lanes 5 and 7). Firefly luciferase, a protein that does not bind dsRNA used as a negative control showed no binding to the beads. The quantification of percentage binding indicates that both wt PACT and P222L appear to have a similar affinity for dsRNA under the condition that the assay was carried out (Fig. 3.1 C). We next examined if P222L mutation affects PACT's interaction with PKR using co-immunoprecipitation assays (Fig. 3.2 A and B). <sup>35</sup>S-methionine labeled flag-PACT, flag-P222L mutant, and untagged PKR were *in vitro* translated using rabbit reticulocyte system. The flag-tagged PACT or P222L mutant was immunoprecipitated using anti-flag mAb-agarose and the co-immunoprecipitation of untagged wt PKR was measured. As

### A. PACT substitution mutation identified in dystonia patients



### B. dsRNA binding



### C. % dsRNA binding

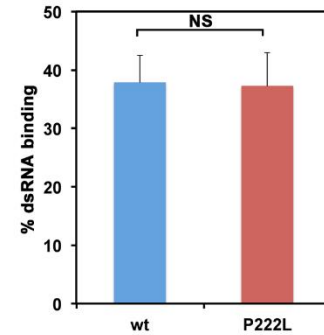


**Figure 3.1: Effect of P222L mutation on dsRNA-binding. (A) Domain structure of PACT.** Grey boxes: dsRNA-binding M1 and M2 motifs, blue box: M3 motif that does not bind dsRNA but is essential for PKR activation. Vertical blue lines: phosphoserines 246 and 287. Red arrow: P222L mutation. **(B) dsRNA-binding assay.** dsRNA-binding activity of wt PACT and P222L was measured by polyI:polyC-agarose binding assay with *in vitro* translated <sup>35</sup>S-labeled proteins. T, total input; B, proteins bound to polyI:polyC-agarose. Competition lanes: competition with 100-fold molar excess of ssRNA (ss) or dsRNA (ds). The bands below the parent PACT bands represent products of *in vitro* translation from internal methionine codons and thus are not produced in similar quantities in all translation reactions and thus are of variable intensity in lanes 1-8. **(C) Quantification of dsRNA-binding assay.** Bands were quantified by phosphorimager analysis and % bound was calculated. Error bars: standard deviation from 3 independent experiments. The p value (0.43) calculated using statistical analyses indicated no significant difference between % dsRNA-binding of wt (blue bar) and P222L mutant (red bar) as indicated by the bracket marked as “NS”.

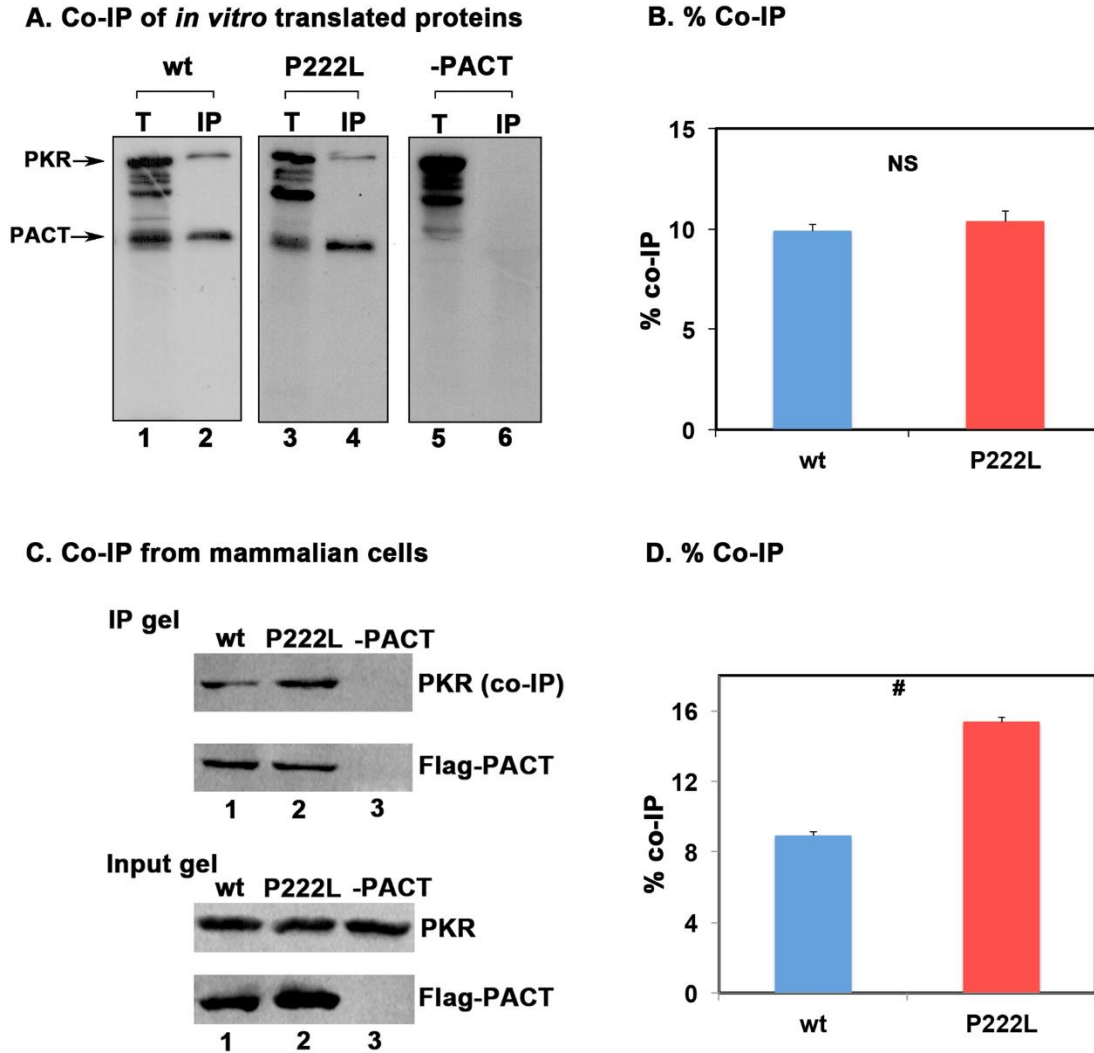


**Figure 3.2: Effect of P222L mutation on PACT-PKR interaction. (A) Co-IP of *in vitro* translated proteins.** 5  $\mu$ l of *in vitro* translated,  $^{35}$ S-labeled flag-tagged wt PACT and P222L proteins were mixed with 5  $\mu$ l of *in vitro* translated,  $^{35}$ S-labeled wt PKR. Flag-PACT proteins were immunoprecipitated using anti-flag mAb-agarose, and wt PKR co-immunoprecipitation was analyzed by SDS-PAGE. T, total input (20% of the IP samples); IP, immunoprecipitates. **(B) Quantification of data in 2 A.** The radioactivity present in the bands was measured by phosphorimager analysis and the % co-IP was calculated as (radioactivity present in the co-immunoprecipitated PKR band/the radioactivity present in the PKR band in the total lane) X 100. This value was normalized to the amount of radioactivity present in the PACT bands in IP lanes to correct for differences in translation/immunoprecipitation. Error bars: standard deviation from 3 independent experiments. The p value (0.391) calculated using statistical analyses indicated no significant difference between % co-IP of wt (blue bar) and P222L mutant (red bar) with PKR as indicated by the bracket marked as “NS”. **(C) Co-IP of wt PACT and P222L proteins from HeLa cells.** HeLa cells were transfected with flag-PACT/pCDNA3.1<sup>-</sup> (lanes 1



**Figure 3.2 (cont.):** and 2) or pCDNA3.1<sup>-</sup> (lane 3). 24h after transfection, Flag-tagged PACT protein was immunoprecipitated for 1 h using anti-flag mAb-agarose. The immunoprecipitates were analyzed by western blot analysis with anti-PKR monoclonal antibody (PKR Co-IP panel). The blot was stripped and re-probed with monoclonal anti-flag M2 antibody (Flag-PACT panel). The input gel (20% of IP lanes) shows western blot analysis of total proteins in the extract, without immunoprecipitation to ascertain equal amount of Flag-PACT expression after transfection in and that equal amount of PKR was present in both samples. **(D) Quantification of Co-IP in 2 C.** The relevant bands were quantified by phosphorimager analysis and % Co-IP was calculated from the band intensities in input and IP lanes. These values were normalized to band intensities of Flag-PACT in IP gel. The error bars: standard deviation calculated from 3 independent experiments. The p value (0.0027) calculated using statistical analyses indicated a significant difference between % co-IP of wt (blue bar) and P222L mutant (red bar) with PKR as indicated by the bracket marked by #.

seen in Fig. 3.2 A and B, both flag-PACT and flag-P222L mutant appear to have a similar affinity for PKR under the condition that the assay was carried out (lanes 2 and 4) and PKR was not immunoprecipitated with Flag-mAb-agarose in the absence of Flag-PACT (lane 6). In this assay, using *in vitro* translated proteins no significant difference in the strength of interaction with PKR was observed between wt and P222L mutant PACT proteins under the condition that the assay was carried out (Fig. 3.2 B). In order to assay for PACT-PKR interaction in a mammalian cells, flag-PACT and flag-P222L mutant were expressed in HeLa cells and co-immunoprecipitation of endogenous wt PKR with the flag-tagged proteins was assayed. Both flag-PACT and flag-P222L were able to pull down wt PKR, and flag-P222L consistently showed a higher efficiency for co-immunoprecipitating PKR as compared to flag-PACT (Fig. 3.2 C, lanes 1 and 2). In the absence of transfected Flag-PACT proteins, no immunoprecipitation of endogenous PKR was observed with anti-Flag mAb-agarose (lane 3). The % co-immunoprecipitation was quantified from 3 separate experiments by analyzing band intensities (Fig. 3.2 D) and the results consistently showed a significantly stronger interaction of flag-P222L with PKR as compared to flag-PACT interaction with PKR. These results establish that P222L mutant retains the ability to bind to PKR and compared to wt PACT, exhibits an enhanced PKR interaction in mammalian cells.

*P222L mutation makes PACT a more efficient PKR activator:*

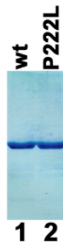
The effect of P222L mutation on PACT's ability to activate PKR was assayed by using the *in vitro* PKR activity assay. Hexahistidine tagged wt PACT and P222L proteins

expressed in bacteria were purified on Ni affinity beads. (Fig.3.3 A). These purified recombinant proteins were used as activators for *in vitro* PKR kinase activity assay using PKR immunoprecipitated from HeLa cells (Patel and Sen 1998). The assay measures autophosphorylation and activation of PKR. As seen in Fig. 3.3 B, there is a basal level of PKR activity seen in the absence of exogenous PKR activator (lane 1), and significantly elevated PKR activity in the dsRNA (ds) positive control (lane 2). There is a dose dependent increase in PKR autophosphorylation in response to increasing amounts of wt PACT (lanes 3-7). In response to increasing amounts of P222L there is significantly higher autophosphorylation of PKR (lanes 8-12) as compared to that seen with equivalent amounts of wt PACT (lanes 3-7). The quantification of radioactive signal in PKR band using phosphorimager analysis is shown in Fig. 3.3 C. Statistical analyses were performed on results from five independent experiments and all concentrations of wt and P222L protein showed significant PKR activation. Three of these p-values are as indicated in Figure 3.3 C with brackets. These results indicate that the P222L mutant activates PKR more efficiently *in vitro* as compared to wt PACT.

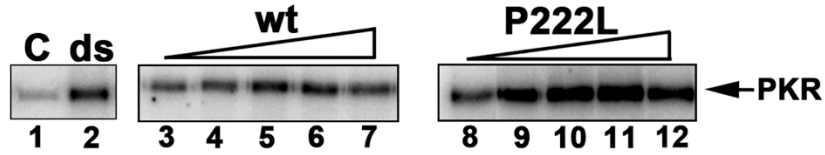
*Patient lymphoblasts homozygous for P222L mutation exhibit enhanced sensitivity to the ER stressor tunicamycin:*

To analyze the effect of P222L mutant's increased ability to activate PKR in a cellular context, apoptosis in response to the ER stressor tunicamycin was evaluated in patient and wt lymphoblasts. Tunicamycin inhibits protein glycosylation in the ER causing misfolded proteins to accumulate thereby inducing the ER stress response pathway

**A. recombinant proteins**



**B. Kinase activity assay**



**C. Kinase assay quantification**

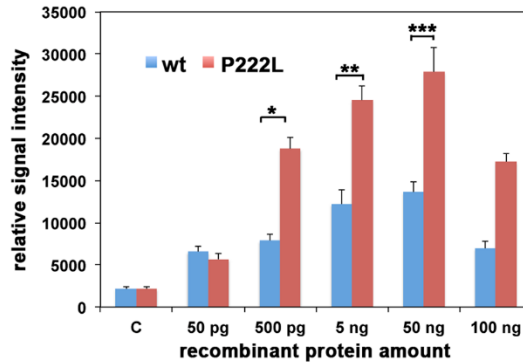


**Figure 3.3: Effect of P222L mutation on PKR activation. (A) Purification of recombinant PACT proteins.** 500 ng of purified, recombinant hexahistidine-tagged wt PACT and P222L proteins analyzed by SDS-PAGE and Coomassie blue staining. **(B) Kinase activity assay.** PKR immunoprecipitated from HeLa cell extracts using PKR monoclonal antibody that immunoprecipitates total PKR (R & D systems) was used to measure PKR kinase activity without any activator (C) or activators added as indicated above the lanes. Lane 1: PKR activity without any activator, lane 2: 100 ng/ml polyI·polyC as activator. Purified recombinant wt PACT or P222L in amounts of 50 pg (lanes 3 and 8), 500 pg (lanes 4 and 9), 5 ng (lanes 5 and 10), 50 ng (lanes 6 and 11), and 100 ng (lanes 7 and 12). **(C) Quantification of kinase assay.** The radioactivity present in the bands was measured by phosphorimager analysis and the relative signal intensities are plotted. The error bars: standard deviation from 5 independent experiments performed with two independent preparations of recombinant wt PACT and P222L proteins. Student T-tests performed indicated that the relative signal intensity increases in radioactive PKR bands as compared to control lanes at all wt and P222L protein concentrations were very significant with all p-values lower than 0.05. Three of these values were also analyzed further to investigate if the differences observed between wt and P222L activation of PKR were significant, and are as indicated: 500 pg (bracket \*) = 0.0015; 5 ng (bracket \*\*) = 0.0017; 50 ng (bracket \*\*\*) = 0.003, n=5.

(Schonthal 2012). Apoptosis was measured using DNA fragmentation, flow cytometry, and caspase 3 and 7 activity. As seen in Figure 3.4 A, the wt lymphoblast cells show some increase in fragmented DNA with tunicamycin treatment (lanes 2 and 4). In contrast to this, the patient lymphoblasts show markedly increased DNA fragmentation in response to tunicamycin (lanes 6, 8, and 10) indicating enhanced sensitivity to the ER stress. Quantification of DNA fragmentation was performed to calculate fold increases in band intensities after tunicamycin treatment compared to untreated samples (Figure 3.4 B). Statistical analysis revealed that the patient lymphoblasts show significantly more DNA fragmentation as compared to wt lymphoblast in response to tunicamycin (bracket marked by #). In addition, the patient lymphoblasts also show significantly more DNA fragmentation as compared to wt lymphoblasts even in untreated samples (bracket marked by \*). These results indicate that patient lymphoblasts are more sensitive to apoptosis in response to the stress and show significantly higher level of apoptosis even in the absence of any deliberately applied external ER stress. To further compare the apoptotic response of wt and patient lymphoblasts, we measured the caspase activity in response to tunicamycin. As seen in Figure 3.4 C, there is a dramatic increase in caspase 3/7 activity in patient lymphoblasts as compared to the wt lymphoblasts, even in the absence of the ER stress (bracket \*). In addition, a significant increase in caspase activity is seen 6 hours after treatment in the patient lymphoblasts (bracket \*\*\*) whereas the wt lymphoblasts show a very modest increase in caspase activity at 6 hours (bracket #). Although there is a more significant increase in caspase activity in wt lymphoblasts at 24 hours (bracket \*\*), the overall caspase activity in the

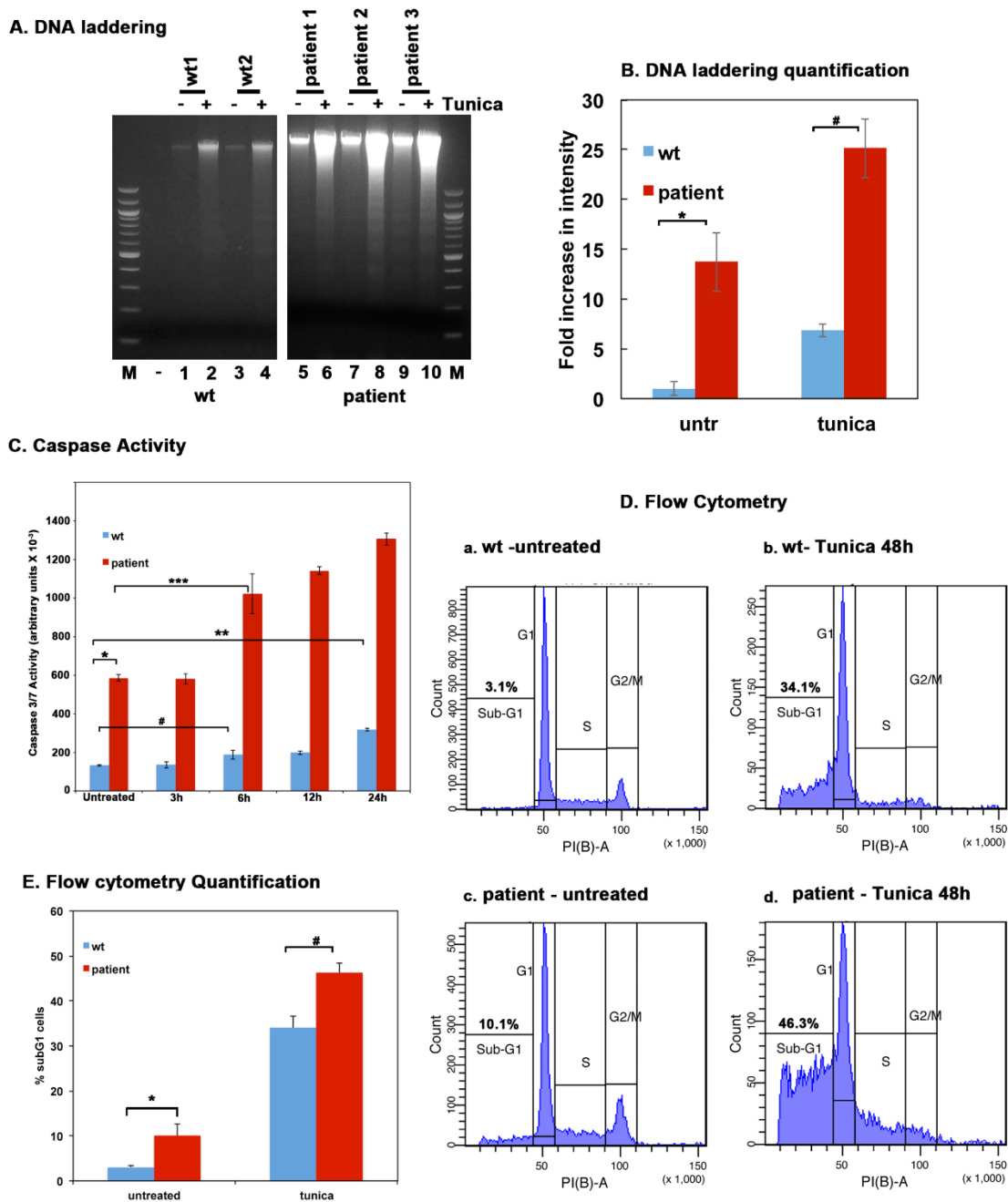


**Figure 3.4: Tunicamycin-induced apoptosis is enhanced in dystonia patient lymphoblasts. (A) DNA fragmentation analysis.** Lymphoblast cell lines established from 2 normal (wt) individuals and 3 dystonia patients were treated with 0.5  $\mu\text{g/ml}$  tunicamycin for 48h. The DNA fragmentation was analyzed as described under experimental procedures. Lanes 1-4: wt (normal) lymphoblasts, lanes 5-10: dystonia patient (affected) lymphoblasts. The - lanes (1, 3, 5, 7, and 9): untreated cells; and the + lanes (lanes 2, 4, 6, 8, and 10): tunicamycin treated cells. Lane M: 100-bp ladder. **(B) Quantification of DNA fragmentation.** The inverted images from all four experiments as

**Figure 3.4 (cont.):** in Fig. 4 A were analyzed by GE Lifesciences ImageQuant TL software to calculate total band intensities in each lane from top to bottom. Blue bars: normal (wt) lymphoblasts and the red bars: dystonia patient lymphoblasts. Band intensities in wt untreated samples were considered as 1.0 and all other samples were expressed as fold increases compared to that value. Student T-tests were performed, and p values are as follows \* = 0.00012 (significant), # = 0.00015 (significant), n=4. **(C) Caspase-Glo 3/7 assay.** Lymphoblast cell lines established from 2 normal (wt) individuals and 3 dystonia patients were treated with 0.5 µg/ml tunicamycin for indicated time points. Caspase 3 and 7 activities were measured, blue bars: normal (wt) lymphoblasts and the red bars: dystonia patient lymphoblasts. Student T-tests were performed, and p values are as follows \* = 0.00016 (significant), \*\* = 0.00041 (significant), # = 0.002 (significant), and \*\*\* = 0.0037 (significant), n=4. **(D) Flow cytometry analysis.** Lymphoblasts from 2 normal (wt) or 3 affected (dystonia patient) individuals were treated with 0.5 µg/ml tunicamycin. Cells were harvested at 48 h after the treatment and subjected to flow cytometry analysis. The sub-G0/G1 cell population represents the dying cells. The sub-G0/G1 percentages are displayed in each panel. These experiments were repeated four times. The most representative profiles from a single experiment with one wt and one patient line are shown. **(E) Flow cytometry quantification and statistical analysis.** The percentage of sub G1 cells from the experiment in panel D is represented as a bar graph and the percentages of sub G1 cells from 4 different experiments were subjected to student T-tests, and p values are as follows \* = 0.00022 (significant), # = 0.00025 (significant).

wt lymphoblasts is fairly low even at 24 hours after treatment as compared to the patient lymphoblasts. These results further establish that patient lymphoblasts exhibit enhanced sensitivity to the ER stressor tunicamycin and in agreement with our DNA fragmentation results (Figure 3.4 A), also show higher caspase activity without any external stressor. In order to further quantify the difference in apoptosis between wt and patient lymphoblasts, flow cytometry analysis was performed. As seen in Figure 3.4 D only 3.1% of the wt cells had a subG1 DNA content in the absence of the ER stress (panel a), whereas 10.1% of the patient cells had a SubG1 DNA content in the absence of the ER stress (panel c). When the lymphoblast lines were treated with tunicamycin for 48 hours prior to analysis, the subG1 population increased to 34.1% for wt lymphoblasts (panel b) and to 48.3% in patient lymphoblast (panel d). Figure 3.4 E shows a bar graph representing this data with the error bars and statistical analyses performed for 4 different experiments. The difference in % apoptosis between wt and dystonia patient cells both in untreated as well as in tunicamycin treated samples is statistically significant as indicated by the brackets \* and #. These results demonstrate that the patient cells exhibit significantly higher levels of apoptosis in the absence of an extrinsic stress signal, and are markedly more sensitive to the ER stressor tunicamycin.

*Patient lymphoblasts homozygous for P222L mutation show a delayed but enhanced and prolonged PKR activation in response to tunicamycin:*

To understand the mechanism of enhanced sensitivity of patient lymphoblasts to the ER stress we compared PKR activation kinetics by western blot analysis in wt and patient



lymphoblasts at indicated time points after tunicamycin treatment. As shown in Figure 3.5 A, PKR phosphorylation is observed at 1h (lane 2) and 2h (lane 3) after treatment, begins to decrease at 4h (lane 4) and is barely detectable after 8h (lanes 5-7) in wt cells. In contrast to this, the patient cells do not show an increase in PKR phosphorylation until 2 h after treatment (lane 9) but this phosphorylation is maintained and continually increased until 24 h after treatment (lanes 10-13). These results demonstrate that PKR activation follows a slow albeit prolonged kinetics in patient cells as opposed to rapid and short duration in wt cells. The ratio of phosphorylated PKR to total PKR was calculated based on phosphorimager quantification of band intensities and is represented in Fig. 3.5 B and the p-values calculated from student T-tests indicate a significant difference in PKR phosphorylation between wt and patient lymphoblasts as represented by brackets marked \*, \*\*, and \*\*\*. We next examined if eIF2 $\alpha$  phosphorylation in response to tunicamycin followed kinetics similar to PKR activation. Similar to the kinetics of PKR activation, eIF2 $\alpha$  phosphorylation is seen as early as 1 h (lane 2) after treatment and is maintained high until 4 h (lanes 2-4) after which the levels gradually decreased (lanes 5-7) in wt cells. In patient lymphoblasts, a comparable increase is not seen until 8h after treatment (lane 12) and these levels slowly rise until 24h after treatment (lanes 11-14). These results indicate that eIF2 $\alpha$  phosphorylation is delayed in response to tunicamycin in patient lymphoblasts, but persists for a prolonged duration compared to wt cells. The ratio of phosphorylated eIF2 $\alpha$  to total eIF2 $\alpha$  was calculated based on phosphorimager quantification of band intensities and is represented in Fig. 3.5 D and the p-values calculated from student T-tests indicate a

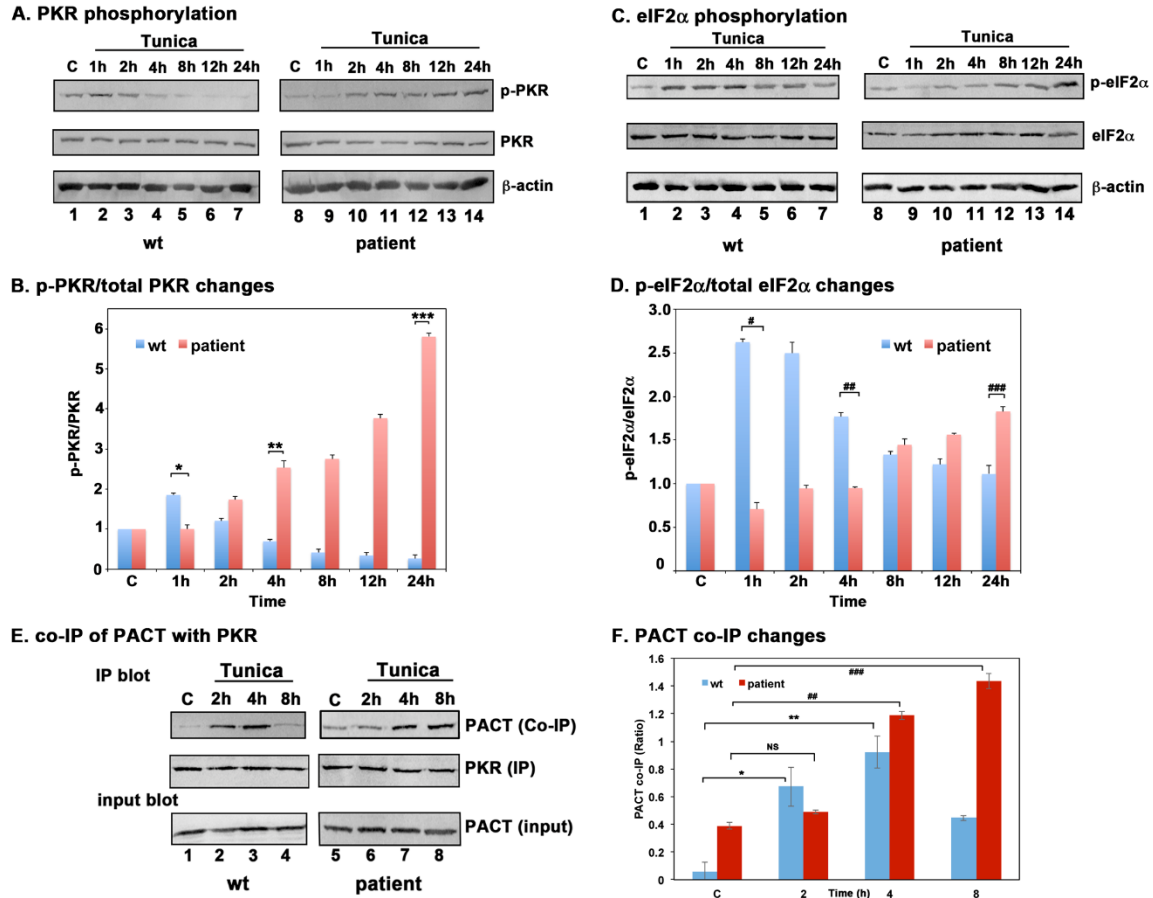


**Figure 3.5: PACT-PKR interaction, PKR activation, and eIF2 $\alpha$  phosphorylation in response to tunicamycin in normal and dystonia patient lymphoblasts. (A) PKR phosphorylation kinetics.** Lymphoblasts from normal (wt), or affected (dystonia patient) individuals were treated with 0.5  $\mu$ g/ml tunicamycin. The cell extracts were prepared at indicated times and analyzed by western blot analysis. The same blot was stripped and re-probed with all antibodies. The analysis was repeated four times with each line and the best representative blots are shown. **(B) Quantification of p-PKR and total PKR signals.** The ratio of phosphorylated PKR to total PKR, calculated using the Imagequant software is represented. The value for ratio obtained for control samples was considered 1.0 for each experiment and all other ratios obtained with treated samples were expressed relative to this value for comparisons between experiments. The fold increases in ratios wt after tunicamycin treatment compared to the control samples were calculated at each time point. Error bars represent standard deviation from 3 experiments. **(C) eIF2 $\alpha$  phosphorylation kinetics in response to tunicamycin.** Same as in (A), except eIF2 $\alpha$  phosphorylation and total eIF2 $\alpha$  was analyzed. **(D) Quantification of p-eIF2 $\alpha$  and total eIF2 $\alpha$  signals.** The ratio of phosphorylated eIF2 $\alpha$  to total eIF2 $\alpha$ , calculated using the Imagequant software and phosphorimager is represented. The analysis was done as in 2 B. **(E) Co-immunoprecipitation of endogenous PKR and PACT proteins.** Lymphoblasts from normal (wt), or dystonia patients (P222L) were treated

**Figure 3.5 (cont.):** with 0.5 µg/ml tunicamycin. The cell extracts were prepared at indicated times and endogenous PKR protein was immunoprecipitated using anti-PKR mAb that immunoprecipitates total PKR and proteinA-sepharose. The immunoprecipitates were analyzed by western blot analysis with anti-PACT monoclonal antibody (PACT co-IP panel). The blot was stripped and re-probed with anti-PKR mAb to ascertain an equal amount of PKR in each lane (PKR panel). The input blot: western blot analysis of total proteins in the extract with anti-PACT mAb showing equal amount of PACT in all samples. **(F) PACT-PKR co-IP quantification and statistical analysis.** The ratio of PACT co-IP signals to total input PACT signals were calculated using GE Life sciences ImageQuant TL software and was further normalized to PKR IP signals. The averages from 3 experiments were plotted as bar graphs. The error bars represent standard error and the data from different experiments were subjected to student T-tests, and p values are as follows \* = 0.0025 (significant), NS = 0.0531 (not significant), \*\* = 0.0003 (significant), ## = 0.0002 (significant), and ### = 0.0006 (significant).

significant difference in eIF2 $\alpha$  phosphorylation between wt and patient lymphoblasts as represented by brackets marked #, ##, and ###. We next evaluated the association of PACT with PKR in response to tunicamycin using a co-immunoprecipitation analysis. PKR was immunoprecipitated from wt and patient lymphoblast cell lysates at indicated time points after tunicamycin treatment using a PKR monoclonal antibody. The immunoprecipitates were analyzed by western blot analysis using anti-PACT antibody. As seen in Fig. 3.5 E, in wt cells, compared to control (lane 1) PACT association with PKR is increased at 2h and 4h (lanes 2 and 3) after tunicamycin treatment and returns to basal levels by 8h (lane 4). However, in patient cells PACT association with PKR stays at basal levels at 2h after treatment (lane 6) similar to control (lane 5) and only shows increase at 4h (lane 7) and 8h (lane 8). These results suggest that PACT association with PKR shows delayed kinetics in patient lymphoblasts in response to tunicamycin. It is interesting to note that in absence of tunicamycin an increase in P222L association with PKR is seen in patient cells as compared to PACT association with PKR in wt cells, further confirming increased association of P222L with PKR in absence of stress (Fig. 3.2 C). PACT's co-immunoprecipitation with PKR was quantified from 3 separate experiments and is shown as a bar graph in Figure 3.5 F. The ratio of PACT co-IP signals to PACT input signals were normalized to PKR IP signals for each lane. The delayed kinetics of PACT association with PKR in response to tunicamycin in dystonia patient cells is further confirmed by this analysis. The p-values calculated from student T-tests are as indicated in the figure legend and demonstrates that the difference observed in kinetics of PACT-PKR association between wt and patient cells is statistically significant. The data shown

is representative of results from 3 different patient samples, all of which showed a similar trend.

*P222L mutation enhances PACT-TRBP as well as PACT-PACT interactions:*

We next examined if the P222L mutation affects PACT's interaction with TRBP consequently resulting in altered kinetics of PKR association and activation. In the absence of stress, PKR-TRBP and PACT-TRBP heterodimers prevail and prevent PACT from activating PKR. In response to stress PACT is phosphorylated on serine 287, which decreases its affinity for TRBP thus reducing TRBP-PACT heterodimers (Singh et al. 2011). This phosphorylation also increases PACT's binding affinity for PKR while simultaneously stabilizing PACT-PACT interactions. Thus we reasoned that the altered kinetics of PKR activation in patient cells may result from P222L's effect on PACT-TRBP interaction. We examined the interactions between PACT-TRBP and PACT-PACT using co-immunoprecipitation assays with PACT and TRBP marked by two different epitope tags. Fig. 3.6 A represents analysis of PACT-TRBP interaction. As seen in lanes 1 and 3, myc-TRBP interacts with both FLAG-wt as well as FLAG-P222L. The interaction between FLAG-wt PACT and myc-TRBP is significantly reduced to almost undetectable levels 2h after tunicamycin treatment (lane 2). In contrast to this, FLAG-P222L stays associated with myc-TRBP strongly at 2h after treatment (lane 4). In absence of Flag-PACT, no myc-TRBP was immunoprecipitated (lanes 5 and 6) thereby indicating that myc-TRBP immunoprecipitation is solely due to interaction with Flag-PACT. These results indicate that the delayed activation of PKR in patient cells could result from an enhanced

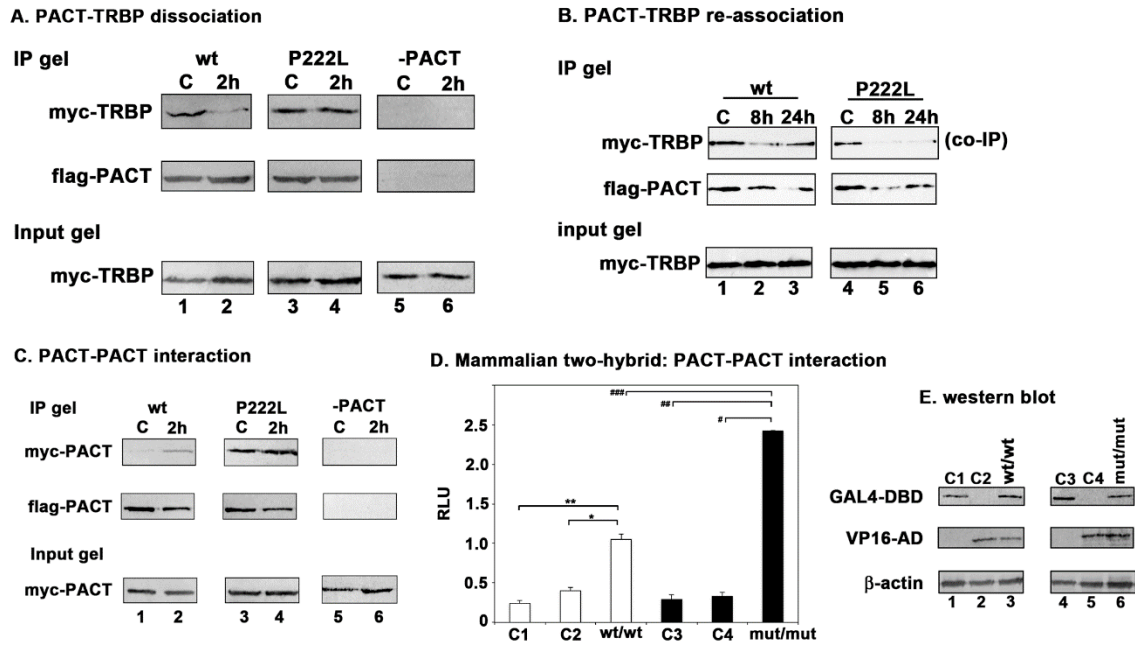


**Figure 3.6: P222L mutation affects TRBP-PACT and PACT-PACT interactions. (A) Co-immunoprecipitation of flag-PACT with myc-TRBP at early time point after ER stress.** HeLa cells were transfected with either flag- wt PACT or flag-P222L mutant and myc-TRBP. 24 hours after transfection, cells were either left untreated or treated with 50  $\mu$ g/ml tunicamycin. 2 hours after treatment, cells were harvested and flag-PACT was immunoprecipitated using anti-flag mAb-sepharose and co-immunoprecipitation of myc-TRBP was analyzed by western blot analysis with anti-myc mAb (myc-TRBP panel). The blot was stripped and re-probed with anti-flag mAb to ascertain an equal amount of flag-PACT protein in each lane (flag-PACT panel). The input blot: western blot analysis of total proteins in the extract with anti-myc mAb. **(B) Co-immunoprecipitation of flag-PACT with myc-TRBP at late time points after ER stress.** HeLa cells were transfected with either flag- wt PACT or flag-P222L mutant and myc-TRBP. 24 hours after transfection, cells were either left untreated or treated with 50  $\mu$ g/ml tunicamycin. AT 8 and 24 hours after tunicamycin treatment, cells were harvested and flag-PACT was immunoprecipitated using anti-flag mAb-sepharose and co-immunoprecipitation of myc-TRBP was analyzed by western blot analysis with anti-myc mAb (myc-TRBP panel). The blot was stripped and re-probed with anti-flag mAb to ascertain an equal amount of flag-PACT protein in each lane (flag-PACT panel). The input blot: western blot analysis of total proteins in the extract with anti-myc mAb. **(C) Co-immunoprecipitation of flag-PACT and myc-PACT.** HeLa cells were transfected with either flag- wt PACT and myc-wt PACT or flag-P222L mutant and myc-P222L mutant. 24 hours after transfection, cells were either left untreated or treated with 50  $\mu$ g/ml tunicamycin. 2 hours after treatment, cells were harvested and flag-PACT was immunoprecipitated using anti-flag mAb-sepharose and co-immunoprecipitation of myc-PACT was analyzed by western blot analysis with anti-myc mAb (myc-PACT panel). The blot was stripped and re-probed with anti-flag mAb to ascertain an equal amount of flag-PACT protein in each lane (flag-PACT

**Figure 3.6 (cont.):** panel). The input blot: western blot analysis of total proteins in the extract with anti-myc mAb. **(D) Mammalian two-hybrid assay.** COS-1 cells were transfected with 250 ng of each of the two test plasmids encoding proteins to be tested for interaction, 50 ng of the reporter plasmid pG5Luc, and 1 ng of plasmid pRL-Null to normalize transfection efficiency. Cells were harvested 24 h after transfection, cell extracts were assayed for luciferase activity. The plasmid combinations are as indicated. C1: wt PACT/GAL4DBD and VP16AD EV (negative control), C2: GAL4DBD EV and wt PACT/VP16AD (negative control), wt/wt: wt PACT/GAL4DBD and wt PACT/VP16AD, C3: P222L/GAL4DBD and VP16AD EV (negative control), C4: GAL4DBD EV and P222L/VP16AD (negative control), mut/mut: P222L /GAL4DBD and P222L/VP16AD. The experiment was repeated twice with each sample in triplicates, and the averages with standard error bars are presented. Student T-tests performed to calculate p-values indicated that the differences observed between the negative controls and test values (C1, C2 and wt/wt, C3, C4 and mut/mut) were highly significant: bracket \* (0.0071), bracket \*\* (0.0001), bracket # (0.0037), bracket ## (0.0002). The difference between wt/wt and mut/mut interaction was also highly significant as indicated by the p value represented by bracket ### (0.0001). **(E) Western blot analysis.** COS-1 cell extracts were examined by western blot analysis using an anti-GAL4-DBD mAb (Santa Cruz), anti-VP16AD Ab (Santa Cruz), and anti- $\beta$ -actin mAb. The samples are indicated on top of the lanes.

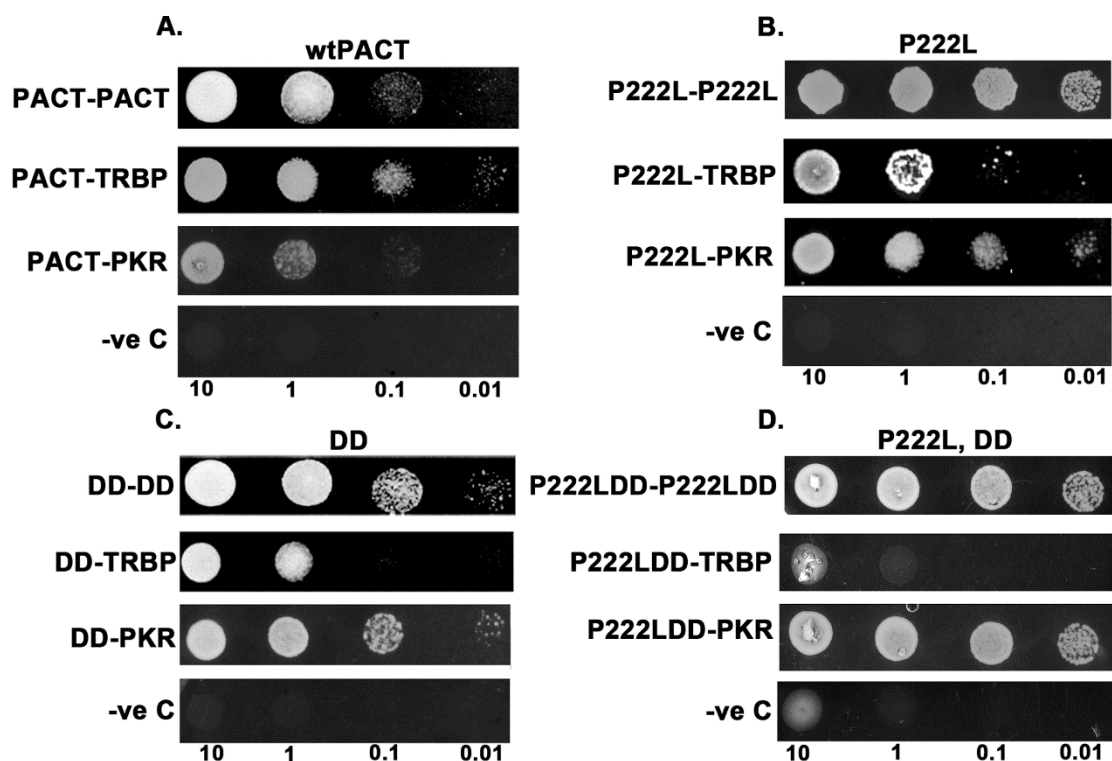
interaction of P222L with TRBP that sequesters P222L mutant away from PKR. Since we observed altered PKR phosphorylation as well as eIF2 $\alpha$  phosphorylation kinetics in patient lymphoblasts as compared to wt lymphoblasts, we examined if this change in kinetics could result from a lack of TRBP re-association with PACT at later time points after ER stress. Fig. 3.6 B represents analysis of PACT-TRBP interaction at 8 and 24 hours after tunicamycin treatment. As seen in lanes 1 and 4, myc-TRBP interacts with both FLAG-wt as well as FLAG-P222L in untreated cells. The FLAG-wt PACT and myc-TRBP begin to re-associate 8h after tunicamycin treatment (lane 2). In contrast to this, myc-TRBP stays dissociated from FLAG-P222L at 8h after treatment (lane 5). At 24h after tunicamycin treatment myc-TRBP shows a strong re-association with flag-wt (lane 3) and in contrast to this, myc-TRBP shows no re-association with flag-P222L even at 24h. These results indicate that the delayed but prolonged activation of PKR in patient cells could result from an enhanced interaction of P222L with TRBP that initially sequesters P222L mutant away from PKR but once dissociated from TRBP, P222L mutant does not re-associate rapidly with TRBP and thus continues to activate PKR even at 24h after the ER stress. Since PKR activation in response to stress is efficiently achieved by PACT-PACT homodimers after serine 287 phosphorylation, we examined if P222L mutation affects formation of PACT-PACT homodimers in response to tunicamycin. As seen in Fig. 3.6 C, myc-wt PACT and FLAG-wt PACT do not associate with high affinity in absence of stress (lane 1), but their interactions is detected 2h after tunicamycin treatment (lane 2). In contrast, Flag-P222L binds strongly to myc-P222L molecules even in absence of stress (lane 3) and this interaction is somewhat intensified at 2h after treatment (lane 4) and is



significantly stronger than the interaction between wt PACT molecules. In the absence of Flag-PACT, no myc-PACT was immunoprecipitated thereby validating that myc-PACT was immunoprecipitated solely by its interaction with Flag-PACT (lanes 5 and 6). These results suggest that the prolonged activation of PKR seen in patient cells results from more efficient formation of PACT homodimers that may be stable for a longer duration after initial onset of stress. Since we detected an enhanced interaction between P222L molecules in the absence of stress, we further examined this by using a mammalian two-hybrid assay to determine the relative increase in homomeric interactions due to P222L mutation in comparison with the wt PACT homomeric interactions. As shown in Fig. 3.6 D, P222L-P222L homomeric interaction (P222L/P222L) activated the reporter gene 1.5 fold higher than wt PACT-wt PACT homomeric interactions (wt/wt) thus validating that P222L mutation enhances interaction between PACT molecules. Student T-tests indicated the observed differences to be statistically significant as indicated in the figure legend. It is worth noting that the wt PACT-wt PACT as well as P222L-P222L interactions are statistically significant as compared to all negative controls (brackets \*, \*\*, #, and ##), and the difference between wt PACT-wt PACT and P222L-P222L interactions is also statistically significant (bracket ###). Fig. 3.6 E shows results of a western blot analysis to ensure that wt and P222L proteins were expressed at similar levels in cells and the observed enhanced P222L-P222L interaction was not due to differences in expression levels of wt PACT and P222L.

In order to ensure that the P222L mutation affects the affinity of PACT-PACT, PACT-TRBP, and PACT-PKR directly without the involvement of a third partner, we measured

the relative affinities of these interactions using a yeast two hybrid system. We have used this system extensively to demonstrate that stress-induced phosphorylation of PACT results in changes in affinity of its interaction with TRBP and PKR. Thus, this system is sensitive enough to detect changes in affinity between these proteins, and measures direct interaction between two proteins. Such changes in relative affinities of the binding partners have been demonstrated to change the cellular outcome in response to a stressor. As seen in fig. 3.7 A and B, in comparison to wtPACT, the P222L mutant shows significant increase in interaction between two PACT molecules (P222L-P222L in panel B versus PACT-PACT in panel A). P222L mutation also increases P222L-PKR (panel B) interaction as compared to wtPACT-PKR (panel A). In contrast, the interaction with TRBP (P222L-TRBP in panel B versus PACT-TRBP in panel A) is not affected to a significant extent by P222L mutation. These results are in agreement with our co-immunoprecipitation data in fig. 3.6. PACT is constitutively phosphorylated on serine 246 and gets phosphorylated at serine 287 in response to the ER stress. We have previously established that a phosphomimetic double mutation S246D,S287D (termed DD) increases interactions with PKR (DD-PKR in panel C versus PACT-PKR in panel A) and another molecule of PACT (DD-DD in panel C versus PACT-PACT in panel A) while decreasing the interaction with TRBP (DD-TRBP in panel C versus PACT-TRBP in panel A). In order to test the effect of stress-induced phosphorylation on the molecular interactions under study, we combined the two mutants to generate P222L,DD mutant. Thus, the P222L,DD mutant represents the P222L dystonia mutant under conditions of the ER stress caused by tunicamycin. As seen in panel D, P222L,DD mutant shows the



**E.**

| PACT type | PACT homodimers | PACT-TRBP heterodimers | PACT-PKR heterodimers |
|-----------|-----------------|------------------------|-----------------------|
| PACT      | +               | ++                     | +                     |
| P222L     | +++             | ++                     | ++                    |
| DD        | ++              | +                      | ++                    |
| P222L,DD  | +++             | +/-                    | +++                   |

**Figure 3.7: Effect of P222L mutation on molecular interactions with PACT's binding partners in yeast two-hybrid assay. A. Interaction of wtPACT with wtPACT, TRBP, and PKR, B. Interaction of P222L mutant with P222L, TRBP, and PKR, C. Interaction of PACT mutant S246D,S287D (DD) with DD, TRBP, and PKR, D. Interaction of PACT mutant P222LDD with P222LDD, TRBP, and PKR.** Various plasmid constructs as indicated in methods section were transformed into yeast strain AH109 and selected on double dropout medium lacking tryptophan and leucine. 10  $\mu$ l of serial dilutions (of OD<sub>600</sub> = 10, 1.0, 0.1, 0.01) were spotted for each transformant on quadruple dropout SD medium plate that lacks adenine, tryptophan, leucine and histidine and have 25 mM 3-Amino-1,2,4-triazole (3-AT). Plates were incubated for three days at 30°C. Transformation of PACT constructs in pGBKT7 and empty vector pGADT7 served as negative controls. **E. Relative affinities of PACT-PACT, PACT-TRBP, and PACT-PKR interactions.** The growth obtained in the yeast two-hybrid interaction assay was scored and is represented in the table. +++ indicates strong growth, ++ indicates moderate growth, + indicates good growth, and +/- indicates poor growth.

strongest interaction with itself (P222L,DD-P222L,DD) and with PKR (P222L,DD-PKR) and the least interaction with TRBP (P222L,DD-TRBP) when compared to results in panels A-C. Thus, these results clearly indicate that the P222L mutation found in dystonia patients leads to increased homodimer formation and PKR interaction under conditions of the ER stress. The altered kinetics of PKR activation and eIF2a phosphorylation that we observe in dystonia patient cells can be attributed to these changes in relative affinities of the binding partners.

### 3.5 Discussion

Dystonia is a genetically heterogeneous neurological movement disorder that is characterized by intermittent or sustained muscle contractions causing abnormal repetitive movements, and postures. In recent years, genetic diagnostic tools have led to identification of several monogenic forms of dystonia and dystonia-related disorders designated as DYT1-25 in OMIM (Online Mendelian Inheritance in Man) and many causative mutations in respective genes have been described (Xiao et al. 2014). Of these, DYT16 is associated with mutations in PACT and was initially described in two unrelated Brazilian families (Camargos et al. 2008) and a single German patient (Seibler et al. 2008). The affected individuals displayed symptoms of generalized dystonia in childhood with mean age being 9 years. All seven Brazilian patients shared the same substitution mutation (c.655C>T;P222L) in exon 7 of the PACT gene. The German patient had a heterozygous frameshift mutation (c.266-267delAT;p.H89fsX20) in exon 3. Recently another genetically confirmed case of DYT16 with an early presentation was

described and whole exome sequencing revealed 2 mutations in PACT (Lemmon et al. 2013). The first c.665C>T;P222L was inherited from the mother and was the same as the Brazilian cohort. The second mutation c.637T>C;C213R was a *de novo* event and was absent in both parents. Two other recessive mutations have been identified that manifest as substitution mutations in PACT C77S and C213F (de Carvalho Aguiar et al. 2015). Recently three additional point mutations were reported in Polish and German patients (Zech et al. 2014).

We examined the effect of the P222L mutation on cellular stress response since regulation of apoptosis in response to stress is PACT's well-characterized function (Patel et al. 2000; Daher et al. 2009; Singh et al. 2011; Singh and Patel 2012). The lymphoblasts derived from three dystonia patients carrying the P222L mutation exhibited significantly enhanced apoptosis in response to ER stress. The mechanisms leading to the enhanced sensitivity to tunicamycin were explored and our results indicated that the P222L mutation leads to PACT's increased interaction with TRBP and consequently causes altered kinetics of PKR and eIF2 $\alpha$  phosphorylation in response to the ER stress. In patient cells, the dissociation of PACT from TRBP in response to the ER stress is delayed, and thus formation of PACT-PKR homodimers is delayed. However, PACT-PACT homodimers appear to be more stable and thus PKR activation is enhanced and persists for a significantly longer duration after an ER stress event. Consequently eIF2 $\alpha$  phosphorylation also is delayed but persists for a longer duration in patient cells. The reason for relative eIF2 $\alpha$  phosphorylation levels in patient cells not reaching as high as that in wt cells is unclear but may be due differences in the level of eIF2 $\alpha$  phosphatases

at early and late time points after the initial stress. The phosphorylation of eIF2 $\alpha$  on serine 51, which is a single regulatory stress-induced modification is of significant functional relevance (Donnelly et al. 2013). Our work presented here highlights the importance of regulating the speed and duration of eIF2 $\alpha$  phosphorylation in determining cellular fate.

As represented in a schematic model in Fig. 3.8, in normal cells PACT-TRBP interaction has an inhibitory effect on PKR activation, and phosphorylation of PACT in response to stress disrupts TRBP-PACT interaction (Daher et al. 2009; Singh et al. 2011). Free PACT then forms homodimers that associate with PKR to activate its kinase activity resulting in eIF2 $\alpha$  phosphorylation (Fig. 3.8 A) (Singh and Patel 2012). The P222L mutant remains associated with TRBP longer under the ER stress conditions thereby causing a delayed PKR activation (Fig. 3.8 B). However P222L associates with PKR with higher affinity and thus remains associated with PKR for a longer duration thereby causing stronger and persistent PKR activation and eIF2 $\alpha$  phosphorylation. In accordance with this, P222L-P222L homodimers are more stable even in the absence of the ER stress (Fig. 3.6 B and C). It is interesting to note that although P222L-P222L homodimers form efficiently in the absence of a stress signal, the P222L homodimers are unable to cause PKR activation in the absence of a stress signal (Fig. 3.6 B, Fig. 3.5 A, and Fig. 3.7). Thus, stress-induced phosphorylation at serine 287 possibly serves an additional function than simply promoting formation of PACT-PACT homodimers. It is also interesting to note that P222L mutation enhances PACT's interaction with PKR as measured by cell-based co-immunoprecipitation assays from mammalian cell extracts (Figure 3.2 C and D).

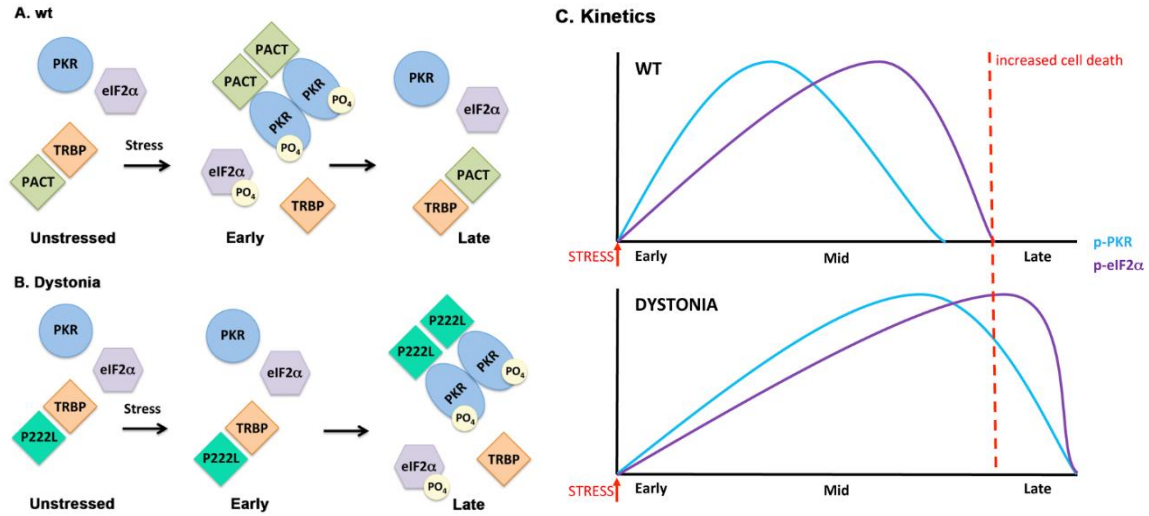


**Figure 3.8: A schematic model of PKR activation in wt and dystonia cells. (A) wt cells.** As previously established (references 19, 21, 22), in the absence of stress, PACT heterodimerizes with TRBP, PKR is catalytically inactive and eIF2 $\alpha$  is not phosphorylated. At early time points after ER stress, PACT dissociates from TRBP due to its phosphorylation, forms homodimers that bind to PKR with high affinity, activate its kinase activity leading to eIF2 $\alpha$  phosphorylation. At late time points after ER stress, cells recover by forming TRBP-PACT heterodimers and turning off PKR and eIF2 $\alpha$  phosphorylation. **(B) Dystonia cells.** In absence of stress, P222L mutant forms heterodimers with TRBP, PKR is catalytically inactive and eIF2 $\alpha$  is not phosphorylated. At early time points after ER stress, P222L remains bound to TRBP, and PKR and eIF2 $\alpha$  phosphorylation is inhibited. At late time points after ER stress, P222L dissociates from TRBP, forms homodimers that bind to PKR with high affinity and activate its kinase activity leading to eIF2 $\alpha$  phosphorylation. Thus, at late time point cells are unable to recover efficiently from ER stress because PKR and eIF2 $\alpha$  remain phosphorylated. **(C) Schematic representation of the altered PKR activation and eIF2 $\alpha$  phosphorylation kinetics in dystonia cells.** The blue line: PKR phosphorylation, purple line: eIF2 $\alpha$  phosphorylation. The red dotted line: a threshold time point. If PKR and eIF2 $\alpha$  remain in their phosphorylated state beyond this time point, recovery from ER stress is prevented resulting in increased apoptosis.

However, co-immunoprecipitation assays performed with the *in vitro* translated proteins shows no enhancement of P222L interaction with PKR (Figure 3.2 A and B). This indicates a possible role of post-translational modifications on P222L in enhancing interaction with PKR that possibly take place in mammalian cells but not in reticulocyte lysates. Further molecular analysis of other substitution mutations (C77S, C213F, C213R, T34S, N102S) recently described in DYT16 patients (Zech et al. 2014; de Carvalho Aguiar et al. 2015) would be important to determine if an altered ER stress response is a common theme in DYT16 dystonia. Our preliminary results indicate that the frameshift mutant protein reported in dominantly inherited dystonia case causes potent PKR activation and also leads to cellular death in cell culture (unpublished results). For efficient recovery and cellular survival after the ER stress, it is essential that the temporary inhibition of protein synthesis caused by phosphorylated eIF2 $\alpha$  is reversed and synthesis of survival related proteins takes place at late time points (Hetz 2012). As depicted in Fig. 3.8 C, the perturbation of this survival pathway due to the P222L mutation leading to delayed but prolonged PKR activation and eIF2 $\alpha$  phosphorylation can result in increased cell death as recovery and survival mechanisms may not be induced optimally in dystonia patients.

Our results presented here elucidate the cellular consequence of dystonia causing PACT mutations for the first time. Based on our results, it is conceivable to imagine that in P222L homozygotes, the neuronal cells may not cope well with cellular stress. Although, apoptosis of neurons is a possible extreme outcome of such detrimental events, survival of neurons that may not function at an optimal level could also be



equally detrimental. Analysis of whole exome sequencing in one particular patient (Lemmon et al. 2013) revealed two mutations within PACT gene. The first c.665C>T (p.P222L) was inherited from his mother and is the same mutation described in the Brazilian cohort and analyzed here. The second mutation c.637T>C (p.C213R) was not present in either parent, and indicated a de novo event. Thus, this patient is heterozygous for each mutation, but has both copies of PACT gene mutated, and thus has no wt PACT protein present. Similar to other DYT16 patients, this patient developed dystonia symptoms in early childhood and imaging revealed progressive MRI abnormalities with significant bilateral volume loss in the basal ganglia (Brashear 2013), which is interesting in view of the observed enhanced apoptosis in our experiments. This patient developed dystonia after a febrile illness, which could be a possible cellular stress event that may have triggered progressive cellular dysfunction or loss. Although our results are obtained using patient lymphoblasts, the PACT-PKR stress response pathway is present ubiquitously in all cell types including neurons (Chen et al. 2006; Paquet et al. 2012; Vaughn et al. 2014). Although neurodegeneration would be the expected long-term outcome of neuronal apoptosis neither apoptosis nor neurodegeneration has been systematically investigated in blood or brain of dystonia patients, but possible similarities and links between neurodegenerative Parkinson's disease and dystonia have recently been noted (Stoessl et al. 2014). Thus, neurodegeneration has not been investigated in any form of dystonia patients and this lack of information is usually interpreted as neurodegeneration generally being absent in dystonia patients. At the same time, PKR activation and ER stress due to misfolded

proteins has also been observed in pathologies of many neurodegenerative diseases such as Alzheimer's, Parkinson's, Huntington's, and Amyotrophic Lateral Sclerosis (ALS) (Marchal et al. 2014). Any contribution of PACT in PKR activation in these neurodegenerative diseases also remains unexplored at present. Nevertheless, possible neurodegeneration should be explored in DYT16 patients in the future especially in light of our results indicating increased apoptosis in P222L patient cells. It is also unknown at present if DYT16 patients exhibit any deficiencies in the innate immune system and respond differently to infections; and in the future this may be something worth investigating considering PACT's involvement in innate immunity. It is interesting to note that DYT16 patient lymphoblasts show higher levels of apoptosis in the absence of a stress signal as seen in the results of our flow cytometry analysis and caspase activity assays. It is unclear at present if this results from chronic low levels of PKR activation or is via a PKR independent mechanism. Similarly, any effect of PACT on activation of PKR-like endoplasmic reticulum kinase (PERK) has not been explored and could have a yet unidentified role on higher levels of apoptosis observed in patient cells.

In addition to activating PKR in response to cellular stress, PACT is known to function in the RNAi (Yong et al. 2014) and innate immune pathways (Heyam et al. 2015) and it is possible that the P222L mutation could affect these pathways. Although our research certainly does not rule out this possibility, it definitely establishes that at least one pathway regulated by the PACT-PKR interaction is significantly altered by the P222L mutation and results in major changes in the cell survival in response to the ER stress. Importance of such perturbation by the P222L mutation is further underscored by the

fact that the change in response to ER stress is reflected in increased apoptosis in patient cells.

The involvement and importance of the ER stress response for dystonia has been noted before for two other genes. Torsin A mutations were the first mutations to be described as the genetic basis of DYT1 dystonias (Bressman 2007). Torsin A functions as a molecular chaperone within the ER/secretory pathways and the mutant forms of torsin A have been shown to either misfold and trigger the ER stress response or cause a secretion defect causing a chronic, low level ER stress (Hewett et al. 2007; Gordon et al. 2011; Thompson et al. 2014). THAP1 (thanatos-associated domain-containing apoptosis-associated protein-1) mutations were described as the genetic basis of DYT6 dystonia (Fuchs et al. 2009). THAP1 is a transcription factor and has a nuclear function; however, it is also localized to the cytoplasm and possesses a N-terminal THAP domain that is homologous to the THAP0 domain found in p52rIPK or PRKRIR (protein-kinase, interferon-inducible double stranded RNA dependent inhibitor, repressor of p58 repressor) (Bragg et al. 2011). Thus, THAP1 may be involved in the ER stress response pathway by regulating PKR activity by inhibiting the function of the PKR inhibitor protein p58. Functionally, THAP1 may work similarly to PACT if it enhanced PKR activation. This can be tested in the future in DYT6 patient cells. Our results strongly emphasize the importance of the proper regulation of the ER stress response pathway and underscore the possibility that any dysregulation may sensitize cells to apoptosis.

## CHAPTER 4: OPPOSING ROLES OF TWO DSRNA-BINDING PROTEINS PACT AND TRBP ON

### RIG-I MEDIATED SIGNALING

---

<sup>1</sup>Vaughn LS and Patel RC. *To be submitted 2015.*

#### 4.1 Abstract:

An integral aspect of innate immunity is the ability to detect non-self molecules to initiate antiviral signaling via pattern recognition receptors (PRRs). One such receptor is the RNA helicase RIG-I (retinoic acid inducible gene 1), which has the ability to detect and be activated by 5'triphosphate uncapped double stranded RNA (dsRNA) as well as the viral mimic dsRNA polyI:C. Once activated, RIG-I's CARD domains oligomerize and initiate downstream MAVS (mitochondrial antiviral signaling protein) signaling ultimately inducing interferon (IFN) production. Another dsRNA binding protein PACT, originally identified as the cellular protein activator of PKR, has recently been shown to enhance RIG-I signaling in response to polyI:C treatment, in part by stimulating RIG-I's ATPase and helicase activities thereby causing an increased induction of IFN. TRBP (TAR-RNA-binding protein), which is about 45% homologous to PACT, inhibits PKR signaling by binding to PKR as well as by sequestration of its' activators, dsRNA and PACT. Despite the domain homology and similar structure of PACT and TRBP, the role of TRBP has not been explored in RIG-I like receptor (RLR) signaling. This work focuses on the effect of TRBP on RIG-I signaling and IFN production. Our results indicate that TRBP acts as an inhibitor of RIG-I signaling in a PACT- and PKR-independent manner. Surprisingly, this is independent of TRBP's post-translational modifications shown to be important for other signaling functions of TRBP, but does implicate TRBP's dsRNA-binding ability. This work has major implications on viral susceptibility, disease progression, and antiviral

immunity as it demonstrates the regulatory interplay between two dsRNA binding proteins PACT and TRBP on RIG-I mediated IFN production.

#### **4.2 Introduction:**

Key to the effectiveness of innate immunity is the ability of the host cell to discriminate between self and non-self molecules (Ahmad and Hur 2015). Detection of pathogenic molecules is done by pattern recognition receptors (PRRs), which are able to detect pathogen-associated molecular patterns (PAMPs) or microbe-associated molecular patterns (MAMPs) (Weber 2015, Schlee 2012). After detection of foreign molecular patterns, PRRs can initiate signaling pathways associated with innate immunity (Ahmad and Hur 2015). One such receptor is RIG-I (retinoic acid inducible gene 1), a cytoplasmic PRR which is activated by long double stranded (ds) RNAs, highly structured RNA molecules, 5' mono-, di-, or triphosphorylated dsRNA structures, polyU/UC rich RNA, or by 3' monophosphorylated RNA (Weber 2015). Once bound to an identified non-self molecule, RIG-I initiates downstream signaling by oligomerization of its two caspase activation and recruitment domains or CARDs (Figure 4.1). Once oligomerized, RIG-I's CARD domains in turn oligomerize with CARD domains in Mitochondrial Anti-Viral Signaling Protein (MAVS) (also known as IPS-1, VISA, and Cardif) and activate downstream signaling (Schlee 2012, Wu and Hur 2015). After MAVS activation, the transcription factors IRF-3 and NFκB are activated, which induce type 1 interferon (IFN) genes (Schlee 2012, Seth et al 2005). The induced IFNs then initiate anti-

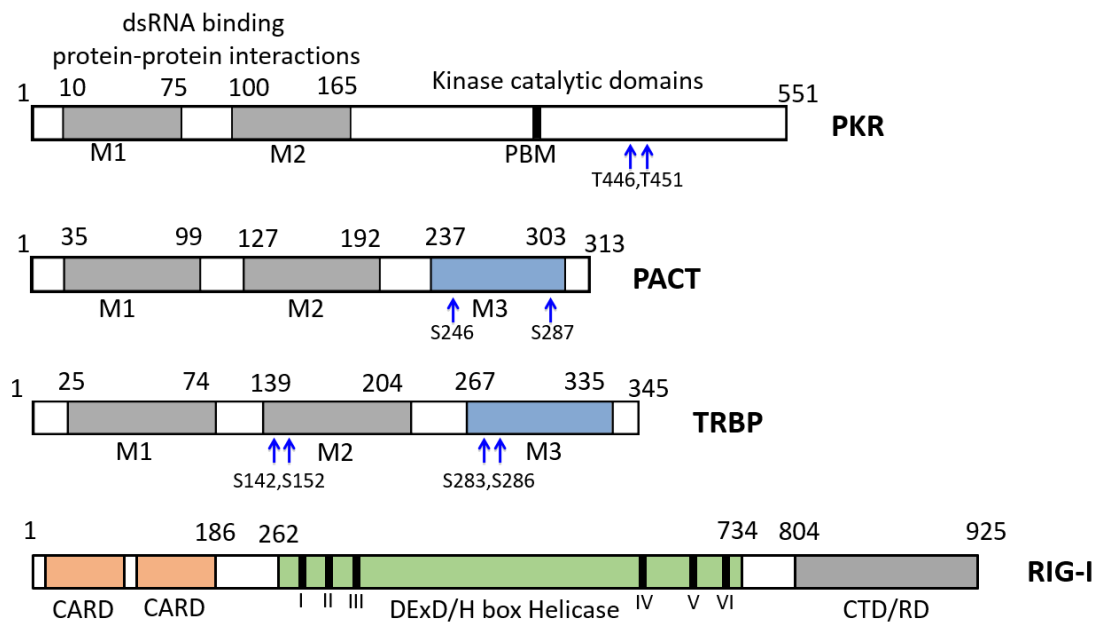


**Figure 4.1 Domain structure of PKR, PACT, TRBP, and RIG-I.** *M1* and *M2* of PKR, PACT, and TRBP are evolutionarily conserved dsRNA binding motifs (dsRBMs) that also mediate protein-protein interactions. *PBM*, PACT Binding Motif. *M3* of PACT is essential for PKR activation. *M3* (aka medial domain) of TRBP mediates TRBP's interactions with Merlin, Dicer, and PACT. *Blue Arrows* indicate known sites of phosphorylation on each protein. *CARD*, Caspase activation and recruitment domain, site of oligomerization with other *CARD* domains. *DExD/H Helicase*, helicase domain with inherent ATPase activity. *CTD/RD*, C-terminal domain and regulatory domain, interaction site of PACT. *I-VI*, conserved helicase motifs.

viral signaling responses in an autocrine and paracrine manner by inducing additional gene products.

PACT, a dsRNA-binding protein first identified as the endogenous protein activator of PKR, has recently been shown also to function as an endogenous activator of RIG-I (Kok et al. 2011). PACT activates RIG-I in the absence of dsRNA, but the presence of both PACT and dsRNA further enhances RIG-I activation, and amplifies downstream IFN signaling (Kok et al. 2011). PACT has been shown to directly interact with RIG-I through RIG-I's C-terminal or regulatory domain (CTD/RD) and increase RIG-I's ATPase activity (Figure 4.1) (Kok et al. 2011). PACT contains two well-characterized and evolutionarily conserved dsRNA-binding motifs (dsRBM), also found in the proteins PKR and TRBP.

TRBP (TAR RNA-binding protein, named for its ability to bind TAR RNA made during HIV infection) has been implicated in a multitude of signaling pathways. TRBP has been shown to aid HIV replication in infected cells (Gatignol et al 1991, Dorin et al. 2003), to regulate dicer activity during RNA interference (RNAi) in all cells (Lee et al. 2006, Lee et al. 2013, Chendrimada et al. 2005, Haase et al. 2005), and to inhibit PKR kinase activity during cellular and viral stress (Park et al 1994, Daher et al. 2009, Singh et al 2011, Dorin et al. 2003). Interest in investigating TRBP's effect on RIG-I activity stems from the fact that PACT and TRBP are about 45% homologous and have been implicated in the same cellular pathways, performing overlapping functions in some instances (Koscianska et al. 2011, Wilson et al. 2015, Heyam et al. 2015, Kok et al. 2007) and exerting opposing effects in other instances (Gupta et al 2003, Patel and Sen 1998,



Gatignol et al. 1991). Previous work has shown that TRBP and PACT have opposite effects on PKR signaling during non-viral cellular stresses (Daher et al. 2009, Singh et al. 2011, Singh and Patel 2012, Nakamura et al. 2015). This makes it interesting to investigate the effect of TRBP on RIG-I signaling, especially since it functions as a negative regulator of PKR, another major PRR and a viral restriction factor.

In this study, we examined if TRBP has a redundant role similar to PACT, an inhibitory role opposite of PACT, or exerts no effect on RIG-I signaling. Our results establish that TRBP inhibits RIG-I signaling and uncovers key differences in PACT and TRBP mediated RIG-I regulation. Our results demonstrate for the first time, an additional pathway involved in innate immunity that is regulated in an opposite manner by these two dsRNA-binding proteins.

#### **4.3 Materials and Methods:**

##### *Reagents and Cell lines*

HEK293Ts, PACT  $-/-$  MEFs (gift from Dr. Ganes Sen), and PKR  $-/-$  MEFs (gift from Bryan Williams) were cultured in Dulbecco's modified Eagle's medium (DMEM) containing 10% fetal bovine serum and penicillin/streptomycin. LMW PolyI:C and 5'ppp dsRNA were purchased from Invivogen. IRF3 antibody (Santa Cruz), p-IRF3 antibody (Cell Signaling),  $\beta$ -actin antibody (Sigma).

### Generation of PACT and TRBP mutants

All TRBP and PACT AA and DD point mutations were generated using a mutagenic primer for PCR amplification to change specific codons. The primer sequences were as follows:

| Primer                   | Sequence   |
|--------------------------|--|
| wt TRBP FOR              | 5'GCTCTAGACATATGGAAATGCTGGCCGCCAACCCAGGC 3'  |
| wt TRBP REV              | 5'GGATCCTCACTTGCTGCCTGCCATGC 3'  |
| K59A TRBP REV            | 5'GACTGCTCCCCCTTTGAGGTGTTT GAGGGCCACCTCAGCTGCCTT<br>GTGCTTGGCTGCCTTCGCGCTGGGGCCCTGC 3' |
| K189A TRBP FOR           | 5'CGAATTCACCATGACCTGTGAGTGGAGCGTTTCATTGAGATTGG<br>GAGTGGCACTCCGCAAAATTGGCAAAGC 3'      |
| S131A TRBP FOR           | 5'CGCCATGGAAGTGCAGCCCCCTGTCGCCCTCAGC 3'  |
| S121D TRBP REV           | 5'GTTCCATGGCGGGGTCCCTGGTTAGGACTACAGATGGAAGTGGG<br>3'                                   |
| S121A REV TRBP           | 5'GTTCCATGGCGGGGGCCCTGGTTAGGACTACAGATGGAAGTGGG<br>G 3'                                 |
| S131D TRBP FOR           | 5'CGCCATGGAAGTGCAGCCCCCTGTCGACCCTCAGC 3'   |
| S262D, S265D<br>TRBP REV | 5'CGGAGCTCACTGAGGACACGGCAGCAGGCAGGGCCCAGGGCACC<br>CAGGTCGCCCAGGTGCGAACTG 3'            |
| S262A, S265A<br>TRBP REV | 5'CGGAGCTCACTGAGGACACGGCAGCAGGCAGGGCCCAGGGCACC<br>CAGGGCGCCCAGGGCGACCCTG 3'            |

AA PACT and DD PACT were cloned as stated previously (Singh et al 2011). The PCR products were subcloned into pGEMT-Easy vector (Promega). Once the sequence and correct mutation was verified, we generated full length mutant ORF in pBSIIKS+ by a three piece ligation with the wt remaining sequence (TRBP phosphorylation mutants made from two mutant products and one wt product ligated into pBSIIKS+). Full length sequences are amino-terminal flag tagged.

PACT dsRNA binding mutants K84A and K189A were cloned using GeneEditor in vitro Site-Directed Mutagenesis System from Promega using the following mutagenic primers:

| Primer         | Sequence                        |
|----------------|---------------------------------|
| K84A PACT FOR  | CGCCAGCTTCGCACTTGTACCTTC        |
| K84A PACT REV  | GAAGGTACAGTGCGAAGCTGGCG         |
| K177A PACT FOR | GAAAGGGGGCATCAGCAAAGCAAGCCAAAAG |
| K177A PACT REV | CTTTTGGCTTGCTTTGCTGATGCCCCCTTTC |

#### *ATPase activity assay*

HEK293T cells were transfected with flag-RIG-I/pEFBOS+ for 24-48hrs. Cells were harvested, washed twice with 1X PBS, then lysed in 100µl lysis buffer (20mM Tris-HCl pH 7.5, 150mM NaCl, 1mM EDTA, 1mM DTT, 20% glycerol, 1% Triton-X, 0.2mM PMSF, 100u/mL aprotonin, 1:100 phosphatase inhibitor cocktail [Sigma]), lysate was then transferred to flag-conjugated agarose beads. After 2 hours of IP, lysate was washed three times with lysis buffer, then eluted with 3X flag peptide (Sigma). 20µl of eluted flag-RIG-I was then mixed with polyI:C, recombinant PACT, or recombinant TRBP as indicated. After 5 minute incubation, mixtures were further incubated in Activity Buffer (500µM ATP, 8.3nM [ $\gamma$ -<sup>32</sup>p] ATP, 50mM Tris-acetate (pH 6.0), 5mM dithiothereitol (DTT), and 1.5mM MgCl<sub>2</sub>) and reaction incubated at 37°C for 30 minutes. 10% of total reaction was then spotted onto TLC PEI Cellulose F plates (Millipore) and resolved in a buffer containing 1M formic acid and 0.5M LiCl. Resulting TLC plate was then scanned using a phosphorimager (Typhoon FLA7000).

### *Recombinant Protein*

The protein coding regions (PACT or TRBP) were subcloned into pET15b (Novagen) to generate in-frame fusion of PACT/TRBP ORF to the histidine tag. The recombinant proteins were expressed and purified as described (Patel and Sen 1998, Singh et al 2011).

### *Transfection*

Transfections of reporters, proteins, and polyI:C was done using Effectene (Qiagen). 5'ppp dsRNA was transfected using 5'ppp dsRNA-lyovec purchased from Invivogen. dsRNA treatment was for 16 hours overnight, 24 hours after reporter and protein vectors were transfected.

### *Luciferase assay*

Luciferase activity was determined using the Dual-Luciferase Reporter Assay System from Promega. Luciferase readings were normalized to Renilla expressed from pRL null. For all luciferase experiments, 200ng of IFN $\beta$ -luc, 1ng of Renilla, 50ng of RIG-I, 50ng of PACT, and 50ng of TRBP (unless otherwise stated) was transfected into HEK293Ts, PACT -/- MEFs, and PKR -/- MEFs. TRBP and PACT concentrations are listed for each experiment. HEK293T cells were harvested 16 hours after dsRNA treatment (50ng of polyI:C and 1 $\mu$ g/mL) 5'ppp dsRNA were used for indicated experiments). Each sample was washed twice with 1X PBS then lysed in 200 $\mu$ l of 1X Passive Lysis Buffer for 5 min. Lysates were spun at 13.2 k for 5 minutes and 15 $\mu$ l of each lysate was transferred to a new tube. 25 $\mu$ l of both Luciferase and Stop and Glo-Renilla reagents were used for

readings. Enzymatic activity was measured using a femtomaster luminometer. Each test was done in triplicate. For each test, luciferase numbers were first normalized to Renilla to account for transfection efficiency. Then, RIG-I + dsRNA stimulation was set as 100 and all samples within that set normalized to this positive control.

#### *dsRNA-binding assay*

The in vitro translated, 35S-labeled PACT proteins were synthesized using the TNT-T7 coupled reticulocyte lysate system from Promega and the dsRNA-binding activity was measured by using the previously established poly(I)-poly(C)-agarose binding assay (Patel 1992, Patel 1998). 4  $\mu$ l of in vitro translation products were diluted with 25  $\mu$ l of binding buffer (20 mM Tris, pH 7.5, 0.3 M NaCl, 5 mM MgCl<sub>2</sub>, 1 mM DTT, 0.1 mM PMSF, 0.5% IGEPAL, 10% glycerol) and incubated with 25  $\mu$ l of poly(I)-poly(C)-agarose beads at 30 °C for 30 min. The beads were washed 4 times with 500  $\mu$ l of binding buffer and the bound proteins were analyzed by SDS-PAGE and fluorography. For competition assay with soluble ssRNA or dsRNA, 1  $\mu$ g of poly(C) or poly(I)-poly(C) was incubated with the proteins for 15 min at 30 °C before the addition of poly(I)-poly(C)-agarose beads. To ascertain specific interaction between PACT proteins and poly(I)-poly(C)-agarose beads, in vitro translated, 35S-labeled firefly luciferase protein was assayed for binding to the poly(I)-poly(C)-agarose beads using same conditions. The T lanes represent total radioactive proteins in the reticulocyte lysate and B lanes represent the proteins that remain bound to poly(I)-poly(C)- agarose beads after washing. The poly(I)-poly(C)- agarose binding was quantified on Typhoon FLA7000 by analyzing the band intensities in

T and B lanes. The percentage of PACT proteins bound to poly(I)·poly(C)-agarose was calculated from these values (% binding = 100 X band intensity in B lane/band intensity in T lane), and was plotted as bar graphs

#### *Quantification*

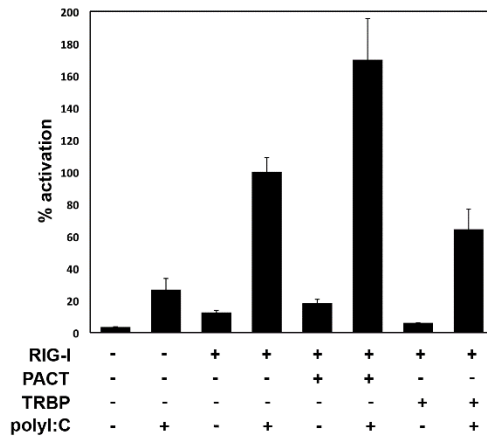
All radioactive TLC and SDS-PAGE gel scans (Typhoon FLA7000) were quantified using GE Life Sciences ImageQuant TL software. Each experiment was normalized to internal controls.

#### **4.4 Results:**

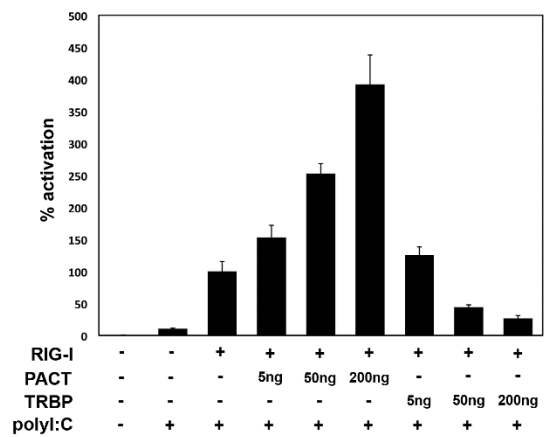
*TRBP is a robust inhibitor of RIG-I signaling.*

As PACT is an established activator of RIG-I signaling, but PACT and TRBP have opposite effects on PKR signaling, we examined the effect of TRBP on RIG-I induced activation of IFN- $\beta$  production in HEK293T cells. As seen in Figure 4.2 A, PACT augments RIG-I mediated IFN- $\beta$  production in response to polyI:C as previously documented. In contrast to this, TRBP inhibits RIG-I mediated IFN $\beta$  production in response to polyI:C by approximately 40%. Previously, LGP2 was reported to act as an inhibitor of MDA5 mediated IFN- $\beta$  production at high concentrations but act as an activator at lower concentrations (Bruns et al. 2014). In order to examine any concentration-dependent effects of TRBP on RIG-I signaling, a dose response curve was performed (Figure 4.2 B). The results exhibit a PACT concentration-dependent gradual increase in IFN- $\beta$  production, and a dose-dependent decrease in IFN- $\beta$  production with TRBP. It is also

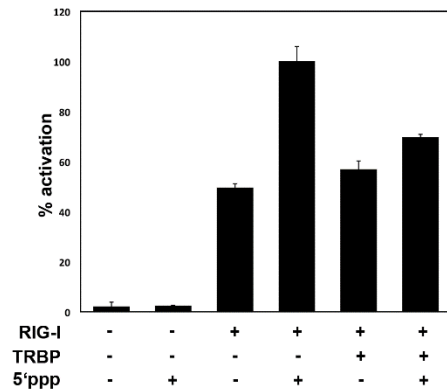
A. IFN- $\beta$  luc



B. IFN- $\beta$  luc



C. IFN- $\beta$  luc



D. IFN- $\beta$  luc

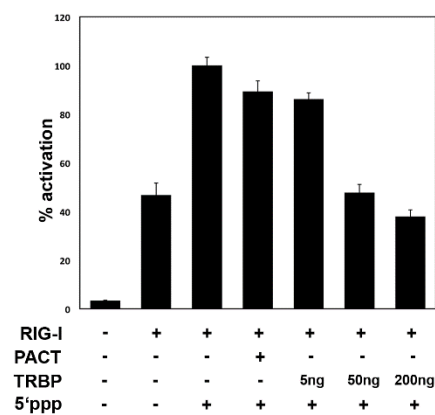


**Figure 4.2 TRBP inhibits RIG-I mediated interferon production in response to polyI:C and 5'ppp dsRNA. (A and B) IFN- $\beta$  induction after polyI:C treatment.** HEK293Ts were transfected with IFN- $\beta$  reporter, expression constructs for RIG-I, and either 50ng of PACT or TRBP as indicated, then treated with polyI:C. pRLnull plasmid was co-transfected for normalization of transfections. Cell extracts were assayed for dual luciferase activity. **(C and D) IFN- $\beta$  induction after 5'ppp dsRNA treatment.** HEK293Ts were transfected with IFN- $\beta$  reporter, RIG-I, and 50ng of PACT or 5ng, 50ng, or 200ng of TRBP as indicated, then treated with 5'ppp dsRNA. pRLnull plasmid was co-transfected for normalization of transfections. Cell extracts were assayed for dual luciferase activity.

important to note that TRBP inhibits RIG-I signaling even in the absence of polyI:C (Figure 4.2 A, Figure 4.2 D). This indicates that TRBP may function as an inhibitor of RIG-I mediated signaling in response to activators of RIG-I other than polyI:C.

It has been shown previously that PACT can enhance RIG-I signaling in the absence of any RNA activator as well as in response to polyI:C, but shows no additional enhancement in response to RIG-I's best-characterized activator, 5'ppp-dsRNA. We wanted to examine TRBP's effect on RIG-I signaling in the presence of 5'ppp-dsRNA. As seen in Figure 4.2C, unlike PACT, TRBP inhibits RIG-I signaling in response to 5'ppp-capped dsRNA, which is in agreement of results in Figure 4.2B and indicate a direct inhibition of RIG-I signaling by TRBP regardless of the activator. A dose response curve with increasing concentrations of TRBP in the presence of 5'ppp-dsRNA shows a concentration-dependent inhibition of RIG-I signaling (Figure 4.2 D). These results establish that TRBP inhibits RIG-I mediated IFN- $\beta$  production in response to various RIG-I ligands.

*TRBP-Mediated inhibition of RIG-I is independent of PACT as well as PKR.*

Previous work has shown that TRBP interacts directly with both PACT as well as PKR to inhibit PKR's kinase activity. Since TRBP, PACT, and PKR interact with each other to influence PKR activation and signaling during cellular stress and viral infections, we next examined if TRBP's inhibition of RIG-I signaling was direct or was mediated via the actions of PACT or PKR. In addition, PKR has been shown to enhance IFN production during viral infections (Taghavi and Samuel 2012, McAllister et al. 2012). To determine if



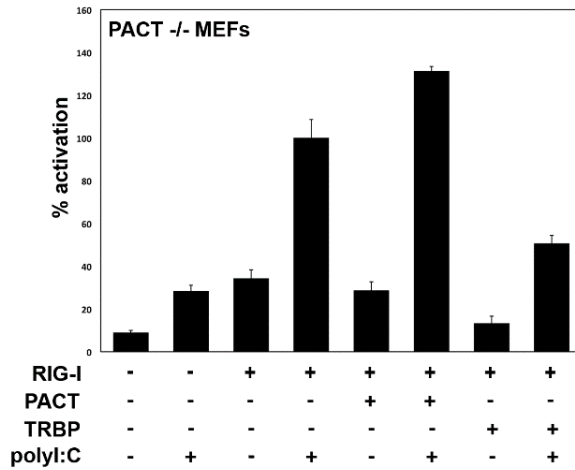
TRBP could inhibit RIG-I in the absence of PACT, we performed experiments similar to the ones shown in Figure 4.2 in PACT  $-/-$  MEFs. As seen in Figure 4.3 A, in the absence of PACT, TRBP is still able to inhibit RIG-I signaling in untreated and polyI:C treated cells. Similarly, the role of PKR in TRBP mediated inhibition of RIG-I signaling was addressed by using PKR  $-/-$ MEFs. As seen in Figure 4.3 B, TRBP is able to inhibit RIG-I signaling in response to polyI:C treatment in the absence of PKR. As the absence of both PACT and PKR have no effect on TRBP's ability to inhibit RIG-I signaling, PACT and PKR likely do not play any role in TRBP-mediated inhibition of RIG-I.

*Mapping PACT and TRBP domains required for effect on RIG-I mediated signaling.*

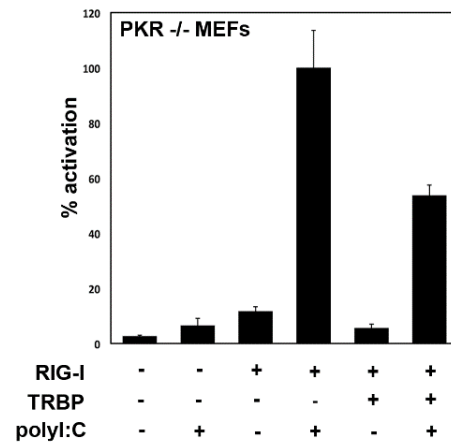
In order to map the domains of PACT required for enhancement of RIG-I signaling, deletion constructs of PACT were utilized as represented in Figure 4.4 A. The three dsRBDs by themselves and the combinations of two dsRBDs were tested for their effect of RIG-I mediated signaling (Huang et al 2002) (Figure 4.4 A).

Figure 4.4 B shows that full length PACT increases activation of RIG-I signaling in response to polyI:C by about 65%, whereas M1M2 and M1 alone can only activate by about 30%. Interestingly, M2M3 inhibits RIG-I signaling by about 30%, but M2 and M3 domains alone have no effect on downstream signaling. This indicates that M1 domain of PACT is important for PACT's ability to activate RIG-I and deletion of M1 domain surprisingly results in an inhibition of RIG-I signaling. As M2M3 of PACT is able to inhibit signaling similar to TRBP, understanding the structural differences between PACT and TRBP become more important. Given the high degree of sequence similarity between

A. IFN-β luc



B. IFN-β luc



**Figure 4.3 TRBP-mediated inhibition of RIG-I requires neither PACT nor PKR. A. PACT requirement for TRBP inhibition of RIG-I signaling.** PACT  $-/-$  MEFs were transfected with IFN-β reporter, RIG-I, PACT, and/or TRBP as indicated, then treated with polyI:C. pRLnull plasmid was co-transfected for normalization of transfections. Cell extracts were assayed for dual luciferase activity. **B. PKR requirement for TRBP inhibition of RIG-I signaling.** PKR  $-/-$  MEFs were transfected with IFN-β reporter, RIG-I, and TRBP as indicated, then treated with polyI:C. pRLnull plasmid was co-transfected for normalization of transfections. Cell extracts were assayed for dual luciferase activity.

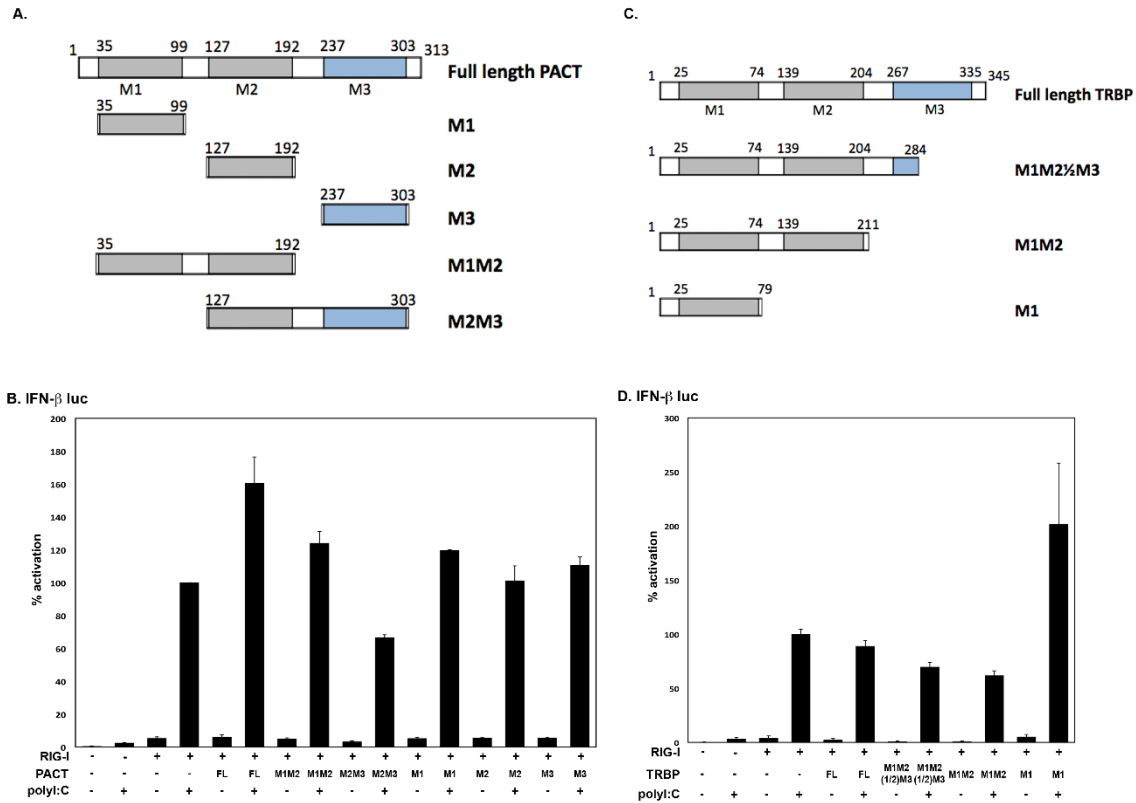


**Figure 4.4 Mapping the domains of PACT and TRBP required for influencing RIG-I mediated signaling. A. Schematic of PACT domain constructs.** Deletion constructs for each of PACT's functional domains were made to assess effect on RIG-I signaling. **B. Ability of PACT domains to affect RIG-I mediated IFN- $\beta$  induction.** HEK293Ts were transfected with IFN- $\beta$  reporter, RIG-I, and 50ng of the expression constructs for either full length PACT or domains of PACT as indicated, then treated with polyI:C. pRLnull plasmid was co-transfected for normalization of transfections. Cell extracts were assayed for dual luciferase activity. **C. Schematic of TRBP domain constructs.** Deletion constructs for each of PACT's functional domains were made to assess effect on RIG-I signaling. **D. Ability of TRBP domains to affect RIG-I mediated IFN- $\beta$  induction.** HEK293Ts were transfected with IFN- $\beta$  reporter, RIG-I, and 50ng of either wt TRBP or domains of TRBP as indicated, then treated with polyI:C. pRLnull plasmid was co-transfected for normalization of transfections. Cell extracts were assayed for dual luciferase activity.

PACT and TRBP, it is interesting to note that the differences that possibly result in structural changes are important for their dramatically different cellular functions and effects on signaling.

Similarly, In order to map the domains of TRBP required for inhibition of RIG-I signaling, deletion constructs of TRBP were utilized as represented in Figure 4.4 C. Figure 4.4 D shows that full length TRBP is able to inhibit RIG-I signaling in response to polyI:C, and with progressive C-terminal M3 domain deletions, the inhibition increases with M1M2 of TRBP inhibiting RIG-I signaling significantly more than full length TRBP. Surprisingly, the M1 domain of TRBP is able to robustly activate RIG-I signaling similar to full length PACT and M1 of PACT. These results point to the importance of the M2 domain of TRBP for inhibition of RIG-I signaling. Together, this demonstrates that both PACT and TRBP's M1 domain is able to enhance RIG-I signaling and that TRBP's M2 domain appears to be important for inhibitory effect on RIG-I signaling (Figure 4.4 B and D).

*Neither PACT nor TRBP's phosphorylation state influences RIG-I mediated signaling.*

Phosphorylation of PACT and TRBP in response to cellular stress influences their interactions with various binding partners including PKR and result in significant changes in signaling outcomes (Peters et al. 2006, Singh et al. 2009, Singh et al. 2011, Paroo et al. 2009, Nakamura et al. 2015, Vaughn et al. 2015). Thus, we wanted to know if PACT and TRBP's phosphorylation status changes their effects on RIG-I mediated signaling. PACT has two known phosphorylation sites that are involved in signaling in response to

oxidative and endoplasmic reticulum (ER) stress; serine 246 (constitutive) and serine 287 (stress induced) (Peters et al. 2006, Singh et al. 2009, Singh et al. 2011). To address the effect of PACT phosphorylation on RIG-I signaling, both serine 246 and 287 were mutated to either alanine to mimic unphosphorylated (inactive state during PKR signaling) PACT or to aspartic acid to mimic phosphorylated (activated state during PKR signaling) PACT (Figure 4.5 A). As seen in Figure 4.5B, neither the phospho-defective AA, or phospho-mimic DD mutant showed any difference in the ability to enhance RIG-I signaling in comparison to wt PACT. These results indicate that the sites that are known to be phosphorylated during oxidative and endoplasmic reticulum stress have no influence in regulation of PACT mediated enhancement of RIG-I signaling.

Similarly, phosphorylation of TRBP has been linked to changes in its ability to inhibit PKR during metabolic stress as well as to stabilize miRNA-generating complexes (Paroo et al. 2009, Nakamura et al. 2015). Four phosphorylation sites in TRBP (serines 142, 152, 283, and 286) are targets of mitogen-activated protein kinase (MAPK) Erk and JNK, and are of functional significance during RNAi and metabolic stress (Paroo et al. 2009, Nakamura et al. 2015). It has been shown that changes in phosphorylation state of TRBP alter TRBP's stability in cells (Paroo et al. 2009, Nakamura et al. 2015). *In vitro* PKR activity assays showed that phospho-defective TRBP could inhibit PKR activity, but that phospho-mimetic TRBP was unable to inhibit PKR signaling (Nakamura et al. 2015). Phosphorylation status of TRBP also influences binding affinity for PKR (Nakamura et al. 2015). These findings indicate the importance of phosphorylation in determining TRBP's activity and suggest a possible role of TRBP phosphorylation in its ability to inhibit RIG-I

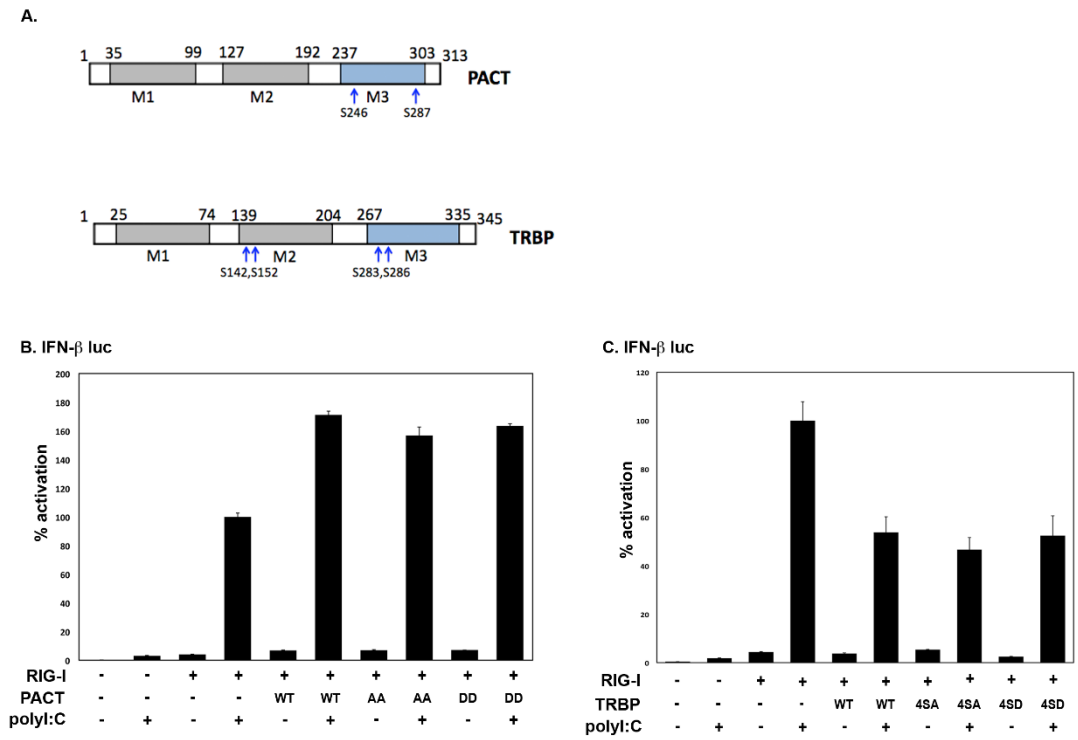


**Figure 4.5 Phosphorylation of PACT and TRBP does not influence RIG-I mediated signaling. A. Schematic of phosphorylation sites of PACT and TRBP.** Residues previously determined to be phosphorylated and important for PKR signaling were mutated from serine to alanine (phospho-defective) or aspartic acid (phospho-mimic). **B. Phosphorylation of PACT does not affect RIG-I signaling.** HEK293Ts were transfected with IFN- $\beta$  reporter, RIG-I, and 50ng of either wt PACT or phosphorylation mutants AA or DD of PACT as indicated, then treated with polyI:C. pRLnull plasmid was co-transfected for normalization of transfections. Cell extracts were assayed for dual luciferase activity. **C. Phosphorylation of TRBP does not affect RIG-I signaling.** HEK293Ts were transfected with IFN- $\beta$  reporter, RIG-I, and 50ng of either wt TRBP or phosphorylation mutants 4SA or 4SD of TRBP as indicated, then treated with polyI:C. pRLnull plasmid was co-transfected for normalization of transfections. Cell extracts were assayed for dual luciferase activity.

signaling. All serines that are known to be phosphorylated in TRBP were mutated to alanines to mimic unphosphorylated state (4SA) or aspartic acids to mimic a phosphorylated state (4SD) (Figure 4.5 A). In Figure 4.5 C, a comparison of the ability of wt TRBP, 4SA, and 4SD to inhibit RIG-I signaling is shown. Neither mutant 4SA nor mutant 4SD exhibited a significantly different inhibitory activity towards RIG-I signaling. This indicates that while TRBP phosphorylation status has been shown to play a crucial role during PKR signaling and RNAi, it appears to have no significant effect on the ability of TRBP to inhibit RIG-I signaling. This demonstrates that TRBP activity may be regulated differently in response to various stress signals, a feature it shares with PACT.

*TRBP but not PACT's dsRNA-binding ability influences RIG-I signaling.*

Being a cytoplasmic PRR that detects non-self dsRNA in cells to initiate anti-viral signaling, RIG-I's dsRNA-binding activity is critical for its ability to identify non-self molecules. Both PACT and TRBP have two conserved dsRBMs that can bind to dsRNA, and thus they may affect RIG-I activity via their ability to sequester such RNAs. PACT and TRBP have opposite effects on PKR activity, another non-traditional PRR for dsRNA, and TRBP sequesters dsRNA to keep it from activating PKR during HIV infection. This leads to the question if PACT or TRBP's ability to bind dsRNA could affect its ability to activate or inhibit RIG-I signaling. PACT activation of RIG-I signaling could be via dsRNA recruitment and TRBP inhibition through sequestration of dsRNA away from RIG-I. To test this, PACT and TRBP mutants defective in dsRNA-binding were made based on the knowledge of similar mutations in conserved domains of PKR (Patel et al. 1996), each a single

mutation in either the M1 or M2 dsRBM (Figure 4.6 A). dsRNA-binding activity was tested and compared to wt PACT and wt TRBP dsRNA-binding ability (Figure 4.6 B and C). Both single mutations in PACT and TRBP showed significantly less dsRNA-binding as compared to wt proteins (Figure 4.6 B and C).

After verification of a reduction in dsRNA-binding activities, both PACT and TRBP mutants' ability to alter RIG-I signaling was assessed (Figure 4.6 D and E). Surprisingly, mutants of PACT lacking the ability to bind dsRNA were still able to activate RIG-I similar to wt PACT (Figure 4.6 D). This indicates that dsRNA-binding of PACT is not required for its ability to enhance RIG-I signaling.

Single point mutations in TRBP's dsRNA-binding domains were not as effective at abolishing dsRNA-binding as those in PACT, but only were able to reduce dsRNA-binding by about 45% (Figure 4.6 B and C). Though dsRNA-binding was not completely compromised, a decrease in ability to inhibit RIG-I signaling was seen (Figure 4.6 E). This indicates a potential role of dsRNA sequestration away from RIG-I, thereby blocking RIG-I's activation by dsRNA.

*Neither PACT nor TRBP affect RIG-I's ATPase activity in the presence of a dsRNA activator.*

Previous work with RIG-I has linked RIG-I's helicase and ATPase activity with initiation of downstream signaling, though it has been shown that ATPase activity is not essential for signaling (Bamming and Horvath 2009). PACT was shown previously to activate RIG-I's ATPase activity *in vitro*, giving a possible mechanism for PACT mediated



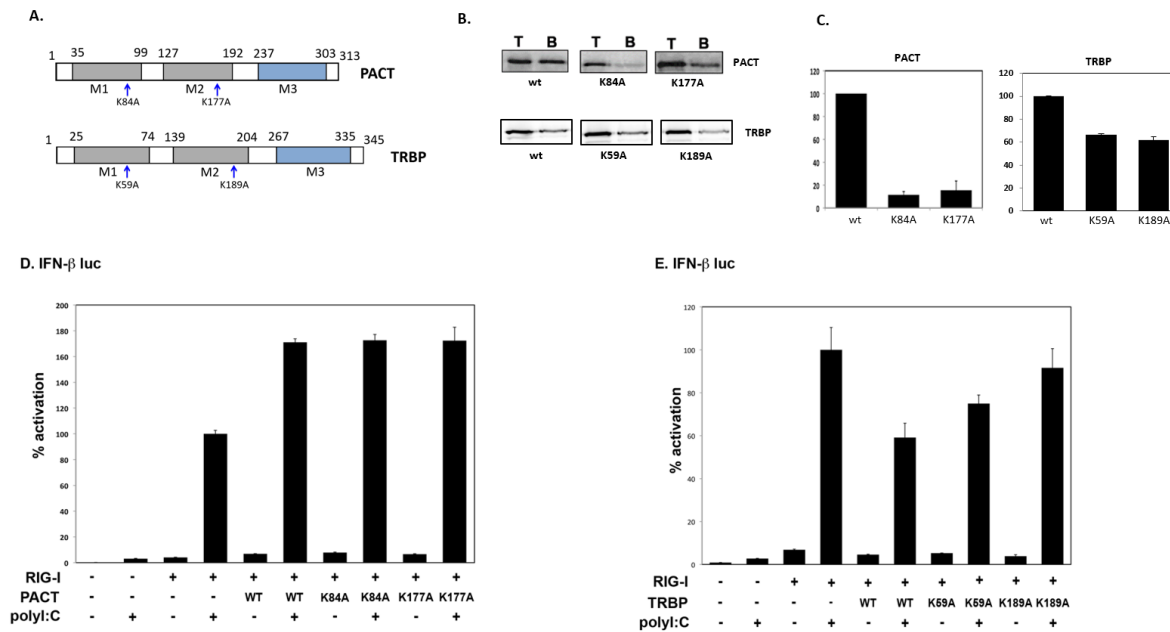


**Figure 4.6 dsRNA binding ability of TRBP but not that of PACT influences RIG-I induced IFN production. A. Schematic of dsRNA-binding mutations of PACT and TRBP.** Residues mutated from lysine to alanine based on previously established mutations that abolish dsRNA binding. **B. dsRNA-binding assay.** dsRNA-binding ability of wt and mutant PACT and TRBP was measured by polyI:C-agarose binding assay with *in vitro* translated  $^{35}\text{S}$ -labeled proteins. T, total input; B, protein bound to polyI:C agarose. **C. Quantification of data in 5.5 B.** Radioactivity in both total input and bound protein bands was quantified, and % bound was calculated by (bound protein/total input) \* 100. The error bars represent standard deviation calculated from 2 experiments. **D. dsRNA-binding ability of PACT does not affect RIG-I signaling.** HEK293Ts were transfected with IFN- $\beta$  reporter, RIG-I, and 50ng of either wt PACT or dsRNA-binding mutants K84A or K177A of PACT as indicated, then treated with polyI:C. pRLnull plasmid was co-transfected for normalization of transfections. Cell extracts were assayed for dual luciferase activity. **E. dsRNA-binding ability of TRBP aids in inhibition of RIG-I signaling.** HEK293Ts were transfected with IFN- $\beta$  reporter, RIG-I, and 50ng of either wt TRBP or dsRNA-binding mutants K59A or K189A of TRBP as indicated, then treated with polyI:C. pRLnull plasmid was co-transfected for normalization of transfections. Cell extracts were assayed for dual luciferase activity.

enhancement of RIG-I signaling (Kok et al. 2011). To investigate TRBP's effect on RIG-I's ATPase activity, an *in vitro* ATPase activity assay was performed with purified RIG-I and a combination of polyI:C and either recombinant PACT or TRBP (Figure 4.7).

First, a polyI:C curve was performed to identify the lowest concentration of polyI:C necessary to activate RIG-I to allow for an increase or decrease in ATPase activity to be visualized. Figure 4.7 A and B shows that as little as 10ng of polyI:C was sufficient to activate immunoprecipitated RIG-I, but an additional activation by increasing amounts of polyI:C could still be seen. Using 10ng of polyI:C, either recombinant PACT or TRBP was added to address changes in ATPase activity. As seen in Figure 4.7 C and D, neither PACT nor TRBP were able to affect RIG-I's ATPase activity. To ensure that the lack of effect was not a result of using recombinant proteins produced in bacteria, this experiment was repeated with PACT and TRBP immunoprecipitated from mammalian cells and identical results were seen (data not shown). These results indicate that TRBP inhibits RIG-I signaling without affecting RIG-I's ATPase activity.

#### **4.5 Discussion:**

In this study, we investigated the effect of the dsRNA-binding protein TRBP on RIG-I induced IFN production in response to dsRNA. Our results indicate that TRBP inhibits RIG-I signaling in response to both polyI:C and 5'ppp dsRNA viral mimics (Figure 4.2). TRBP's actions on RIG-I differ from the actions of PACT, which enhances RIG-I signaling only in response to polyI:C and not in response to 5'ppp dsRNA. TRBP inhibition of RIG-I is independent of PACT or PKR, indicating that TRBP affects RIG-I

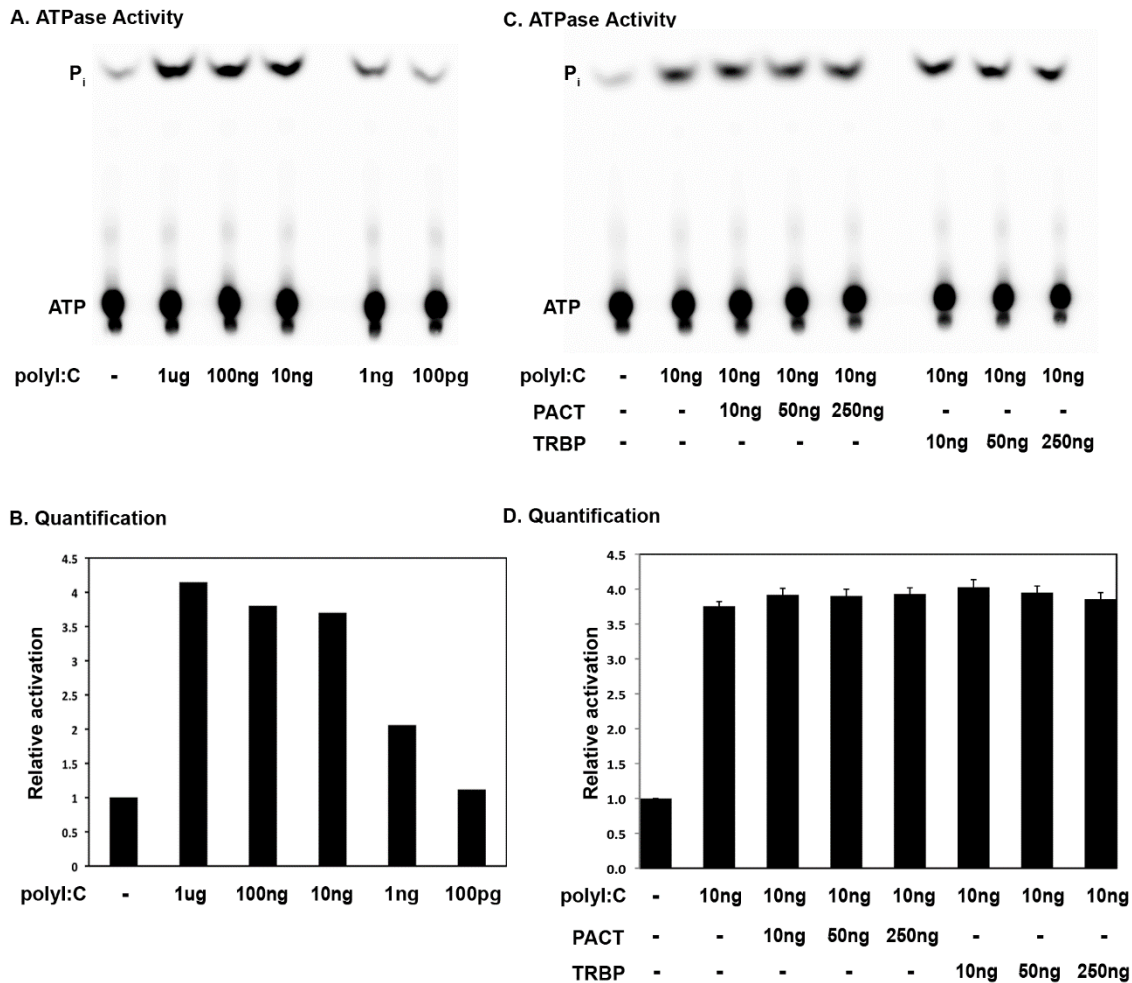


**Figure 4.7 Neither PACT nor TRBP affect RIG-I's ATPase activity in the presence of dsRNA. A. polyI:C dose response for RIG-I activation.** RIG-I immunoprecipitated from HEK293T cells was activated by increasing amounts of polyI:C as indicated to measure RIG-I ATPase activity as determined by ATP hydrolysis. The positions of ATP and free phosphate are as indicated. **B. Quantification of data in 5.6 A.** Radioactivity in the free phosphate and ATP spots was quantified, and samples were first normalized by dividing free phosphate by total (free phosphate plus ATP). To calculate relative fold activation, these normalized numbers were compared to polyI:C control values, which were as considered as 1. **C. Effect of PACT and TRBP on RIG-I's ATPase activity.** RIG-I immunoprecipitated from HEK293T cells was activated by incubation with 1ng polyI:C, and varying amounts of recombinant PACT or TRBP were added as indicated to measure changes in ATPase activity as determined by ATP hydrolysis. **D. Quantification of data in 5.6 C.** Radioactivity in the free phosphate and ATP spots was quantified, and samples were first normalized by dividing free phosphate by total (free phosphate plus ATP). To calculate relative fold activation, these normalized numbers were compared to polyI:C control values, which were as considered as 1.

pathway directly and not by inhibiting PACT from activating RIG-I or via inhibiting PKR activity (Figure 4.3). To help to determine how PACT and TRBP are able to affect RIG-I signaling in opposing ways despite the high degree of homology between them, deletion constructs of both proteins were tested for their effect on RIG-I signaling (Figure 4.4). One surprising finding in this analysis was that the stand-alone M1 domain of TRBP enhances RIG-I signaling instead of inhibiting it, thus indicating that carboxy-terminal region of TRBP serves a strong inhibitory function on RIG-I signaling. Furthermore, The M1 domains of PACT and TRBP both have a positive effect on RIG-I signaling in spite of the full-length proteins having opposite effects. This demonstrates that overall differences protein structure and resulting differences in protein or RNA interactions likely are responsible for their opposing activities. In support of this, it was previously reported that PACT and TRBP exhibit different preferences and affinities for binding to their interacting partners; PACT preferred to form homodimers over binding to dsRNA while TRBP preferred to bind to dsRNA over forming homodimers (Takahashi et al. 2013).

Phosphorylation state of neither PACT nor TRBP showed any effect on RIG-I signaling, which is noteworthy as changes in these phosphorylation sites are essential for changes in signaling through PKR (Figure 4.5). This could indicate that these proteins' activities are constitutive and that post-translational modifications are unable to affect their activities, or that previously unidentified phosphorylation sites or other post-translation modifications are necessary to change PACT and TRBP activity in response to RNA signals. Interestingly, dsRNA-binding ability of PACT was unimportant for activation

of RIG-I signaling during polyI:C treatment, but TRBP's dsRNA-binding activity seems essential for RIG-I inhibition at least in part (Figure 4.6). Inhibition of signaling via sequestration of dsRNA by TRBP has been previously observed for PKR signaling during viral infections. Since the dsRNA-binding mutants of TRBP we tested were not able to eliminate dsRNA-binding completely, it is yet to be determined if dsRNA sequestration can account for all of TRBP's inhibitory capacity. To further test the implications of dsRNA-binding of TRBP on its ability to inhibit RIG-I, the two single point mutations will be combined to create a more effective dsRNA-binding mutant.

While it may be surprising that dsRNA-binding is not necessary for PACT's activities with RIG-I, it has been shown previously that LGP2 which acts as an endogenous activator of MDA5 also does not have a requirement for dsRNA-binding for its activity (Bamming and Horvath 2009). This suggests an alternative form of activation by PACT independent of dsRNA binding. It has been demonstrated previously that PACT forms homodimers readily within stressed cells, and this has been shown to aid in PKR activation. During viral stress, PACT oligomerization may aid in RIG-I's CARD domain oligomerization during viral stress (Vaughn et al 2015, Singh and Patel 2012). RIG-I CARD domain oligomerization has been shown to be either induced by ubiquitination induced oligomerization or through an ubiquitin independent, filament mediated oligomerization (Wu and Hur 2015). Previously, this RIG-I CARD filament has been shown to be induced near dsRNA ends, implicating proximity-induced oligomerization. This proximity-induced oligomerization could be recapitulated through an artificial fusion protein, which could sufficiently enhance anti-viral signaling (Wu and Hur 2015).

This leads to the possibility that multimers of PACT are able to localize RIG-I CARD domains with in close enough proximity to induce oligomerization. A dramatic increase in homodimer formation of PACT during non-viral cellular stress has been demonstrated to be heavily influenced by phosphorylation of PACT at serines 246 and 287, which we have demonstrated here is unable to affect RIG-I signaling (Figure 4.5), thus indicating that additional regulatory modifications on PACT that are yet to be characterized may be involved on its effects on RIG-I.

Last, TRBP does not inhibit RIG-I's ATPase activity in the presence of polyI:C activator *in vitro* (Figure 4.7). This clearly distinguishes TRBP's mode of action on RIG-I signaling pathway compared to that of PACT, as it was previously reported that PACT mediated enhancement of RIG-I signaling occurred mainly via PACT directly binding to RIG-I and stimulating RIG-I's ATPase activity in the absence of a dsRNA (Kok et al 2011). This differs from results previously seen indicating that PACT could activate RIG-I's ATPase activity (Kok et al. 2011), which could possibly be attributed to differences in the use of recombinant RIG-I and immunoprecipitated RIG-I in the RIG-I ATPase activity assay. A schematic model is presented in Figure 4.8, which shows the known activities of PACT and dsRNA in activating RIG-I signaling and the additional novel aspect of RIG-I regulation by TRBP partially through dsRNA sequestration.

Tight regulation of innate immunity is crucial during viral infections and is essential for host survival, while aberrant activation of innate immunity can lead to excessive inflammation and IFN production leading to various pathologies (Crow 2011). Anomalous production of IFN leads to a group of disorders termed interferonopathies,

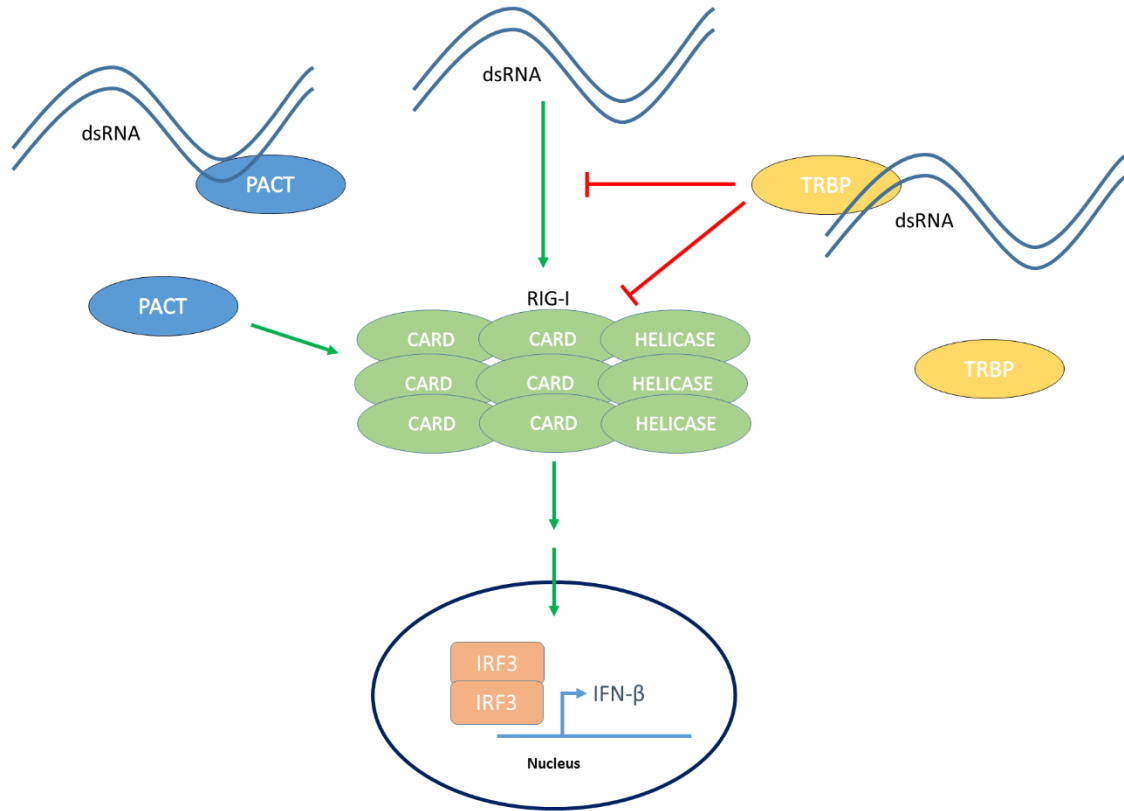


**Figure 4.8 Regulation of RIG-I activation by dsRNA-binding proteins PACT and TRBP.**

During most viral infections, dsRNA is produced as either a replicative intermediate or a by-product during viral replication. This dsRNA is sensed by RIG-I, the cytoplasmic PRR. RIG-I can be activated by both dsRNA itself and by a dsRNA-binding protein PACT. TRBP, another cytoplasmic dsRNA-binding protein, inhibits RIG-I signaling independently of PACT and at least in part through dsRNA sequestration.

highlighting the importance of negative regulation of these pathways when not under a pathogenic threat (Crow 2011). Various types of Interferonopathies have been linked with mutations in RLR and dsRNA binding proteins, which lead to aberrant IFN production and development of disease (Crow 2011, Crow and Manel 2015). PACT activation and TRBP inhibition of RIG-I signaling may help to maintain the delicate balance of IFN production so the host can mount a rapid anti-viral response, and ascertain that the IFN response is not sustained once the pathogen threat is cleared. Lack of TRBP or mutations in TRBP may also lead to increased steady state levels of IFN, though no mutations have yet been identified. The regulatory interplay between these two dsRNA-binding proteins helps to maintain homeostasis during times of cellular stress and during recovery. This work demonstrates that TRBP has a broad ability to inhibit RIG-I regardless of dsRNA activator, highlighting TRBP's importance as a negative regulator in innate immunity. Further research needs to address whether TRBP inhibition of RIG-I signaling is via a direct interaction with RIG-I or a result of inhibition of the signaling steps downstream of RIG-I activation. It also remains to be tested if TRBP can inhibit other PRRs during viral stress.



## CHAPTER 5: GENERAL DISCUSSION

This dissertation focuses on the regulatory roles of the dsRNA-binding proteins PACT, TRBP, PKR, and RIG-I during cellular stress and innate immunity and how these roles might be altered in DYT16 dystonia. Collectively, these dsRNA binding proteins have diverse functions in both discrete and overlapping signaling pathways, which help to maintain homeostasis in the face of cellular stress. This work demonstrates the levels of regulation that dsRNA-binding proteins exert, and how any deviation of this regulation results in disease.

In **Chapter 2**, it was shown that by inhibiting PKR activity by overexpression of a trans-dominant negative mutant during tunicamycin-induced endoplasmic reticulum (ER) stress, we could rescue neuroblastoma cells from an apoptotic fate. The expression of the transcription factor ATF4 and of its transcriptional target CHOP were both drastically inhibited in response to PKR inhibition. In addition, caspase-3 activation, which is a marker of apoptosis, was also significantly inhibited in cells when PKR was inhibited. This establishes that PKR signaling during ER stress regulates apoptosis in neuronal cells and further establishes the ubiquitous nature of the PKR stress response pathway. The ability of PKR to control apoptosis during cellular stress is especially pertinent to disease pathologies, including neurodegenerative diseases like Alzheimer's. In addition to neurodegenerative diseases, this research indicates the possibility of an altered stress response in neurons as a possible mechanism where the DYT16 PACT mutations lead to the movement disorders seen in dystonia patients. This work also

demonstrates that PKR inhibition during cellular stress may be beneficial in preventing apoptosis and neurodegeneration in patients and therefore, PKR may be a good target for drug development for the treatment of neurodegenerative diseases.

In **Chapter 3**, changes in PACT activity caused by the P222L mutation found in DYT16 dystonia were investigated in the context of tunicamycin-induced ER stress. Lymphoblasts derived from patients bearing the P222L homozygous mutations exhibited enhanced apoptosis in response to ER stress as compared to wt lymphoblasts. This enhanced apoptotic response resulted from altered interactions leading to a delayed PKR-eIF2 response. First, increased interactions of P222L PACT with TRBP lead to slower kinetics of PKR activation following stress. In addition, P222L PACT mutation also increased PACT-PACT homodimer interactions as well as PACT-PKR heterodimer interactions ultimately resulting in a delayed but more robust and sustained PKR activation contributing to the enhanced apoptosis seen in the patient lymphoblasts. This work highlights the importance of regulating the speed and duration of PKR activation and eIF2 $\alpha$  phosphorylation in determining cellular fate as well as presenting a cellular consequence of one of the dystonia causing point mutations. Our results also suggest that other cellular pathways in which PACT is functionally involved may be affected by the P222L mutation and future work can examine the effect of dystonia-causing P222L mutation on regulation of innate immunity and RNA interference by PACT.

In **Chapter 4**, it was shown that TRBP plays an inhibitory role in RIG-I mediated induction of interferon (IFN) in response to polyI:C dsRNA, a viral mimic. This introduces an additional pathway where PACT acts as an activator and TRBP as an inhibitor of

signaling, reminiscent to the regulation of PKR signaling. The results showed that TRBP inhibits RIG-I induced IFN production, at least in part, by directly inhibiting RIG-I signaling in response to both polyI:C and 5'ppp dsRNA. The results also demonstrated that dsRNA-binding is an important aspect of TRBP's activity (unlike PACT) on RIG-I signaling, suggesting dsRNA sequestration as a main inhibitory mechanism. These results also highlight the importance of negative regulation of innate immunity, as aberrant IFN production can lead to development of diseases termed interferonopathies as well as other auto-inflammatory diseases. This work establishes a regulatory interplay between the two dsRNA-binding proteins PACT and TRBP in RIG-I mediated interferon production and this regulation could have wide implications on viral susceptibility, disease progression, and antiviral immunity.

## REFERENCES

- Aguzzi A and O'Connor T. (2010). "Protein aggregation diseases: pathogenicity and therapeutic perspectives." *Nat Rev Drug Discov* 9: 237-248.
- Ahmad S and Hur S. (2015) "Helicases in Antiviral Immunity: Dual Properties as Sensors and Effectors." *Trends in Biochemical Sciences*. 40(10):576-585.
- Alirezai M, Watry DD, Flynn, CF, Kiosses WB, Masliah E, Williams BR, Kaul M, Lipton SA and Fox HS. (2007). "Human immunodeficiency virus-1/surface glycoprotein 120 induces apoptosis through RNA-activated protein kinase signaling in neurons." *J Neurosci* 27: 11047-11055.
- Anderson MA and Gusella JF. (1984). "Use of cyclosporin A in establishing Epstein-Barr virus-transformed human lymphoblastoid cell lines." *In Vitro* 20: 856-858.
- Bamming D, Horvath CM. (2009) "Regulation of signal transduction by enzymatically inactive antiviral RNA helicase proteins MDA5, RIG-I, and LGP2." *J Biol Chem*. 284(15):9700-12
- Bando Y, Onuki R, Katayama T, Manabe T, Kudo T, Taira K and Tohyama M. (2005). "Double-strand RNA dependent protein kinase (PKR) is involved in the extrastriatal degeneration in Parkinson's disease and Huntington's disease." *Neurochem Int* 46: 11-18.

- Benkirane M, Jin DY, Chun RF, Koup RA and Jeang KT. (1997). "Mechanism of transdominant inhibition of CCR5-mediated HIV-1 infection by ccr5delta32." J Biol Chem 272(49): 30603-30606.
- Benkirane M, Neuveut C, Chun RF, Smith SM, Samuel CE, Gatignol A and Jeang KT. (1997). "Oncogenic potential of TAR RNA binding protein TRBP and its regulatory interaction with RNA-dependent protein kinase PKR." Embo J 16: 611-624.
- Bennett RL, Blalock WL and May WS. (2004). "Serine 18 phosphorylation of RAX, the PKR activator, is required for PKR activation and consequent translation inhibition." J Biol Chem 279(41): 42687-42693.
- Bennett RL, Blalock WL, Choi EJ, Lee YJ, Zhang Y, Zhou L, Oh SP, May WS. (2008) "RAX is required for fly neuronal development and mouse embryogenesis." Mech Dev. 125(9-10):777-85.
- Bennett RL, Blalock WL, Abtahi DM, Pan Y, Moyer SA and May WS. (2006). "RAX, the PKR activator, sensitizes cells to inflammatory cytokines, serum withdrawal, chemotherapy, and viral infection." Blood 108: 821-829.
- Bragg DC, Armata IA, Nery FC, Breakefield XO and Sharma N. (2011). "Molecular pathways in dystonia." Neurobiol Dis 42(2): 136-147.
- Brashear, A. (2013). "Commentary." Mov Disord 28: 1939.
- Bressman SB. (2007). "Genetics of dystonia: an overview." Parkinsonism Relat Disord 13 Suppl 3: S347-355.

- Bruns AM, Leser GP, Lamb RA, Horvath CM. (2014) "The innate immune sensor LGP2 activates antiviral signaling by regulating MDA5-RNA interaction and filament assembly." *Mol Cell*. 55(5):771-81.
- Camargos S, Scholz S, Simon-Sanchez J, Paisan-Ruiz C, Lewis P, Hernandez D, Ding J, Gibbs JR, Cookson MR, Bras J, Guerreiro R, Oliveira CR, Lees A, Hardy J, Cardoso F and Singleton AB. (2008). "DYT16, a novel young-onset dystonia-parkinsonism disorder: identification of a segregating mutation in the stress-response protein PRKRA." *Lancet Neurol* 7(3): 207-215.
- Camargos S, Lees AJ, Singleton A and Cardoso F. (2012). "DYT16: the original cases." *J Neurol Neurosurg Psychiatry* 83: 1012-1014.
- Chang KY and Ramos A. (2005). "The double-stranded RNA-binding motif, a versatile macromolecular docking platform." *FEBS J* 272(9): 2109-2117.
- Chang RC, Suen KC, Ma CH, Elyaman W, Ng HK and Hugon J. (2002). "Involvement of double-stranded RNA-dependent protein kinase and phosphorylation of eukaryotic initiation factor-2alpha in neuronal degeneration." *J Neurochem* 83: 1215-1225.
- Chang RC, Wong AK, Ng HK and Hugon J. (2002). "Phosphorylation of eukaryotic initiation factor-2alpha (eIF2alpha) is associated with neuronal degeneration in Alzheimer's disease." *Neuroreport* 13: 2429-2432.
- Chen G, Ma C, Bower KA, Ke Z and Luo J. (2006). "Interaction between RAX and PKR modulates the effect of ethanol on protein synthesis and survival of neurons." *J Biol Chem* 281: 15909-15915.

Chen HM, Wang L and D'Mello SR. (2008). "A chemical compound commonly used to inhibit PKR, {8-(imidazol-4-ylmethylene)-6H-azolidino[5,4-g] benzothiazol-7-one}, protects neurons by inhibiting cyclin-dependent kinase." *Eur J Neurosci* 28: 2003-2016.

Chendrimada TP, Gregory RI, Kumaraswamy E, Norman J, Cooch N, Nishikura K, Shiekhattar R. "TRBP recruits the Dicer complex to Ago2 for microRNA processing and gene silencing." *Nature*. 436(7051):740-4.

Clerzius G, Shaw E, Daher A, Burugu S, Gélinas JF, Ear T, Sinck L, Routy JP, Mouland AJ, Patel RC, Gatignol A. (2013) "The PKR activator, PACT, becomes a PKR inhibitor during HIV-1 replication." *Retrovirology*. 10:96.

Cole JL. (2007). "Activation of PKR: an open and shut case?" *Trends Biochem Sci* 32(2): 57-62.

Cosentino GP, Venkatesan S, Serluca FC, Green SR, Mathews MB and Sonenberg N. (1995). "Double-stranded-RNA-dependent protein kinase and TAR RNA-binding protein form homo- and heterodimers in vivo." *Proc Natl Acad Sci USA* 92(21): 9445-9449.

Crow YJ and Manel N. (2015) "Aicardi-Goutieres syndrome and the type-I interferonopathies" *Nature Reviews Immunology*. 15:429-440.

Crow YJ. (2011) "Type I interferonopathies: a novel set of inborn errors of immunity." *Ann N Y Acad Sci*. 1238:91-8.

Daher A, Laraki G, Singh M, Melendez-Peña CE, Bannwarth S, Peters AH, Meurs EF, Braun RE, Patel RC, Gatignol A. (2009) "TRBP control of PACT-induced



- phosphorylation of protein kinase R is reversed by stress." *Mol Cell Biol.* 29(1):254-65.
- Daher A, Longuet M, Dorin D, Bois F, Segeral E, Bannwarth S, Battisti PL, Purcell DF, Benarous R, Vaquero C, Meurs EF and Gatignol A. (2001). "Two dimerization domains in the trans-activation response RNA-binding protein (TRBP) individually reverse the protein kinase R inhibition of HIV-1 long terminal repeat expression." *J Biol Chem* 276(36): 33899-33905.
- Daniels SM, Melendez-Pena CE, Scarborough RJ, Daher A, Christensen HS, El Far M, Purcell DFJ, Laine S, Gatignol A. (2009) "Characterization of the TRBP domain required for Dicer interaction and function in RNA interference" *BMC Molecular Biology* 10:38.
- Daviet L, Erard M, Dorin D, Duarte M, Vaquero C, Gatignol A. (2000) "Analysis of a binding difference between the two dsRNA-binding domains in TRBP reveals the modular function of a KR-helix motif." *Eur J Biochem.* 267(8):2419-31
- de Carvalho Aguiar P, Borges V, Ferraz HB, Ozelius LJ. (2015) "Novel compound heterozygous mutations in PRKRA cause pure dystonia." *Mov Disord.* 30(6):877-8
- Dickerman BK, White CL, Chevalier C, Nalesso V, Charles C, Fouchécourt S, Guillou F, Viriot L, Sen GC, Hérault Y. (2006). "Missense mutation in the second RNA binding domain reveals a role for Prkra (PACT/RAX) during skull development." *PLoS One.* 6(12):e28537.
- Donnelly N, Gorman AM, Gupta S and Samali A. (2013). "The eIF2alpha kinases: their structures and functions." *Cell Mol Life Sci* 70(19): 3493-3511.

- Dorin D, Bonnet MC, Bannwarth S, Gatignol A, Meurs EF, Vaquero C. (2003) "The TAR RNA-binding protein, TRBP, stimulates the expression of TAR-containing RNAs in vitro and in vivo independently of its ability to inhibit the dsRNA-dependent kinase PKR." *J Biol Chem.* 278(7):4440-8.
- Doyle KM, Kennedy D, Gorman AM, Gupta S, Healy SJ and Samali A. (2011). "Unfolded proteins and endoplasmic reticulum stress in neurodegenerative disorders." *J Cell Mol Med* 15: 2025-2039.
- Eckmann CR, Jantsch MF. (1997). "Xlrpba, a Double-stranded RNA-binding Protein Associated with Ribosomes and Heterogenous Nuclear RNPs." *J. Cell Biol.* 138:239–253.
- Erard M, Barker DG, Amalric F, Jeang KT, Gatignol A. (1998) "An Arg/Lys-rich core peptide mimics TRBP binding to the HIV-1 TAR RNA upper-stem/loop." *J Mol Biol.* 279(5):1085-99
- Fasciano S, Kaufman A, Patel RC. (2007) "Expression of PACT is regulated by Sp1 transcription factor." *Gene* 388(1-2):74-82
- Fawcett TW, Martindale JL, Guyton KZ, Hai T and Holbrook NJ. (1999). "Complexes containing activating transcription factor (ATF)/cAMP-responsive-element-binding protein (CREB) interact with the CCAAT/enhancer-binding protein (C/EBP)-ATF composite site to regulate Gadd153 expression during the stress response." *Biochem J* 339 (Pt 1): 135-141.

- Fuchs T, Gavarini S, Saunders-Pullman R, Raymond D, Ehrlich ME, Bressman SB and Ozelius LJ. (2009). "Mutations in the THAP1 gene are responsible for DYT6 primary torsion dystonia." *Nat Genet* 41: 286-288.
- Galabru J and Hovanessian A. (1987). "Autophosphorylation of the protein kinase dependent on double-stranded RNA." *J Biol Chem* 262(32): 15538-15544.
- Garcia MA, Gil J, Ventoso I, Guerra S, Domingo E, Rivas C and Esteban M. (2006). "Impact of protein kinase PKR in cell biology: from antiviral to antiproliferative action." *Microbiol Mol Biol Rev* 70(4): 1032-1060.
- Garcia MA, Meurs EF and Esteban M. (2007). "The dsRNA protein kinase PKR: Virus and cell control." *Biochimie* 89: 799-811.
- Gatignol A, Buckler C, Jeang KT. (1993) "Relatedness of an RNA-binding motif in human immunodeficiency virus type 1 TAR RNA-binding protein TRBP to human P1/dsl kinase and *Drosophila* staufen." *Mol Cell Biol.* 13(4):2193-202
- Gatignol A, Buckler-White A, Berkhout B, Jeang KT. (1991) "Characterization of a human TAR RNA-binding protein that activates the HIV-1 LTR." *Science.* 251(5001):1597-600.
- Geyer HL and Bressman SB. (2006) "The diagnosis of dystonia." *Lancet Neurol.* 5(9):780-90.
- Gordon KL, Glenn KA, and Gonzalez-Alegre P. (2011). "Exploring the influence of torsinA expression on protein quality control." *Neurochem Res* 36: 452-459.
- Gorman AM, Healy SJ, Jager R and Samali A. (2012). "Stress management at the ER: regulators of ER stress-induced apoptosis." *Pharmacol Ther* 134: 306-316.

- Green SR and Mathews MB. (1992). "Two RNA-binding motifs in the double-stranded RNA-activated protein kinase, DAI." *Genes Dev* 6: 2478-2490.
- Gupta V and Patel RC. (2002) "Proapoptotic protein PACT is expressed at high levels in colonic epithelial cells in mice." *Am J Physiol Gastrointest Liver Physiol.* 283(3):G801-8.
- Gupta V, Huang X, Patel RC. (2003). "The carboxy-terminal, M3 motifs of PACT and TRBP have opposite effects of PKR activity." *Virology* 315(2):283-291.
- Haase AD, Jaskiewicz L, Zhang H, Lainé S, Sack R, Gatignol A, Filipowicz W. (2005) "TRBP, a regulator of cellular PKR and HIV-1 virus expression, interacts with Dicer and functions in RNA silencing." *EMBO Rep.* 6(10):961-7.
- Harding HP, Novoa I, Zhang Y, Zeng H, Wek R, Schapira M and Ron D. (2000). "Regulated translation initiation controls stress-induced gene expression in mammalian cells." *Mol Cell* 6: 1099-1108.
- Hetz C. (2012). "The unfolded protein response: controlling cell fate decisions under ER stress and beyond." *Nat Rev Mol Cell Biol* 13: 89-102.
- Hewett JW, Tannous B, Niland BP, Nery FC, Zeng J, Li Y. and Breakefield, X.O. (2007). "Mutant torsinA interferes with protein processing through the secretory pathway in DYT1 dystonia cells." *Proc Natl Acad Sci U S A* 104: 7271-7276.
- Heyam A, Lagos D, Plevin M. (2015) "Dissecting the roles of TRBP and PACT in double-stranded RNA recognition and processing of noncoding RNAs." *Wiley Interdiscip Rev RNA.* 6(3):271-89.

- Hoozemans JJ and Scheper W. (2012). "Endoplasmic reticulum: the unfolded protein response is tangled in neurodegeneration." *Int J Biochem Cell Biol* 44: 1295-1298.
- Huang X, Hutchins B and Patel RC. (2002). "The C-terminal, third conserved motif of the protein activator PACT plays an essential role in the activation of double-stranded-RNA-dependent protein kinase (PKR)." *Biochem J* 366(Pt 1): 175-186.
- Hugon J, Paquet C, and Chang RC. (2009). "Could PKR inhibition modulate human neurodegeneration?" *Expert Rev Neurother* 9: 1455-1457.
- Ito T, Yang M and May WS. (1999). "RAX, a cellular activator for double-stranded RNA-dependent protein kinase during stress signaling." *J Biol Chem* 274(22): 15427-15432.
- Iwamura T, Yoneyama M, Koizumi N, Okabe Y, Namiki H, Samuel CE, Fujita T. (2001) "PACT, a double-stranded RNA binding protein acts as a positive regulator for type I interferon gene induced by Newcastle disease virus." *Biochem Biophys Res Commun.* 282(2):515-23.
- Katze MG. (1995). "Regulation of the interferon-induced PKR: can viruses cope?" *Trends Microbiol* 3: 75-78.
- Kew C, Lui PY, Chan CP, Liu X, Au SW, Mohr I, Jin DY, Kok KH. (2013) "Suppression of PACT-induced type I interferon production by herpes simplex virus 1 Us11 protein." *J Virol.* 87(24):13141-9
- Klein C. (2008). "DYT16: a new twist to familial dystonia." *Lancet Neurol* 7(3): 192-193.

- Kok KH, Lui PY, Ng MH, Siu KL, Au SW, Jin DY. (2011) "The double-stranded RNA-binding protein PACT functions as a cellular activator of RIG-I to facilitate innate antiviral response." *Cell Host Microbe*. 9(4):299-309.
- Kok KH, Ng MH, Ching YP, Jin DY. (2007) "Human TRBP and PACT directly interact with each other and associate with dicer to facilitate the production of small interfering RNA." *J Biol Chem*. 282(24):17649-57.
- Koscianska E, Starega-Roslan J, Krzyzosiak WJ. (2011) "The role of Dicer protein partners in the processing of microRNA precursors." *PLoS One*. 6(12):e28548.
- Laraki G, Clerzius G, Daher A, Melendez-Pena C, Daniels S and Gatignol A. (2008). "Interactions between the double-stranded RNA-binding proteins TRBP and PACT define the Medipal domain that mediates protein-protein interactions." *RNA Biol* 5(2): 92-103.
- Lee HY, Zhou K, Smith AM, Noland CL, Doudna JA. (2013) "Differential roles of human Dicer-binding proteins TRBP and PACT in small RNA processing." *Nucleic Acids Res*. 41(13):6568-76.
- Lee SB, Green SR, Mathews MB and Esteban M. (1992). "Activation of the double-stranded RNA (dsRNA)-activated human protein kinase in vivo in the absence of its dsRNA binding domain." *Proc Natl Acad Sci U S A* 91(22): 10551-10555.
- Lee Y, Hur I, Park SY, Kim YK, Suh MR, Kim VN. (2006) "The role of PACT in the RNA silencing pathway." *EMBO J*. 25(3):522-32.

- Lemmon ME, Lavenstein B, Applegate CD, Hamosh A, Tekes A, Singer HS. (2013) "A novel presentation of DYT 16: acute onset in infancy and association with MRI abnormalities." *Mov Disord.* 28(14):1937-8.
- Li S, Peters GA, Ding K, Zhang X, Qin J, Sen GC. (2006) "Molecular basis for PKR activation by PACT or dsRNA." *Proc Natl Acad Sci USA.* 103(26):10005-10
- Li S and Sen GC. (2003) "PACT-mediated enhancement of reporter gene expression at the translational level." *J Interferon Cytokine Res.* 23(12):689-97.
- Luthra P, Ramanan P, Mire CE, Weisend C, Tsuda Y, Yen B, Liu G, Leung DW, Geisbert TW, Ebihara H, Amarasinghe GK, Basler CF. (2013) "Mutual antagonism between the Ebola virus VP35 protein and the RIG-I activator PACT determines infection outcome." *Cell Host Microbe.* 14(1):74-84.
- Marchal JA, Lopez GJ, Peran M, Comino A, Delgado JR, Garcia-Garcia JA, Conde V, Aranda, FM, Rivas C, Esteban M and Garcia MA. (2014). "The impact of PKR activation: from neurodegeneration to cancer." *Faseb j* 28: 1965-1974.
- McAllister CS, Taghavi N, Samuel CE. (2012) "Protein kinase PKR amplification of interferon  $\beta$  induction occurs through initiation factor eIF-2 $\alpha$ -mediated translational control." *J Biol Chem.* 287(43):36384-92.
- McCormack SJ, Thomis DC and Samuel CE. (1992). "Mechanism of interferon action: identification of a RNA binding domain within the N-terminal region of the human RNA-dependent P1/eIF-2 alpha protein kinase." *Virology* 188: 47-56.

- McCullough KD, Martindale JL, Klotz LO, Aw TY and Holbrook NJ. (2001). "Gadd153 sensitizes cells to endoplasmic reticulum stress by down-regulating Bcl2 and perturbing the cellular redox state." *Mol Cell Biol* 21: 1249-1259.
- Mencacci NE, Rubio-Agusti I, Zdebik A, Asmus F, Ludtmann MH, Ryten M, Plagnol V, Hauser AK, Bandres-Ciga S, Bettencourt C, Forabosco P, Hughes D, Soutar MM, Peall K, Morris HR, Trabzuni D, Tekman M, Stanescu HC, Kleta R, Carecchio M, Zorzi G, Nardocci N, Garavaglia B, Lohmann E, Weissbach A, Klein C, Hardy J, Pittman AM, Foltynie T, Abramov AY, Gasser T, Bhatia KP, Wood NW. (2015) "A missense mutation in KCTD17 causes autosomal dominant myoclonus-dystonia." *Am J Hum Genet.* 96(6):938-47.
- Meurs E, Chong K, Galabru J, Thomas NS, Kerr IM, Williams BR and Hovanessian AG. (1990). "Molecular cloning and characterization of the human double-stranded RNA-activated protein kinase induced by interferon." *Cell* 62(2): 379-390.
- Mittelstadt M, Frump A, Khuu T, Fowlkes V, Handy I, Patel CV, Patel RC. (2008) "Interaction of human tRNA-dihydrouridine synthase-2 with interferon-induced protein kinase PKR." *Nucleic Acids Research* 36(3):998-1008.
- Nakamura T, Kunz RC, Zhang C, Kimura T, Yuan CL, Baccaro B, Namiki Y, Gygi SP, Hotamisligil GS. (2015) "A critical role for PKR complexes with TRBP in Immunometabolic regulation and eIF2 $\alpha$  phosphorylation in obesity." *Cell Rep.* 11(2):295-307.



- Nakamura T, Furuhashi M, Li P, Cao H, Tuncman G, Sonenberg N, Gorgun CZ and Hotamisligil GS. (2010). "Double-stranded RNA-dependent protein kinase links pathogen sensing with stress and metabolic homeostasis." *Cell* 140: 338-348.
- Nanduri S, Rahman F, Williams BR and Qin J. (2000). "A dynamically tuned double-stranded RNA binding mechanism for the activation of antiviral kinase PKR." *EMBO J* 19(20): 5567-5574.
- Nekhai S, Bottaro DP, Woldehawariat G, Spellerberg A and Petryshyn R. (2000). "A cell-permeable peptide inhibits activation of PKR and enhances cell proliferation." *Peptides* 21: 1449-1456.
- Onuki R, Bando Y, Suyama E, Katayama T, Kawasaki H, Baba T, Tohyama M, Taira K. (2004) "An RNA-dependent protein kinase is involved in tunicamycin-induced apoptosis and Alzheimer's disease." *EMBO J.* 23(4):959-68.
- Ortega LG, McCotter MD, Henry GL, McCormack SJ, Thomis DC and Samuel CE. (1996). "Mechanism of interferon action. Biochemical and genetic evidence for the intermolecular association of the RNA-dependent protein kinase PKR from human cells." *Virology* 215: 31-39.
- Oyadomari S and Mori M. (2004). "Roles of CHOP/GADD153 in endoplasmic reticulum stress." *Cell Death Differ* 11: 381-389.
- Oyadomari S, Koizumi A, Takeda K, Gotoh T, Akira S, Araki E and Mori M. (2002). "Targeted disruption of the Chop gene delays endoplasmic reticulum stress-mediated diabetes." *J Clin Invest* 109: 525-532.

- Paccalin M, Pain-Barc S, Pluchon C, Paul C, Besson MN, Carret-Rebillat AS, Rioux-Bilan A, Gil R and Hugon J. (2006). "Activated mTOR and PKR kinases in lymphocytes correlate with memory and cognitive decline in Alzheimer's disease." *Dement Geriatr Cogn Disord* 22: 320-326.
- Page G, Rioux Bilan A, Ingrand S, Lafay-Chebassier C, Pain S, Perault Pochat MC, Bouras C, Bayer T and Hugon J. (2006). "Activated double-stranded RNA-dependent protein kinase and neuronal death in models of Alzheimer's disease." *Neuroscience* 139: 1343-1354.
- Paquet C, Mouton-Liger F, Meurs EF, Mazot P, Bouras C, Pradier L, Gray F, Hugon J. (2012) "The PKR activator PACT is induced by A $\beta$ : involvement in Alzheimer's disease." *Brain Pathol.* 22(2):219-29.
- Paquet C, Bose A, Polivka M, Peoc'h K, Brouland JP, Keohane C, Hugon J and Gray F. (2009). "Neuronal phosphorylated RNA-dependent protein kinase in Creutzfeldt-Jakob disease." *J Neuropathol Exp Neurol* 68: 190-198.
- Park H, Davies MV, Langland JO, Chang HW, Nam YS, Tartaglia J, Paoletti E, Jacobs BL, Kaufman RJ, Venkatesan S. (1994) "TAR RNA-binding protein is an inhibitor of the interferon-induced protein kinase PKR." *Proc Natl Acad Sci U S A.* 91(11):4713-7.
- Paroo Z, Ye X, Chen S, and Liu Q. (2009) "Phosphorylation of the human micro-RNA generating complex mediates MAPK/Erk signaling" *Cell* 1139(1):12-122.
- Patel CV, Handy I, Goldsmith T and Patel RC. (2000). "PACT, a stress-modulated cellular activator of interferon-induced double-stranded RNA-activated protein kinase, PKR." *J Biol Chem* 275(48): 37993-37998.

- Patel RC and Sen GC. (1992). "Construction and expression of an enzymatically active human-mouse chimeric double-stranded RNA-dependent protein kinase." J Interferon Res 12(5): 389-393.
- Patel RC and Sen GC. (1998). "PACT, a protein activator of the interferon-induced protein kinase, PKR." EMBO J 17(15): 4379-4390.
- Patel RC, Stanton P, McMillan NM, Williams BR and Sen GC. (1995). "The interferon-inducible double-stranded RNA-activated protein kinase self-associates in vitro and in vivo." Proc Natl Acad Sci U S A 92(18): 8283-8287.
- Patel RC, Stanton P, Sen GC. (1996) "Specific mutations near the amino terminus of double-stranded RNA-dependent protein kinase (PKR) differentially affect its double-stranded RNA binding and dimerization properties." J Biol Chem. 271(41):25657-63.
- Patel RC and Sen GC. (1992). "Identification of the double-stranded RNA-binding domain of the human interferon-inducible protein kinase." J Biol Chem 267: 7671-7676.
- Peall KJ, Kuiper A, de Koning TJ, Tijssen MA. (2015) "Non-motor symptoms in genetically defined dystonia: Homogenous groups require systematic assessment." Parkinsonism Relat Disord. 21(9):1031-40
- Peel AL and Bredesen DE. (2003). "Activation of the cell stress kinase PKR in Alzheimer's disease and human amyloid precursor protein transgenic mice." Neurobiol Dis 14: 52-62.
- Peel AL, Rao RV, Cottrell BA, Hayden MR, Ellerby LM and Bredesen DE. (2001). "Double-stranded RNA-dependent protein kinase, PKR, binds preferentially to

- Huntington's disease (HD) transcripts and is activated in HD tissue." *Hum Mol Genet* 10: 1531-1538.
- Peters GA, Hartmann R, Qin J, and Sen GC. (2001). "Modular structure of PACT: distinct domains for binding and activating PKR." *Mol Cell Biol* 21(6): 1908-1920.
- Peters GA, Li S, and Sen GC. (2006). "Phosphorylation of specific serine residues in the PKR activation domain of PACT is essential for its ability to mediate apoptosis." *J Biol Chem* 281(46): 35129-35136.
- Peters GA, Seachrist DD, Keri RA, Sen GC. (2009). "The double-stranded RNA-binding protein, PACT, is required for postnatal anterior pituitary proliferation." *Proc Natl Acad Sci U S A.* 106(26):10696-701
- Peters GA, Khoo D, Mohr I, Sen GC. (2002) "Inhibition of PACT-mediated activation of PKR by the herpes simplex virus type 1 Us11 protein." *J Virol.* 76(21):11054-64.
- Rao RV and Bredesen DE. (2004). "Misfolded proteins, endoplasmic reticulum stress and neurodegeneration." *Curr Opin Cell Biol* 16: 653-662.
- Ron D and Walter P. (2007). "Signal integration in the endoplasmic reticulum unfolded protein response." *Nat Rev Mol Cell Biol* 8: 519-529.
- Ross CA and Poirier MA. (2004). "Protein aggregation and neurodegenerative disease." *Nat Med* 10 Suppl: S10-17.
- Rowe TM and Sen GC. (2001) "Organizations and promoter analyses of the human and the mouse genes for PACT, the protein-activator of the interferon-induced protein kinase, PKR." *Gene.* 273(2):215-25.

- Rowe TM, Rizzi M, Hirose K, Peters GA, Sen GC. (2006) "A role of the double-stranded RNA-binding protein PACT in mouse ear development and hearing." *Proc Natl Acad Sci U S A.* 103(15):5823-8.
- Sadler AJ and Williams BR. (2007). "Structure and function of the protein kinase R." *Curr Top Microbiol Immunol* 316: 253-292.
- Scheuner D, Patel R, Wang F, Lee K, Kumar K, Wu J, Nilsson A, Karin M and Kaufman RJ. (2006). "Double-stranded RNA-dependent protein kinase phosphorylation of the alpha-subunit of eukaryotic translation initiation factor 2 mediates apoptosis." *J Biol Chem* 281: 21458-21468.
- Schlee M. (2012) "Master sensors of pathogenic RNA - RIG-I like receptors" *Immunobiology.* 218:1322-1335.
- Schonthal AH. (2012). "Endoplasmic reticulum stress: its role in disease and novel prospects for therapy." *Scientifica (Cairo)* 2012: 857516.
- Seibler P, Djarmati A, Langpap B, Hagenah J, Schmidt A, Bruggemann N, Siebner H, Jabusch HC, Altenmuller E, Munchau A, Lohmann K and Klein C. (2008). "A heterozygous frameshift mutation in PRKRA (DYT16) associated with generalized dystonia in a German patient." *Lancet Neurol* 7(5): 380-381.
- Seth RB, Sun L, Ea C, Chen ZJ. (2005) "Identification and Characterization of MAVS, a Mitochondrial Antiviral Signaling Protein that Activates NF- $\kappa$ B and IRF3" *Cell* 122(5):669-682.
- Shi Y, Taylor SI, Tan SL. and Sonenberg, N. (2003). "When translation meets metabolism: multiple links to diabetes." *Endocr Rev* 24: 91-101.

- Shimazawa M and Hara H. (2006). "Inhibitor of double stranded RNA-dependent protein kinase protects against cell damage induced by ER stress." *Neurosci Lett* 409: 192-195.
- Singh M and Patel RC. (2012) "Increased Interaction between PACT Molecules in Response to Stress Signals is required for PKR Activation" *Journal of Cellular Biochemistry*. 113:2754-2764.
- Singh M, Castillo D, Patel CV and Patel RC. (2011). "Stress-induced phosphorylation of PACT reduces its interaction with TRBP and leads to PKR activation." *Biochemistry* 50(21): 4550-4560.
- Singh M, Fowlkes V, Handy I, Patel CV and Patel RC. (2009). "Essential role of PACT-mediated PKR activation in tunicamycin-induced apoptosis." *J Mol Biol* 385(2): 457-468.
- Siu KL, Yeung ML, Kok KH, Yuen KS, Kew C, Lui PY, Chan CP, Tse H, Woo PC, Yuen KY, Jin DY. (2014) "Middle east respiratory syndrome coronavirus 4a protein is a double-stranded RNA-binding protein that suppresses PACT-induced activation of RIG-I and MDA5 in the innate antiviral response." *J Virol*. 88(9):4866-76
- Soto C. (2003). "Unfolding the role of protein misfolding in neurodegenerative diseases." *Nat Rev Neurosci* 4: 49-60.
- Srivastava SP, Davies MV and Kaufman RJ. (1995). "Calcium depletion from the endoplasmic reticulum activates the double-stranded RNA-dependent protein kinase (PKR) to inhibit protein synthesis." *J Biol Chem* 270: 16619-16624.

- Stefani IC, Wright D, Polizzi KM and Kontoravdi C. (2012). "The role of ER stress-induced apoptosis in neurodegeneration." *Curr Alzheimer Res* 9: 373-387.
- Stoessel AJ, Lehericy S and Strafella AP. (2014). "Imaging insights into basal ganglia function, Parkinson's disease, and dystonia." *Lancet* 384: 532-544.
- Suen KC, Yu MS, So KF, Chang RC and Hugon J. (2003). "Upstream signaling pathways leading to the activation of double-stranded RNA-dependent serine/threonine protein kinase in beta-amyloid peptide neurotoxicity." *J Biol Chem* 278: 49819-49827.
- Tabas I and Ron D. (2011). "Integrating the mechanisms of apoptosis induced by endoplasmic reticulum stress." *Nat Cell Biol* 13: 184-190.
- Taghavi N, Samuel CE. (2012) "Protein kinase PKR catalytic activity is required for the PKR-dependent activation of mitogen-activated protein kinases and amplification of interferon beta induction following virus infection." *Virology*. 427(2):208-16.
- Takacs AM, Das T and Banerjee AK. (1993). "Mapping of interacting domains between the nucleocapsid protein and the phosphoprotein of vesicular stomatitis virus by using a two-hybrid system." *Proc. Natl. Acad. Sci. USA* 90: 10375-10379.
- Takahashi T, Miyakawa T, Zenno S, Nishi K, Tanokura M, Ui-Tei K. (2013) "Distinguishable in vitro binding mode of monomeric TRBP and dimeric PACT with siRNA." *PLoS One*. 8(5):e63434.
- Takeuchi O and Akira S. (2010) "Pattern Recognition Receptors and Inflammation." *Cell*. 140(6):805-820.

- Tang NM, Korth MJ, Gale M, Jr., Wambach M., Der, S.D., Bandyopadhyay, S.K., Williams, B.R. and Katze, M.G. (1999). "Inhibition of double-stranded RNA- and tumor necrosis factor alpha-mediated apoptosis by tetratricopeptide repeat protein and cochaperone P58(IPK)." *Mol Cell Biol* 19: 4757-4765.
- Tawaratsumida K, Phan V, Hrinčius ER, High AA, Webby R, Redecke V, Häcker H. (2014) "Quantitative proteomic analysis of the influenza A virus nonstructural proteins NS1 and NS2 during natural cell infection identifies PACT as an NS1 target protein and antiviral host factor." *J Virol*. 88(16):9038-48
- Thomis DC and Samuel CE. (1995). "Mechanism of interferon action: characterization of the intermolecular autophosphorylation of PKR, the interferon-inducible, RNA-dependent protein kinase." *J Virol* 69: 5195-5198.
- Thompson ML, Chen P, Yan X, Kim H, Borom AR, Roberts NB, Caldwell KA, and Caldwell GA. (2014). "TorsinA rescues ER-associated stress and locomotive defects in *C. elegans* models of ALS." *Dis Model Mech* 7: 233-243.
- Vaughn LS, Bragg DC, Sharma N, Camargos S, Cardoso F, Patel RC. (2015) "Altered Activation of Protein Kinase PKR and Enhanced Apoptosis in Dystonia Cells Carrying a Mutation in PKR Activator Protein PACT." *J Biol Chem*. 290(37):22543-57.
- Vaughn LS, Snee B and Patel RC. (2014). "Inhibition of PKR protects against tunicamycin-induced apoptosis in neuroblastoma cells." *Gene* 536: 90-96.
- Walter P and Ron D. (2011). "The unfolded protein response: from stress pathway to homeostatic regulation." *Science* 334: 1081-1086.



- Weber F. (2015) "The catcher in the RIG-I" Cytokine. 76:38-41.
- Wek RC and Cavener DR. (2007). "Translational control and the unfolded protein response." Antioxid Redox Signal 9: 2357-2371.
- Wek RC, Jiang HY and Anthony TG. (2006). "Coping with stress: eIF2 kinases and translational control." Biochem Soc Trans 34: 7-11.
- Williams BR. (1999). "PKR; a sentinel kinase for cellular stress." Oncogene 18: 6112-6120.
- Wilson RC, Tambe A, Kidwell MA, Noland CL, Schneider CP, Doudna JA. (2015) "Dicer-TRBP complex formation ensures accurate mammalian microRNA biogenesis." Mol Cell. 57(3):397-407.
- Wu B and Hur S. (2015) "How RIG-I like receptors activate MAVS" Current Opinion in Virology. 12:91-98.
- Xiao J, Vemula SR and LeDoux MS. (2014). "Recent advances in the genetics of dystonia." Curr Neurol Neurosci Rep 14: 462.
- Xing J, Wang S, Lin R, Mossman KL, Zheng C. (2012) "Herpes simplex virus 1 tegument protein Us11 downmodulates the RLR signaling pathway via direct interaction with RIG-I and MDA-5." J. Virol. 86:3528-3540.
- Xu Z, Wang S, Lee X, and Williams BR. (2004). "Biochemical analyses of multiple fractions of PKR purified from Escherichia coli." J Interferon Cytokine Res 24(9): 522-535.
- Yeung, M.C. (2002). "Accelerated apoptotic DNA laddering protocol." Biotechniques 33: 734, 736.

Yong Y, Meng Y, Ding H, Fan Z, Tang Y, Zhou C, Luo J, Ke ZJ. (2015) "PACT/RAX regulates the migration of cerebellar granule neurons in the developing cerebellum." *Sci Rep.* 5:7961

Yong Y, Luo J, and Ke ZJ. (2014). "dsRNA binding protein PACT/RAX in gene silencing, development and diseases." *Front Biol (Beijing)* 9: 382-388.

Zech M, Castrop F, Schormair B, Jochim A, Wieland T, Gross N, Lichtner P, Peters A, Gieger C, Meitinger T, Strom TM, Oexle K, Haslinger B, Winkelmann J. (2014) "DYT16 revisited: exome sequencing identifies PRKRA mutations in a European dystonia family." *Mov Disord.* 29(12):1504-10.

Zech M, Castrop F, Haslinger B, Winkelmann J. (2015) "Reply to Letter: Novel Compound Heterozygous Mutations in *PRKRA* Cause Pure Dystonia." *Movement Disorders.* 30(6)

Zhang W, Feng D, Li Y, Iida K, McGrath B and Cavener DR. (2006). "PERK EIF2AK3 control of pancreatic beta cell differentiation and proliferation is required for postnatal glucose homeostasis." *Cell Metab* 4: 491-497.

Zinszner H, Kuroda M, Wang X, Batchvarova N, Lightfoot RT, Remotti H, Stevens JL and Ron D. (1998). "CHOP is implicated in programmed cell death in response to impaired function of the endoplasmic reticulum." *Genes Dev* 12: 982-995.

## APPENDIX A- GENE REPRINT PERMISSION

ELSEVIER  
()



SEARCH



MENU


### Personal use

Authors can use their articles, in full or in part, for a wide range of scholarly, non-commercial purposes as outlined below:

- Use by an author in the author's classroom teaching (including distribution of copies, paper or electronic)
- Distribution of copies (including through e-mail) to known research colleagues for their personal use (but not for Commercial Use)
- Inclusion in a thesis or dissertation (provided that this is not to be published commercially)
- Use in a subsequent compilation of the author's works
- Extending the Article to book-length form
- Preparation of other derivative works (but not for Commercial Use)
- Otherwise using or re-using portions or excerpts in other works

These rights apply for all Elsevier authors who publish their article as either a subscription article or an open access article. In all cases we require that all Elsevier authors always include a full acknowledgement and, if appropriate, a link to the final published version hosted on Science Direct.

## APPENDIX B- JOURNAL OF BIOLOGICAL CHEMISTRY REPRINT PERMISSION



Institution: USC SCHOOL OF MEDICINE Sign In

QUICK SEARCH | Author:  Keyword:  Year:  Vol:  Page:   [\[Advanced Search\]](#) [\[Browse the Archive\]](#)

[Home](#) | [Current issue](#) | [Archive](#) | [Papers in Press](#) | [Minireviews](#) | [Reports](#) | [Classics](#) | [Reflections](#) | [Papers of the Week](#)

### Copyright Permission Policy

These guidelines apply to the reuse of articles, figures, charts and photos in the *Journal of Biological Chemistry*, *Molecular & Cellular Proteomics* and the *Journal of Lipid Research*.

#### For authors reusing their own material:

Authors need **NOT** contact the journal to obtain rights to reuse their own material. They are automatically granted permission to do the following:

- Reuse the article in print collections of their own writing.
- Present a work orally in its entirety.
- Use an article in a thesis and/or dissertation.
- Reproduce an article for use in the author's courses. (If the author is employed by an academic institution, that institution also may reproduce the article for teaching purposes.)
- Reuse a figure, photo and/or table in future commercial and noncommercial works.
- Post a copy of the paper in PDF that you submitted via BenchPress.
- Link to the journal site containing the final edited PDFs created by the publisher.

EXCEPTION: If authors select the Author's Choice publishing option:

- The final version of the manuscript will be covered under the Creative Commons Attribution license (CC BY), the most accommodating of licenses offered. [Click here for details.](#)
- The final version of the manuscript will be released immediately on the publisher's website and PubMed Central.

Please note that authors must include the following citation when using material that appeared in an ASBMB journal:

"This research was originally published in *Journal Name*. Author(s). Title. *Journal Name*. Year; Vol:pp-pp. © the American Society for Biochemistry and Molecular Biology."